University of Alberta

Finite Element Analysis of Nonlinear Wave Propagation in a One-Dimensional Structure

by

Kennedy J. Kirkhope 

A thesis submitted to the Faculty of Graduate Studies and Research in partial fulfillment of the requirements of the degree of *Master of Science.*

in

Department of *Mechanical Engineering*

Edmonton, Alberta,

Spring 2005

Abstract

This thesis presents application-specific finite element analysis program, JIFEA (Jar Impact Finite Element Analysis), as an efficient and accurate tool for solving 1D wave propagation representative of Jarring in a drilling assembly.

Custom elements were created to model the pipe, Coulomb damping, viscous damping and axial contact. The response of each element was verified against analytical solutions and two commercial FEA programs, ANSYS and ADINA showing good agreement. Three time-integration methods were implemented in JIFEA, Central Difference, Newmark and Wilson and verified with ANSYS and ADINA but with JIFEA performing 30 times faster.

A sample drill string model was created to test the elements and solution strategy. Viscous and Coulomb damping rapidly decayed the wave response. Jar placement offers one of the few controls to alter the generated force magnitude.

JIFEA's speed and accuracy makes it a perfect tool for performing this type of analyses.

Acknowledgements

I wish to acknowledge the efforts, contributions and support of the following:

Dr. Trent Kaiser: Dr Kaiser provided his knowledge of nonlinear finite element analysis and dynamics. His contributions were invaluable to the development of the application-specific wave propagation analysis software JIFEA (Jar Impact Finite Element Analysis). Without his contributions this thesis would not have been possible.

Dr. Walied Moussa: Dr Moussa guided me in the masters' process and assisted with preparation of the thesis and defence.

Dr. Ken Fyfe: Dr. Fyfe offered to be my original primary supervisor and assisted with my acceptance into the masters program.

My family and friends: Everyone around me supported me during many of my sleepless rants and understanding me even when I did not understand myself. They showed confidence in my abilities and constantly reminded me: when you put your mind to it, anything is possible.

Table of Contents

List of Tables

List of Figures

Nomenclature

$[M]$	Mass coefficient matrix
$[C]$	Damping coefficient matrix
$[K]$	Stiffness coefficient matrix
$\{x\}$	Displacement vector
$\{\dot{x}\}=\left\{\frac{dx}{dt}\right\}$	Velocity vector (single dot notation for first derivative)
$\{\ddot{x}\}=\left\{\frac{d^2x}{dt^2}\right\}$	Acceleration vector (double dot notation for second derivative)
$\{R\}$	Externally applied load vector
$\{F\}$	Forces equivalent to internal element stress vector
$\{{}^{t}x^{(k)}\}$	The left superscript t denotes the time The right superscript denotes the equilibrium iteration. The brackets are to distinguish between superscripts and mathematical exponents
ω_D	Damped circular natural frequency
ω_N	Circular natural frequency
$\zeta=\frac{c}{c_{crit}}$	Damping coefficient. The ratio of applied damping and the critical damping of the system

Chapter 1

INTRODUCTION

The drilling industry is decades old and from the beginning, problems of the assembly becoming stuck down-hole were common. Specialized tools, known as Drilling Jars, were developed to introduce impulse waves to free the stuck drill string. Jars generate high-amplitude impulses that propagate throughout the drill string. Jar placement within the drilling assembly affects the magnitude and duration of these waves.

Structural and dynamic analyses have long been used to assess the stress or force in drilling components for the oil and gas industry. Specifically, dynamic analysis is used for a variety of reasons such as determining fatigue limits to increase tool and/or pipe lifecycle or used to increase tool efficiency.

Many wave propagation calculation techniques have been employed from simple hand calculations to advanced computer simulations. A common analysis technique for solving wave propagation is time-history integration. This technique is used to assess the force (stress) present in the drilling assembly as a function of induced vibration and/or time.

Time-history analyses are used to study Jar wave propagation attempting to refine placement and maximize Jarring effectiveness. Finite Element Analysis (FEA) is one of the most common methods for solving these problems. FEA is also used to verify or calibrate other methods. Alternate methods are commonly developed as commercial FEA is considered slow for field use and requires extensive training. As the literature shows, commercial FEA methods are generally not used beyond verification, calibration or research purposes for wave propagation in drilling applications.

Application-specific FEA software is superior to commercial FEA software, eliminating extensive training requirements and increasing solution performance. Application-specific software produces direct Jar placement results and requires minimal user input. The wave propagation model of Jarring has specific boundary conditions such as friction and damping that are implemented to minimize user input. The solution strategy and integration controls are fixed, preventing integration settings from generating erroneous or divergent solutions. Result interpretation is built-in, producing placement information such as forces at the stuck point.

This thesis demonstrates that application-specific FEA can be used to efficiently and accurately solve nonlinear one-dimension (1D) wave propagation and is broken into two components:

1. The numerical methods typically used in commercial applications are reviewed and implemented in an application-specific program, known as **JIFEA** (Jar Impact Finite Element Analysis), and verified using analytical methods and commercial FEA.
2. Different integration techniques are used with various control parameters, friction, damping and Jar location to demonstrate sensitivity to each.

The thesis is structured to introduce the concepts systematically. Chapter 2 presents detailed background into Jars and application in the drilling industry and covers the literature review for analysis methods and application. Chapter 3 introduces the numerical methods used in the application-specific software, in the alternate numerical methods and in the manual (hand) calculations. Also, comparisons between JIFEA and commercial FEA software are shown to verify accuracy. Chapter 4 shows solution sensitivity to each controlling factor of the application-specific program and a brief case study on Jar placement. Note: Chapters 3 and 4 were originally written as stand-alone papers and as such have separate introductions and summaries specific to the respective chapter. Finally Chapter 5 provides an overall conclusion and recommended further research.

Considering the diverse use of dynamic analysis, efficient and accurate FEA code created for specific purposes will have industry application.

Chapter 2

LITERATURE REVIEW

2.1 Background

Many of the terms used in the drilling industry may be foreign to people outside the industry. This section provides detailed background of the terms and drilling concepts that are used throughout this thesis.

2.1.1 Drill string

A drilling assembly is a long assembly of pipe joined end-to-end by threaded connections[1]. The pipe outside and inside diameters are chosen to provide weight for the bit, strength for the drilling application and other application-specific requirements. Figure 2.1 shows a basic drilling assembly with a typical Jar placement and location of the stuck point.

The diameter of the pipe is small compared to its length and when assembled acts like a string. Therefore, the assembly is commonly known as the "drill string".

2.1.2 Drilling Jar

The Drilling Jar is a specialized tool designed to generate large stress waves in the drill string. It consists of a locking mechanism that enables the driller to stretch the drill string into tension. This is often referred to as strain or energy storage stage.

Once the tension exceeds the lock-load the Jar travels a free-stroke length (gap) allowing each end of the drill string to accelerate towards each other. These ends are typically referred to as the hammer for the end connected to the upper pipe and the anvil for the lower portion. Figure 2.2 shows a depiction of the hammer and anvil. This is the energy release stage.

When the hammer and anvil strike, momentum is transferred creating an impulse wave that travels in both directions in the pipe. The amount of momentum transferred is a function of the stiffness and mass attached to both the hammer and anvil. As such, Jar placement can be used to modify the impulse wave amplitude and duration.

The process of pulling the Jar into tension, overcoming the lock-load and transferring the momentum is called "Jarring". This process is repeated until either the string is freed (ideal) or the stuck string is otherwise bypassed.

---

[1] There are other methods but threaded connection are the most common.

The wave propagation problem involves compression waves travelling in a tensile pre-stressed pipe. Reflections and refractions cause the wave to split and change sign. Therefore, tension waves could travel into the tensile pre-stressed pipe potentially causing local yielding[2].

2.1.3 Shock tool

The "Shock Tool" is another common tool in a drilling assembly. It is designed to remove vibration generated at the bit from propagating up to the lighter weight pipe. Drilling vibrations can cause fatigue failures or reduce the rate of penetration (ROP) of the bit. Typically, the shock tool is placed as low in the drilling assembly as possible, which places it in close proximity to the Jar.

The shock tool is basically an axial spring with stiffness proportional to the weight on bit (WOB). This enables the shock tool to operate within the maximum displacement range (fixed stroke length) for the desired drilling conditions. Essentially, the shock tool is a vibration isolation system.

The response rate[3] of a shock tool may hinder its performance or effectiveness as a vibration isolation method.

2.1.4 Stuck point

In Jar impact analysis, the key result of interest is the force response generated at the stuck point. By definition, the stuck point is the location where the drill string becomes stuck.

As the drilling progresses, several down-hole occurrences can cause the drill string to become stuck. The mechanisms that cause sticking of the drilling assembly are categorized as follows:

1. **Mechanical.** The sticking mechanism is considered mechanical when the formation is directly responsible for restraining the pipe. For example, when rock from the formation collapses in around the pipe or foreign matter, such as cuttings, is caught between the pipe and the formation.
2. **Hydraulic.** The mechanism is considered hydraulic when the drilling fluid is responsible for restraining the pipe. For example, if cuttings present in the drilling-fluid pack around one side of the pipe and prevent fluid from separating the pipe from the formation, the fluid pressure builds on one side of the pipe effectively pushing the pipe against the formation causing friction.

---

[2] Materials typically exhibit higher yield strengths under rapidly applied loads. Strain rate effects are out of the scope of this paper.

[3] Response rates of tools are out of the scope of this paper. However, this type of dynamic analysis is well suited for response rate studies.

Two other terms are commonly used when discussing Jars and the waves produced: Impact and Impulse. Their use is somewhat inaccurate in strict definition but convenient to describe the different types of wave propagation.

Impact has come to mean a large amplitude force applied over a very small time frame; whereas Impulse means a moderate force applied over a longer period of time. It is commonly said that impacts are better against mechanical sticking and impulse is better for hydraulic sticking. The difficulty in defining the difference is the magnitude of the forces and the times in which they act are relatively similar and therefore subjective. Jars are tools that have certain conditions that must be met in order to use them. These conditions restrict the Jar placement within the drill string limiting how much "Impact" vs. "Impulse" is generated.

As the following study will show, most of the waves of interest occur within the first half-second or less. The amount of viscous damping and coulomb damping will further limit the control on what type of force is produced by the Jar.

2.1.5 Reason for analysis

As stated previously, the waves generated by a Jar travel in both directions and are impeded by several factors. Understanding how waves travel through the drill string is paramount in determining the most effective location to place the Jar in the drilling assembly.

Initially simple hand-calculations were employed to determine Jar placement based on simple impulse-momentum relations and stress-wave propagation. As technology advanced, more and better methods were used to increase the accuracy and add complexity to the computations.

One of the most significant contributions was finite element analysis (FEA) performed by Kalsi, Wang et al in 1985. Kalsi used ANSYS commercial FEA software to evaluate the Jar impact analysis. At that time, the solution took approximately 3 hours to solve with that version of the software on the computing power of the day (Kalsi *et al.*, 1985). Kalsi demonstrated an advantage to performing the analysis using FEA but the solution time and cost of computers and software made commercial FEA impractical for most end-users.

Kalsi et al required alternate methods to perform the impact analysis producing similar results but much faster if impact analysis was going to be used as a design and field placement tool. Kalsi, Wang et al and Eustes set out to find such methods. ANSYS was used by both Kalsi (Wang) and Eustes to verify and calibrate their respective methods (Eustes, 1996; Wang *et al.*, 1990).

2.1.6 Modelling difficulties

The wave propagation problem representative of drilling conditions has several difficult features to handle numerically.

1. **Friction.** The action of friction distributed along the drill pipe is a discontinuous function. The elements are created to capture the discontinuities as an idealized function of displacement.
2. **Damping.** The damping term in d'Alembert's principle (equation of motion) adds complexity to the integration and additional elements to the model.
3. **Contact.** Contact is used to represent the Jar in the model. The ratio of closed stiffness to open stiffness is very large making contact elements highly discontinuous.

The modelling utilizes all of these features creating a very discontinuous and consequently nonlinear problem. Iterative solvers and integrators are required to solve the system of equations. The elements are implemented with continuous functions and used to represent a discontinuous system response.

2.2 Literature Review

Wave propagation and mode superposition analysis have been used extensively in the drilling industry for decades to evaluate the effect vibrations have on the drill string, other tools or even the rig. From the 1960's on, methods have evolved from simple hand calculations producing force distributions to advanced nonlinear finite element analysis producing force, stress and kinematics at any location within the string.

Dynamic analysis is either structural dynamics or wave propagation. In structural dynamics, the system is commonly excited by harmonic or periodic forcing functions. The system response will exhibit a limited number of frequencies. For these types of analysis, depending on the frequency or number of frequencies of interest, a spectral (frequency domain) analysis may be preferred. For wave propagation problems often several frequencies are represented and the forcing function is not harmonic or periodic. These types of problems are more commonly solved with time-history techniques.

Many have used wave propagation to determine potential problems within the drilling assembly or to maximize specific efficiencies. The review that follows looks generally at the application of wave propagation but focuses on analysis techniques. The review is presented in ascending chronological order.

2.2.1 Drill string wave propagation analysis

Skeem developed one of the first and most wide-spread methods for determining the drill string dynamics during Jar operations (Skeem *et al.*, 1979). This method was dubbed the "average force" method. Wave propagation and basic impulse-momentum principles were applied to a

simplified drill string model to develop an analytical formulation of Jarring efficiency. Some of the assumptions were: The drilling assembly consisted of drill pipe and drill collar only, the stuck point was represented by a fixed boundary and the entire drill collar instantly reached the contraction velocity. The results from this work indicated that Jar placement could be altered to maximize the force produced or time over which the force was applied at the stuck point.

One of the first uses of FEA was performed by McDaniel (McDaniel, 1982) to verify empirical data from a simple test of a jar in a 267 foot drilling assembly. The method used the Newmark beta method to integrate the equation of motion and featured a bilinear element to represent hammer-anvil contact. The nonlinear behaviour was handled using a brute-force method rather than an incremental solution strategy such as Newton-Raphson. The FEA implementation's response was subject to oscillations due to the brute-force approach. However, with the appropriate element length and time step size, the application-specific FEA did verify the empirical results showing that the numerical techniques provided a viable and valuable tool for Jar placement impact analysis.

One of the most cited works on transient analysis of the drill string under Jar loads is that by Kalsi (Kalsi et al., 1985). The analysis was performed using ANSYS and incorporates viscous damping, friction (stuck point) and contact (Jar). These features require nonlinear solution techniques available in ANSYS. Several of the works cited herein reference this paper and treat it as the definitive FEA work on the analysis of Jar wave propagation. For this reason, the model used to test and verify JIFEA is Kalsi's model. The cost of commercial FEA packages such as ANSYS and the speed of the solutions at the time (1985) made field use impractical.

Lerma used Skeem's method in conjunction with Kalsi's results to determine the effect heavy-weight drill pipe had on the Jarring Operation (Lerma, 1985). The analysis showed that the mass-stiffness relationship altered the Jarring efficiency thus requiring adjustment to Jar placement and concludes by stating that more mass closer to the Jar increases the magnitude of the force propagating. Therefore, running the Jar in the drill collars is preferred. However, the results were based on the physics of a specific model and changing the parameters will alter the results.

Askew presented a paper to the Society of Petroleum Engineering outlining Jar placement refinement using FEA results in combination with experience and static calculations being accurate and practical for field use (Askew, 1986). The paper indicates that finite element analysis was used to perform the Jar placement study but specifically states that the details of the software used will be omitted. It is possible that the software was proprietary FEA code created for Jar placement – force propagation analysis. No further information could be found at the time of this writing. One might consider the performance and cost of commercial nonlinear FEA methods impractical for common application to Jar placement motivating the development of

alternative methods. Fast and simple methods of solving the wave propagation problem were required to produce a field-friendly method to solve Jar impact.

Dynamic analysis was used by Lubinski to assess the fatigue of drill pipe for Sec. 12 of API RP7G. Computer analysis was used to assess the dynamic loading of drill pipe during tripping (Lubinski, 1986). No specific mention is made regarding the software used to perform the analysis other than to say: "two computer programs have been developed ...". From the discussion it would seem the programs use some form of wave-tracking similar to that presented by Skeem.

Kalsi, Wang et al revisited the Jar placement/wave propagation problem by developing a wave-tracking method (Wang et al., 1990). The previous efforts proved tedious due to analysis time using commercial software. Wave-tracking uses the basic premise of wave propagation as Skeem used but with recursive computer algorithms to track all reflections and refractions of the propagating waves. The method consisted of a numerical model of an impulse introduced into a linear assemblage of pipe and tracked as the wave travelled through the pipe. Every encounter with a cross-sectional area change would split the wave, some being reflected and some being transmitted (Clough & Penzien, 1993).

The program results were verified against ANSYS and the wave-tracking method then developed into a commercial Jar placement/analysis program called JarPRO™. The initial input wave was a square pulse with the magnitude computed from basic impulse-momentum relationships and compared to incremental root-mean-square magnitudes of the wave generated by ANSYS. The results were found to be reasonable enough to warrant the creation of JarPRO™. Wave-tracking produced considerably faster solution times making iterative Jar placement possible for field use.

Kalsi produced an information pamphlet outlining the JarPRO™ software and demonstrating the capabilities ("JarPRO™", 1990). JarPRO™ features an intuitive user interface, robust drilling assembly creation and produces a results matrix with force and kinematics information for the entire assembly. Also, it produces similar results compared to ANSYS but in a fraction of the time, solutions in a few seconds rather than several minutes. Further work by Kalsi Engineering produced a new version of the wave-tracking method where nonlinear effects such as friction and damping were added. Again, ANSYS was used to calibrate the results. At the time of this writing, documentation on the verification or implementation of the nonlinear results was unavailable.

Rather than determining the force produced at the stuck point, Aarrestad determined the force waves propagating up through the drill pipe (Aarrestad & Kyllingstad, 1994). This could be used to assess the forces acting on the rig or to determine the fatigue loading of the drill pipe. This paper demonstrates the necessity of performing dynamic analysis on the full drilling assembly even if only in one dimension. Kalsi's FEA model used a reduced model size to

decrease the solution time. In order to analyze the forces reaching the rig, a full model with a longer solution time must be used. An efficient and accurate application-specific solution may facilitate such analyses.

Eustes also considered the wave propagation problem of Jars but considered it from a purely numerical analysis view. Very complex elements (spectral elements) were used to represent the pipe but the complex nature meant very few were required. Elements represent a Fourier series and could only represent frequencies or modes proportional to the number of terms in the series. Eustes used ANSYS to re-create the work of Kalsi and Askew and to calibrate the spectral analysis. As mentioned earlier, spectral analysis is well suited for harmonic or periodic responses but not necessarily for general wave propagation. Eustes concluded that the method produced similar results to ANSYS but in a fraction of the time. However, spectral analysis is not meaningful until the results are transformed into time-history data. Furthermore, the numerical model was found conditionally stable to the damping coefficient[4].

The spectral model proved to be very fast to solve the system but very temperamental to damping and solution control parameters. Slight changes in either would produce large changes in the response or cause numerical instability.

A case history was performed to assess the affects jar accelerators had on the stuck drill string (Broussard *et al.*, 2004). As part of the analysis, proprietary jar analysis software was used. This software was based on the wave-tracking method (Wang et al., 1990). Broussard makes no mention in the publication as to why the proprietary Jar software was used. However, it may have been for two reasons, first, the simplified user input facilitates extensive case studies; and second, the cost of the software and learning time is significantly less than that of commercial analysis software such as ANSYS. Other software such as JIFEA could have been used that is equally accurate and efficient to perform the dynamic analysis.

Companies that produce drilling Jars, such as National Oilwell, publish guidelines on Jar placement and Jar operation ("Basic jar placement", 1995), ("Drilling jars", 1994). These documents discuss the energy transfer that occurs from the hammer-anvil contact within the Jar and provide an overview of how energy travels from the Jar to the stuck point. They do not, however, discuss the wave propagation in detail but do provide cursory results from JarPRO™ analyses.

2.2.2 Other dynamic analyses

The literature shows wave propagation used for several purposes other than Jar placement.

[4] Information conveyed by co-worker.

Stockard discusses case histories performed on Pile Driving in the Gulf of Mexico (Stockard, 1980). Wave propagation is used to study the dynamics of Pile Driving and considers the impact generated from the ram, the damping of the pile cushion, the dynamics of the pile and both the friction and damping of the soil. The software used to perform the analysis is described as a Wave Equation Program, and from the discussion is likely some form of wave-tracking program. The analysis is a 1D wave propagation problem with damping and friction. Piles are modelled as an elastic 1D structure with friction acting at the soil-pile interface. In some models, contact is used to model the hammer-pile interface while in other models a time-based periodic forcing function is used. The top of the pile may have a cushion attached represented by a lower stiffness and viscous damping.

As part of an extensive drilling design optimization, Gibson discusses the use of dynamic analysis to improve Jar firing efficiency (Gibson *et al.*, 1992). The overall drilling optimization is to improve Openhole completions of North Sea horizontal wells. The optimization is performed using drill string stability analysis.

Field describes the use of dynamic analysis to prevent MWD damage from drill string vibration (Field *et al.*, 1993). The analysis produces a critical speed that is used as running criteria for the drilling operations. The use of Critical Speed Analysis (CSA) is recommended as a pre-drilling analysis to better predict the expected dynamics. However, the paper also mentions "judicious post-processing" as a requirement of proper application of the CSA method. Application-specific software could be implemented with the post-processing requirements built-in streamlining the solution process.

Mabsout presents a paper on the simulation of pile driving using finite element analysis (Mabsout & Tassoulas, 1994). The numerical model presented is a two dimensional model making use of the axisymmetric nature of dimensions. The analysis is a nonlinear time-history analysis similar to that performed by JIFEA. The use of the dynamic analysis is used to determine the drivability of concrete piles under various hammering and soil conditions. For this case, the hammer is represented by a periodic forcing function rather than modelling the contact between hammer and pile.

Elnaggar discusses a similar nonlinear model used to analyze the dynamics of piles (Elnaggar & Novak, 1994). Axial dynamic analysis is used to determine the bearing capacity and load-deflection relationships for the pile. The model allows for nonlinear response decay through damping and soil hysteresis. These effects can be modelled using combinations of spring stiffness, damping and friction.

Nonlinear dynamic analysis is used to study the scattering of waves at nonlinear joints between two rods (Nagem & Williams, 1994). Nonlinear joint analysis can be added to wave propagation analysis and used for response prediction, non-destructive testing and space structures. The discussion

indicates the joints are analyzed by using nonlinear damping, nonlinear friction and nonlinear weak springs.

The full transient analysis of a bend-housing BHA enables the determination of the time-dependent bit side load (Jianhong & Taihe, 1996). Finite element analysis was used to determine the speed depended loading on the BHA when used with a bend-housing. The results were used to specify drilling parameters to control trajectory and prevent fatigue. Two or three dimensional analysis was employed due to the geometry but these effects can be applied to a one dimensional model to simulate the results. The paper describes the difficulty in solving these types of analysis and mentions application of harmonic spectral analysis as an alternative simplifying the solution. Application-specific software is viable for solving these types of problems producing the required results.

Badoni discusses pile-to-pile interactions (Badoni & Makris, 1997). The focus of this paper is on the pile-to-pile interaction of waves travelling through the soil. Wave propagation is used to determine the force entering the soil from each pile then visco-elastic soil properties and plain-strain wave theory is used to model the wave propagation through the soil. The analysis was performed to assess the effect pile motions have on one another.

Aadnoy performed a friction analysis on long-reach wells (Aadnoy *et al.*, 1998). Analytical equations are developed to assess the friction in various well geometries. These equations produce a total well friction distribution on the drill string.

Longitudinal wave attenuation in rods was presented by Thorp (Thorp *et al.*, 2001). The waves were effectively filtered out by use of piezoelectric bands placed along the rod. The application of this filtering technique is interesting for application in drilling to remove vibration from sensitive regions of the drill string.

Several other applications for wave propagation analysis were found during the literature review but none other than the references listed addressed development of application-specific software or specific relationships for damping and friction. A few other references typical of documents found are : (Fernandez *et al.*, 2003), (Li & Li, 2002), (Dawson & Paslay, 1984).

2.3 Chapter 2 figures

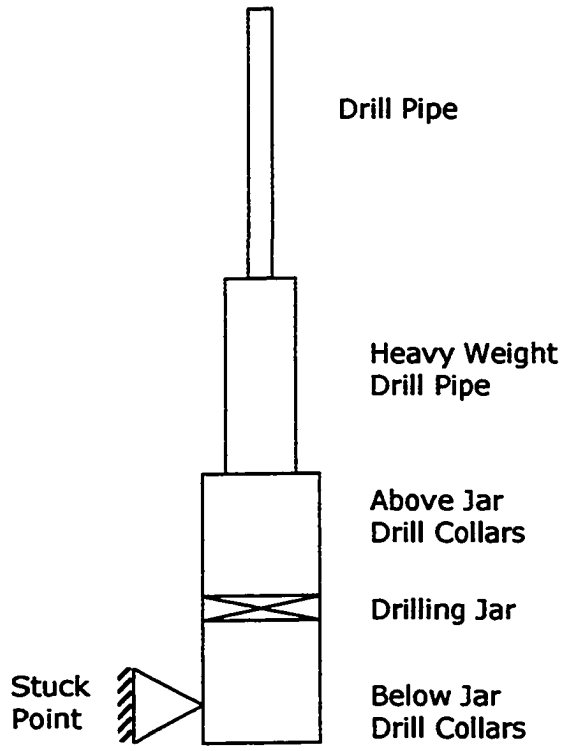

Figure 2.1, Jar location within basic drilling assembly

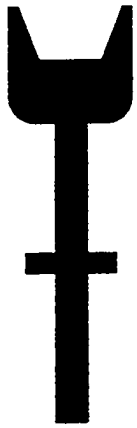

Figure 2.2, Hammer-anvil depiction of Drilling Jar

Chapter 3

SOLUTION STATEGIES FOR FINITE ELEMENT ANALYSIS OF NONLINEAR WAVE PROPAGATION

"... progress in design of new structures seems to be unlimited" (Bathe, 1967).

By today's standards Bathe's statement may appear an extreme view but it is truer today than ever and progress will continue expanding.

Jars have not changed much, although, advancements in analysis and design improved the technology and quality. The use of computers and techniques such as Finite Element Analysis (FEA) enabled designers to better explore geometry variations, materials and part interactions.

The evolution of Drilling Jars largely stems from manufacturers and operators improving their understanding of Jar component behaviour and Jar - drill string interaction. Wave propagation analysis is used to refine Jar placement within the drilling assembly. The analysis is typically used on a comparative basis so absolute forces are not necessarily important.

This thesis focuses on waves introduced into a system and the numerical methods used to analyze them. Several manual methods have been published describing approximations to wave propagation based on impulse-momentum relations. With advancements in numerical methods and computer / software technology, more sophisticated techniques were developed and used to analyze the waves. Commercial FEA was used to calibrate or verify these methods. However, it was not used directly to perform the analysis.

Commercial FEA packages ADINA and ANSYS were used to re-create previously documented models and some of the alternate methods such as spectral analysis and wave-tracking were reviewed. The key numerical techniques for time integration (Central Difference, Newmark and Wilson) and nonlinear solutions (full or modified Newton) were evaluated for implementation in custom finite element software specifically designed to solve a nonlinear one dimensional wave propagation problem.

3.1 Model Description

The waveform and amplitude of the waves are a function of the Jar's position within the drill string but also, the characteristics of the well bore and fluid surrounding the pipe.

In order to perform the desired wave propagation analysis, the basic modelling approach must be defined. This includes the definition of element

type, storage of the stiffness, damping and mass matrices and determination of the solution strategy.

The drill string is idealized as a 1D wave propagation problem with viscous damping, coulomb damping (friction) and contact. The Jar is modelled as a single 1D contact element representative of the hammer-anvil couple. The hole-drag is modelled as friction elements tied from ground to the pipe, distributed along the drilling assembly. Damping from fluid shear is also tied from ground to the pipe, distributed along the drilling assembly. Figure 3.1 shows a depiction of a three-dimensional drilling assembly and the corresponding one-dimensional representation.

The model used to assess the wave propagation is a 1D assembly of link[1] elements. A link element represents simple tension and compression forces with no large displacement, large strain or nonlinear material effects. It is used to capture the longitudinal waves as they propagate along the length of the model. A simple derivation of this element is in Appendix A. Given the 1D nature of this problem, the element is assembled inline to remove any requirements of 2D degrees of freedom. Well curvature contributions were added by imposing the effects onto the 1D geometry. Details of these effects are discussed in the Model Features section. The simplicity of this element suits the application as the internal element forces required for the nonlinear analysis are easily computed without integration. See Bathe (Bathe, Chap 6, 1996) for more information on computation of internal element forces.

The assembled elements form a symmetric tri-diagonal matrix. To reduce the memory requirements, a condensed matrix storage was developed. Only the diagonal and upper off-diagonal terms are stored. Without efficient memory usage the data storage is significant. For example, 1000 link elements require a matrix 1001 by 1001. In the condensed format, the storage is only 1001 by two.

A solver based on simple Guassian elimination was written to solve the condensed system of equations. This solver is used for static linear, static nonlinear, dynamic linear and dynamic nonlinear analyses.

The nonlinear aspects principally come from friction (hole-drag) acting along the length of the model. Friction acts to limit displacement and remove energy from the system. The distribution of friction comes from a simple rationalization of the hole-drag. This provides a nonlinear distribution of a nonlinear effect. The friction elements are connected from each node of the pipe assembly to ground. Therefore, all the relative displacements are related to a zero displacement at ground.

Contact is another nonlinear aspect in the model. Contact elements are highly nonlinear but as only one element is used to model the Jar hammer-anvil interaction, the effects are limited. Furthermore, the element was designed to

[1] ANSYS uses the term "link" for a basic tension/compression element; other texts and software use alternate terms such as spar element or truss element.

reduce the nonlinear severity (see Model Features section). Contact is modelled for two reasons: first, it provides the ability to generate a more natural waveform[2] from the model; and second, it allows the adjacent section of pipe to come out of contact.

In some FEA analyses the waveform is assumed and input as a time-function. Modelling the contact with the simple contact element used here enables a non-uniform wave to propagate.

Many models in the past have made the assumption that once the contact is made the bodies remain in contact for the rest of the analysis. In the contact description used here, the contact surfaces are allowed to contact and separate as the wave travels. This allows subsequent impact to occur between the hammer and anvil generating more waves. Previous models analyzed using similar techniques demonstrated good agreement with empirical data (McDaniel, 1982).

The Jar is represented by the contact element. The element is placed at the desired location of the Jar within the drilling assembly. Several analyses are performed varying the location of the Jar to determine the Jar location that generates maximum force at the stuck point. The stuck point is modelled either as a constrained node for which the reaction force history provides required force information or as a friction element allowing the stuck point to slide if the incoming force is large enough and re-stick once the wave has passed. Re-sticking occurs if down-hole conditions still exist after the initial Jarring. The stuck point friction is large enough that the initial pull force does not free the drill string. Therefore, the stuck point slips only when incoming waves have sufficient magnitude to overcome friction. This provides the ability to assess the time at which the stuck point is mobilized and form other placement acceptance criterion different from wave magnitude. Another possibility is to model the stuck point as a friction point that once free, it remains free. The purpose of Jarring is to free the string but it doesn't always occur upon first attempt. This type of stuck point makes developing a placement acceptance criterion difficult, either the total distance of slip or the total time of slip could be used.

Initially a link element, stiffer than the drill string link elements, is used to bridge the contact element. The assembly is pulled into tension using a static nonlinear solver. This provides the initial displacements in the model. The "bridge element" is removed and the dynamic nonlinear solver is employed to solve the system. Microsoft Excel® is used to analyze the displacement field and the response of the system; in particular, the location of the stuck point, the Jar and the Rig. The desire is to minimize the force acting at the Jar and Rig and maximize the force at the stuck point.

[2] The waveform is a function of the mesh density. As the mesh density increases, the waveform is more accurately represented but at the cost of solution speed.

3.2 Time Integration Techniques

Many of the schemes used in Finite Element Analysis (FEA) are derived from Newton Backward, Central and Forward methods. Other schemes are formed from polynomial approximations to functions and some are formed by simulating the Taylor Series Expansion in different ways from the Newton methods mentioned above. In any case, the fundamental goal is to provide an integration technique that is fast and accurate but also stable. In the work that follows, the evaluated methods were chosen because of to their commonality in FEA and numerical texts.

Many of the derivations and techniques presented were referenced from Bathe (Bathe, 1996). However, the information was verified in other texts such as Tedesco (Tedesco *et al.*, 1999), Logan (Logan, 1992), Clough (Clough & Penzien, 1993) and Chapra (Chapra & Canale, 1988).

The methods are broken down into two basic types with two alternate forms of each.

Explicit Methods – These methods are generally straightforward as the function is evaluated at known locations and/or previously solved locations. The primary advantages of explicit methods are that they are fast and simple to understand and implement. However, if the differential equations being integrated are stiff in nature or have abrupt changes in the response, explicit techniques generally require a small time step size (Tedesco *et al.*, 1999), thus increasing the total number of steps to complete the integration. In many wave propagation problems, the time step size must be considerably smaller than the highest frequency (period) of interest. Many authors suggest the time step size be at least $1/10^{th}$ the shortest period (Logan, 1992). The step size must at least be smaller than the critical time step size, which is discussed in detail in the Central Difference section. Also, the element length must be shorter than the wavelength of interest. ANSYS theory manual suggests 20 elements per wavelength.

Implicit Methods – These methods are more complex to implement and are iterative in nature (Tedesco et al., 1999). They are implicit as the determination of the next step (left hand side) is dependant on a guess of the next step for a function evaluation on the right hand side. Hence, the solution is iterative and often the convergence is dependent on the quality of the initial guess. The main advantage of implicit methods is that they can generally handle stiff differential equations or abrupt changes in the response. The main disadvantages are that they must iteratively solve each integration step and are more difficult to implement. Note that when solving a linear system, only one iteration is required per time step.

Semi-Implicit Methods – These are a class of methods that are implicit but the function evaluation on the right hand side is computed directly rather than iteratively. The computation captures the behaviour from the past and current steps to the next (future) step.

Single-Step Methods – Explicit or Implicit methods may be single-step. This means the determination of the next step is solely based on the previous step. The advantage is that these methods are simpler and require fewer function evaluations. However, by only including the previous step, they generally have significant error associated with the results.

Multi-Step Methods – Explicit and Implicit methods can be multi-step which means that the determination of the next step is based on more than just the previous step. Some schemes may include contributions from the previous two or three steps. While these methods have a lower error, they are not self-starting. As such, they are often used in conjunction with a single-step method as a predictor–corrector pair or require a "special" starting sequence.

Predictor-Corrector Methods – These methods combine the single-step and multi-step techniques (Tedesco et al., 1999). The predictor is a single step method used to compute the first few points then a multi-step algorithm is used from these points to determine the next point more accurately. This process can be used to start the multi-step method or can be employed continuously as the single step is usually faster than multi-step methods switching where the response is more abrupt.

Choosing the numerical integration schemes for a given problem is somewhat subjective given the vast number of schemes available today. For the purpose of this work, three schemes were chosen for evaluation: The Central Difference method, The Newmark method and The Wilson Θ method.

Selection of these methods was a choice of the author. The Central Difference method was chosen because of its simplicity and ease of implementation and to evaluate the speed and accuracy of an explicit method compared to the implicit methods. The Newmark Beta method (referred to as Newmark for the remainder of the text) is the primary integration technique used in commercial Finite Element Analysis (FEA) packages such as ANSYS and ADINA. The Wilson Θ method was found while researching integration schemes. It has similar characteristics to the Newmark method and is discussed in several books including Bathe and Tedesco, McDougal and Ross (Bathe, 1996; Tedesco *et al.*, 1999). The primary difference between the Wilson method and the Newmark method is that the Wilson method is based on a linear variation in acceleration while the Newmark method employs a constant average acceleration. Clough (Clough & Penzien, p330, 1993) suggests that the linear acceleration method is more accurate than the constant average method. In the ADINA theory manual, Bathe indicates that the Wilson Θ method is not suitable for certain types of elements such as multi-layered shell elements. In this work, only 1D link, friction, damping and contact elements are used so this integration technique is applicable.

Additional consideration should be given to the numerical stability of the methods. Texts such as Bathe and others in the bibliography discuss the stability of the numerical methods chosen for consideration in this thesis.

The equation of motion forms the backbone of the analysis being performed. Equation 3.2.1 shows the equation of motion at time = t. If the initial and boundary conditions are known, then the initial acceleration can be computed from equation 3.2.1 at time t=0 shown in equation 3.2.2.

$$[M]\{{}^{t}\ddot{x}\}+[C]\{{}^{t}\dot{x}\}+[K]\{{}^{t}x\}=\{{}^{t}R\} \quad 3.2.1$$

$$\{{}^{t=0}\ddot{x}\}=[M]^{-1}\left(\{{}^{t=0}R\}-[K]\{{}^{t=0}x\}-[C]\{{}^{t=0}\dot{x}\}\right) \quad 3.2.2$$

The calculation of the initial acceleration can be used to start any of the following methods.

3.2.1 Central difference method

The central difference method was chosen as a representation of an explicit method but also as a common integration method used in commercial codes. Simplicity makes it popular for many numerical integration requirements, however, not without trade-offs. Central Difference is based on substitution of the first and second displacement derivatives with the Newton central difference approximation. Re-writing the equation of motion with these approximations provides the future displacement in terms of the current and previous displacements. A partial derivation is in Appendix C. The Central Difference method is more sensitive to time step size than implicit methods and is not well suited for stiff differential equations. In the wave propagation analysis considered in this thesis, nonlinearity comes from friction and contact. The behaviour is very discontinuous and represents a severe nonlinearity. In theory, implicit codes with equilibrium iterations are better suited to handle such system behaviour.

3.2.1.1 Linear derivation

Typically in FEA, the equation being solved is $[K]\{x\}=\{R\}$, where $[K]$ is the global stiffness matrix, $\{x\}$ is the nodal displacement vector and $\{R\}$ is the applied load vector. From the central difference method, the equation being solved is $[M_{eff}]\{x\}=\{R_{eff}\}$. The linear central difference method takes the following form:

$$\left(\frac{[M]}{\Delta t^2}+\frac{[C]}{2\Delta t}\right)\{{}^{t+\Delta t}x\}=\{{}^{t}R\}-\left([K]-\frac{2[M]}{\Delta t^2}\right)\{{}^{t}x\}-\left(\frac{[M]}{\Delta t^2}-\frac{[C]}{2\Delta t}\right)\{{}^{t-\Delta t}x\} \quad 3.2.3$$

Bathe et al present a method of implementing the central difference, which demonstrates that no matrix inversions are required, with lumped mass and damping, the method performs a series of matrix and vector multiplications. However, since JIFEA has efficient storage and solution techniques and includes damping, the full method is employed. Normally the presence of the

damping matrix requires the full method (Bathe, p771, 1996). In this case, the damping elements connect the pipe nodes to ground. This creates a diagonal damping matrix similar to that of the lumped mass matrix so the full implementation is not required. Use of the concise Central Difference method would only reduce the number of operations by approximately a factor of two. The Central Difference method requires a much smaller step size than the implicit methods thus the advantage may be lost for this model. The verification case required a step size 10 times smaller than the implicit methods.

Time step size

An important consideration of using an explicit method is time step size Δt. If the time step is too large then the solution is likely to be erroneous and/or unstable. The basis for choosing a suitable time step is to consider the application and expected response characteristics. Normally the time step is chosen smaller than the shortest natural frequency, however, when a 1D analysis of a bar is performed with lumped mass assumptions and no damping, the ideal time step size is the critical step size (equation 3.2.4) (Bathe, p815, 1996). Using the central difference method in this case with the ideal effective element length yields the exact wave propagation solution. Bathe and Tedesco, McDougal and Ross both discuss the critical time step size and the effective element length (Tedesco et al., 1999). Bathe suggests using the natural frequency (natural period) as the critical time step in the following manner:

$$\Delta t \le \Delta t_{crit} = \frac{T_N}{\pi}, \qquad \text{where } T_N \text{ is the system natural period} \qquad 3.2.4$$

The analysis will capture the natural frequency of the system but higher frequencies are lost. If higher frequency response is desired then the step size must be smaller.

Element length

The effective element length is also a function of the natural period. A wave with a wavelength of 10 mm would not be captured by elements 500 mm in length. As a general rule of thumb, Bathe suggests that the element length be no less than $1/10^{th}$ the wavelength of interest (ANSYS suggests $1/20^{th}$). The solution time becomes very large if high frequency response is desired because of the number of elements combined with the time step size. The element length requirement can be thought of as an analog to digital conversion. A sine wave cannot be adequately described with 3 points. However, it can be reasonably modelled with 10 points and better with 20 points. Bathe suggests that the effective length of an element should be the wave speed in the given material times the time step size.

3.2.1.2 Nonlinear derivation

The primary difference in the nonlinear and linear derivations is the calculation of the element's internal forces. In equation 3.2.5, the stiffness matrix can no longer be multiplied by the nodal displacements to obtain the force because the stiffness itself is a function of the displacement. Therefore, equation 3.2.1 is written as:

$$\left(\frac{[M]}{\Delta t^2}+\frac{[C]}{2\Delta t}\right)\left\{{}^{t+\Delta t}x\right\}=\left\{{}^{t}R\right\}+\frac{2[M]}{\Delta t^2}\left\{{}^{t}x\right\}-\left(\frac{[M]}{\Delta t^2}-\frac{[C]}{2\Delta t}\right)\left\{{}^{t-\Delta t}x\right\}-\left\{{}^{t}F\right\} \qquad 3.2.5$$

$\left\{{}^{t}F\right\}$ is defined as the element's internal forces at time t. The internal force is calculated from the nonlinear effects and is updated at every time step. Since the displacement at time t is known, this method equates to a simple forward marching in time. Depending on the nature of the nonlinearity, the time step size may have to be much smaller than the critical time step discussed above.

3.2.2 Newmark method

The first and principle implicit method of interest is the Newmark method. Based on a constant average acceleration, the equations forming the method are used to directly increment time steps in linear problems or with the addition of equilibrium iterations for incremental nonlinear analysis. As mentioned earlier, if desired, the acceleration, $\{\ddot{x}\}$, can either be assumed zero or calculated at $t=0$ using equation 3.2.2. The Newmark method performs well for the verification case whether the initial acceleration is specified or assumed zero.

3.2.2.1 Linear derivation

The Newmark method is a multi-step semi-implicit method designed to solve second order differential equations extending the constant average acceleration assumption. The multi-step aspect comes from the use of the displacement, velocity and acceleration at the previous time step. The velocity and acceleration are essentially from solutions of displacement further back in time.

Newmark Beta is the second "version" of Newmark's method. The notation used in this derivation is taken from Bathe (Bathe, 1996). The following assumptions are used:

$$\left\{{}^{t+\Delta t}\dot{x}\right\}=\left\{{}^{t}\dot{x}\right\}+\left[(1-\delta)\left\{{}^{t}\ddot{x}\right\}+\delta\left\{{}^{t+\Delta t}\ddot{x}\right\}\right]\Delta t \qquad 3.2.6$$

$$\left\{{}^{t+\Delta t}x\right\}=\left\{{}^{t}x\right\}+\left\{{}^{t}\dot{x}\right\}\Delta t+\left[\left(\frac{1}{2}-\alpha\right)\left\{{}^{t}\ddot{x}\right\}+\alpha\left\{{}^{t+\Delta t}\ddot{x}\right\}\right]\Delta t \qquad 3.2.7$$

When $\delta = {}^1/_2$ and $\alpha = {}^1/_6$ the above equations produce the linear acceleration method and when $\delta = {}^1/_2$ and $\alpha = {}^1/_4$ the above equations produce the constant average acceleration method (trapezoid rule) (Clough & Penzien, 1993). The parameters are chosen for speed, accuracy and stability of the integration method. Newmark is unconditionally stable (solution does not grow unbounded for given time step size) when $\delta \geq {}^1/_2$ and $\alpha \geq {}^1/_4$. The parameters are often set for specific types or classes of problems. For 1D wave propagation, the integration parameters are set to mimic the constant-average-acceleration method.

Unlike the Central Difference method, the equation of motion is considered at time $t + \Delta t$. The full derivation is in Appendix D.

$$[M]\{{}^{t+\Delta t}\ddot{x}\} + [C]\{{}^{t+\Delta t}\dot{x}\} + [K]\{{}^{t+\Delta t}x\} = \{{}^{t+\Delta t}R\} \qquad 3.2.8$$

This method is implemented in both ANSYS and ADINA commercial FEA codes. During the implementation, one feature to note is that the Newmark method requires fewer vector calculations per step than the Wilson method. However, the Wilson method seems to provide a more accurate solution, especially the velocity and acceleration components. In the Verification section comparisons between the various methods and the analytical solution are shown.

3.2.2.2 Nonlinear derivation

In order to develop the nonlinear variation of the Newmark integration scheme two factors must be considered. First, the stiffness matrix, $[K]$, is now a function of the displacement, $\{x\}$. Second, the system needs to be solved incrementally in order to determine equilibrium at any given time step. There are several techniques that can be employed to perform the equilibrium iterations, however, the following derivation uses the full Newton–Raphson method. The discussion on the Newton–Raphson method shows a variation on the full method.

Equation 3.2.8 can be modified to allow for an incremental approach necessary for implementing the full Newton-Raphson iteration technique.

$$[M]\{{}^{t+\Delta t}\ddot{x}\} + [C]\{{}^{t+\Delta t}\dot{x}\} + \left[{}^{t+\Delta t}K^{(k-1)}\right]\{\Delta x^{(k)}\} = \{{}^{t+\Delta t}R\} - \{{}^{t+\Delta t}F^{(k-1)}\} \qquad 3.2.9$$

And with the relationship:

$$\{{}^{t+\Delta t}x^{(k)}\} = \{{}^{t+\Delta t}x^{(k-1)}\} + \{\Delta x^{(k)}\} \qquad 3.2.10$$

Several texts including Bathe take α = 0.25 and δ = 0.50. By using these values, the terms in the equations simplify yielding the constant-average acceleration method. Bathe's derivation of the nonlinear Newmark method is based on the constant-average method, dropping the integration coefficients and only uses the modified Newton-Raphson method (Newton method). However, some codes such as ANSYS use slightly different default values (α = 0.250625 and δ = 0.5050) (*Ansys theory manual*, 2003) for these coefficients. The following derivation keeps the general format for the equations with the full Newton method. The entire derivation is in Appendix D.

$$\left\{{}^{t+\Delta t}\ddot{x}^{(k)}\right\} = a_0\left(\left\{{}^{t+\Delta t}x^{(k-1)}\right\} - \left\{{}^{t}x\right\} + \left\{\Delta x^{(k)}\right\}\right) - a_2\left\{{}^{t}\dot{x}\right\} - a_3\left\{{}^{t}\ddot{x}\right\} \qquad 3.2.11$$

$$\left\{{}^{t+\Delta t}\dot{x}^{(k)}\right\} = \left\{{}^{t}\dot{x}\right\} + a_6\left\{{}^{t}\ddot{x}\right\} + a_7\left\{{}^{t+\Delta t}\ddot{x}^{(k)}\right\} \qquad 3.2.12$$

The final form of the nonlinear Newmark method is:

$$\left[K_{eff}\right]\left\{\Delta x^{(k)}\right\} = \left\{{}^{t+\Delta t}R_{eff}\right\} \qquad 3.2.13$$

$$\left[K_{eff}\right] = a_0[M] + a_1[C] + \left[{}^{t+\Delta t}K^{(k-1)}\right] \qquad 3.2.14$$

$$\begin{aligned}\left\{{}^{t+\Delta t}R_{eff}\right\} &= \left\{{}^{t+\Delta t}R\right\} - \left\{{}^{t+\Delta t}F^{(k-1)}\right\} - \\ &[M]\left(a_0\left(\left\{{}^{t+\Delta t}x^{(k-1)}\right\} - \left\{{}^{t}x\right\}\right) - a_2\left\{{}^{t}\dot{x}\right\} + a_3\left\{{}^{t}\ddot{x}\right\}\right) - \\ &[C]\left(a_1\left(\left\{{}^{t+\Delta t}x^{(k-1)}\right\} - \left\{{}^{t}x\right\}\right) - a_4\left\{{}^{t}\dot{x}\right\} - a_5\left\{{}^{t}\ddot{x}\right\}\right)\end{aligned} \qquad 3.2.15$$

Note that these equations are very similar to the linear counterpart except that the displacement is in terms of the incremental displacement and the internal element force $\{F\}$ has been added to resolve equilibrium. This describes the full Newton-Raphson technique. A modified Newton method is also presented later in the text.

3.2.3 Wilson Θ method

The Wilson Θ method is very similar in implementation to the Newmark method. It is an implicit method that has an integration parameter (Θ) that acts to relax the computations controlling stability. Fundamentally, it is based on the linear acceleration method (Θ = 1). The advantage over the standard linear acceleration method is that for Θ ≥ 1.37 the Wilson method is unconditionally stable (Bathe, p777, 1996; Clough & Penzien, p331, 1993).

3.2.3.1 Linear derivation

The following equations describe the acceleration, velocity and displacement at time $= t + \tau$ in Bathe's notation (Bathe, p777, 1996).

$$\{^{t+\tau}\ddot{x}\} = \{^{t}\ddot{x}\} + \frac{\tau}{\theta\Delta t}\left(\{^{t+\theta\Delta t}\ddot{x}\} - \{^{t}\ddot{x}\}\right) \quad 3.2.16$$

$$\{^{t+\tau}\dot{x}\} = \{^{t}\dot{x}\} + \{^{t}\ddot{x}\}\tau + \frac{\tau^2}{2\theta\Delta t}\left(\{^{t+\theta\Delta t}\ddot{x}\} - \{^{t}\ddot{x}\}\right) \quad 3.2.17$$

$$\{^{t+\tau}x\} = \{^{t}x\} + \{^{t}\dot{x}\}\tau + \frac{1}{2}\{^{t}\ddot{x}\}\tau^2 + \frac{\tau^3}{6\theta\Delta t}\left(\{^{t+\theta\Delta t}\ddot{x}\} - \{^{t}\ddot{x}\}\right) \quad 3.2.18$$

Notice that the acceleration is a linear interpolation assuming $0 \le \tau \le \theta\Delta t$. The velocity is the integration of the acceleration with respect to τ and the displacement is then determined by integrating the velocity. This method is based on solving the system at $t+\theta\Delta t$. The load vector uses a linear extrapolation to get the load at $t+\theta\Delta t$.

$$[M]\{^{t+\theta\Delta t}\ddot{x}\} + [C]\{^{t+\theta\Delta t}\dot{x}\} + [K]\{^{t+\theta\Delta t}x\} = \{^{t+\theta\Delta t}\overline{R}\} \quad 3.2.19$$

$$\{^{t+\theta\Delta t}\overline{R}\} = \{^{t}R\} + \theta\left(\{^{t+\Delta t}R\} - \{^{t}R\}\right) \quad 3.2.20$$

The rest of the derivation is in Appendix E.

3.2.3.2 Nonlinear derivation

The derivation of the nonlinear Wilson method is in Appendix E. The nonlinear concepts were taken from Bathe. Similar derivations are found in other texts such as Tedesco (Tedesco et al., 1999). Bathe's discussion of the nonlinear implicit schemes uses the trapezoid rule (simplification of Newmark) in the derivation (Bathe, p826, 1996). The full Wilson derivation is completed here to implement the method in JIFEA. The behaviour of the Wilson method is similar to Newmark but marginally slower for the same step size. Using the full Newton iteration, the Wilson method can be expressed as:

$$\{^{t+\theta\Delta t}x^{(k)}\} = \{^{t+\theta\Delta t}x^{(k-1)}\} + \{\Delta x^{(k)}\} \quad 3.2.21$$

$$\{^{t+\theta\Delta t}\ddot{x}^{(k)}\} = \frac{6}{\theta^2\Delta t^2}\left(\{^{t+\theta\Delta t}x^{(k)}\} - \{^{t}x\}\right) - \frac{6}{\theta\Delta t}\{^{t}\dot{x}\} - 2\{^{t}\ddot{x}\}$$

$$\{^{t+\theta\Delta t}\ddot{x}^{(k)}\} = \frac{6}{\theta^2\Delta t^2}\left(\{^{t+\theta\Delta t}x^{(k-1)}\} + \{\Delta x^{(k)}\} - \{^{t}x\}\right) - \frac{6}{\theta\Delta t}\{^{t}\dot{x}\} - 2\{^{t}\ddot{x}\} \quad 3.2.22$$

$$\left\{{}^{t+\theta\Delta t}\dot{x}^{(k)}\right\}=\frac{3}{\theta\Delta t}\left(\left\{{}^{t+\theta\Delta t}x^{(k)}\right\}-\left\{{}^{t}x\right\}\right)-2\left\{{}^{t}\dot{x}\right\}-\frac{\theta\Delta t}{2}\left\{{}^{t}\ddot{x}\right\}$$

$$\left\{{}^{t+\theta\Delta t}\dot{x}^{(k)}\right\}=\frac{3}{\theta\Delta t}\left(\left\{{}^{t+\theta\Delta t}x^{(k-1)}\right\}+\left\{\Delta x^{(k)}\right\}-\left\{{}^{t}x\right\}\right)-2\left\{{}^{t}\dot{x}\right\}-\frac{\theta\Delta t}{2}\left\{{}^{t}\ddot{x}\right\} \qquad 3.2.23$$

The main difference in computational effort between Wilson and Newmark is the number of vector calculations that take place every time step. The linear extrapolation adds a few extra operations as does calculating displacement from the equation of motion at time $t+\theta\Delta t$. The following three equations show the equation of motion solved at $t+\theta\Delta t$.

$$\left[{}^{t+\theta\Delta t}K_{eff}\right]=\left[{}^{t+\theta\Delta t}K^{(k-1)}\right]+a_0[M]+a_1[C] \qquad 3.2.24$$

$$\left\{{}^{t+\theta\Delta t}R_{eff}\right\}=\left\{{}^{t}R\right\}+\theta\left(\left\{{}^{t+\Delta t}R\right\}-\left\{{}^{t}R\right\}\right)-$$
$$[M]\left(a_0\left(\left\{{}^{t+\theta\Delta t}x^{(k-1)}\right\}-\left\{{}^{t}x\right\}\right)-a_2\left\{{}^{t}\dot{x}\right\}-2\left\{{}^{t}\ddot{x}\right\}\right)- \qquad 3.2.25$$
$$[C]\left(a_1\left(\left\{{}^{t+\theta\Delta t}x^{(k-1)}\right\}-\left\{{}^{t}x\right\}\right)-2\left\{{}^{t}\dot{x}\right\}-a_3\left\{{}^{t}\ddot{x}\right\}\right)$$

Such that the final form is

$$\left[{}^{t+\theta\Delta t}K_{eff}\right]\left\{\Delta x^{(k)}\right\}=\left\{{}^{t+\theta\Delta t}R_{eff}\right\}-\left\{{}^{t+\theta\Delta t}F^{(k-1)}\right\} \qquad 3.2.26$$

Since $\{R_{eff}\}$ and $\{F\}$ are at time $t+\theta\Delta t$, the calculation of $\{\Delta x\}$ produces displacements at time $t+\theta\Delta t$. These displacements are then used to calculate velocity and acceleration at time $t+\theta\Delta t$ for each equilibrium iteration.

The acceleration, velocity and displacement at $t+\Delta t$ must be calculated using the kinematics calculated at $t+\theta\Delta t$ for each time step. Clough's statement that the linear acceleration scheme is more accurate is supported by the verification tests performed here. (see Verification section). An important consideration in this method is that equilibrium is sought for time $t+\theta\Delta t$ then the displacement, velocity and acceleration results interpolated to $t+\Delta t$.

3.3 Model Features

Since the focus of this work is to understand the solution strategies of nonlinear systems, it is necessary to review the components that add

nonlinearity to the system and the mechanisms to solve them. Subsequently the numerical techniques and their respective controls will be reviewed.

3.3.1 Newton–Raphson method for nonlinear equilibrium

As mentioned previously, the Newton-Raphson or Newton method is an iterative technique used to determine the equilibrium of the system. For the static linear solution of an FEA system, equation 3.3.1 is solved. The time shown on the load vector in a static analysis is just a convenient variable to allow for different load steps. In a dynamic analysis, time would truly represent time.

$$[K]\{x\}=\{{}^{t}R\} \qquad 3.3.1$$

The Newton method requires balance between the external forces and the internal forces as shown in equation 3.3.2. Bathe (Chapter 6) describes, in detail, the computation of the internal forces. In this case, the determination of internal forces is straightforward as the link element has no nonlinear properties. The friction and contact elements are handled more carefully and are discussed later in this section.

$$\begin{aligned} \{{}^{t}R\}&=\{{}^{t}F\} \\ \{{}^{t}R\}-\{{}^{t}F\}&=0 \end{aligned} \qquad 3.3.2$$

The full Newton method uses an iterative approach in solving equation 3.3.1 as shown in equation 3.3.3.

$$[{}^{t}K^{(k-1)}]\{\Delta x^{(k)}\}=\{{}^{t}R\}-\{{}^{t}F^{(k-1)}\} \qquad 3.3.3$$

With the relation:

$$\{{}^{t}x^{(k)}\}=\{{}^{t}x^{(k-1)}\}+\{\Delta x^{(k)}\} \qquad 3.3.4$$

Several texts on nonlinear analysis or numerical analysis, such as Bathe (Bathe, 1996), show the complete derivation, rate of convergence and stability for the Newton method. The appeal of the full Newton method is the quadratic rate of convergence.

The modified Newton method simplifies the solution process by only updating the stiffness matrix at each time step rather than at each equilibrium iteration.

$$[{}^{t}K]\{\Delta x^{(k)}\}=\{{}^{t}R\}-\{{}^{t}F^{(k-1)}\} \qquad 3.3.5$$

For systems that do not exhibit severe nonlinearities, a modified method may be preferred. Systems that have severe nonlinearities generally require the full method for good convergence rates and accuracy.

For either the full or the modified methods, the following initial conditions are used.

$$\left\{{}^{t+\Delta t}x^{(0)}\right\}=\left\{{}^{t}x\right\} \qquad 3.3.6$$

$$\left[{}^{t+\Delta t}K^{(0)}\right]=\left[{}^{t}K\right] \qquad 3.3.7$$

$$\left\{{}^{t+\Delta t}F^{(0)}\right\}=\left\{{}^{t}F\right\} \qquad 3.3.8$$

3.3.2 Friction element

Friction is the primary nonlinear feature of the wave propagation problem. Friction elements are connected to every node to resist motion over the length of the model. The friction element is depicted in Figure 3..

Using a true stick-slip description causes severe nonlinear behaviour and can contribute to oscillations in the response. To help smooth the response an alternate element is formulated. Figure 3.3 shows the response used for the friction element. Initially, when the element is defined, there is a known displacement between node i and node j. The stiffness of the friction element is defined by the maximum friction force and a tolerable amount of displacement. This displacement is referred to as the critical displacement as any amount of displacement over this limit is defined as slipping. Evaluating the incremental displacement provides the indication of direction.

As the element is loaded in tension, the two nodes move apart such that the response is along the sloped part of the friction curve until the critical displacement is reached. Then, as the incremental displacement passes the critical displacement, the element switches behaviour modes from sticking to slipping. If the incremental displacement continues to increase, the element continues to slip. When the incremental displacement changes direction, this indicates that the incremental load has dropped below the maximum force and the element unloads along the sloped portion of the friction curve. The behaviour of this element is analogous to elastic-perfectly plastic material characteristics. Maximum friction force is used in place of the yield stress and the friction stiffness F_{max} / U_{crit} is used for the elastic modulus. The amount of slip that occurs is similar to the plastic strain. Therefore, this friction element is described in terms of force and displacement instead of stress and strain. JIFEA assumes node N_j is "ground" so the displacement is always zero. This simplifies the computation of the slip between the nodes.

3.3.3 Friction distribution

The friction data provided by most drilling operators is very limited. Though techniques exist to measure the hole-drag accurately, cost, time and lack of requirement typically means the total friction is measured as the difference between the string weight and the force required to insert or extract the drilling assembly from the well. A distribution of the total friction (hole-drag) was needed to define the friction acting in each friction element. A rationalization was created to take the total friction and distribute it using several factors: the length of the string, the size (diameter) of the string and the inclination of the string from vertical. Each of these factors was used to create a weighted distribution. The effects were normalized to ensure the total sum of the ratios equalled one (total friction was not exceeded).

The following system was used to distribute the total friction:

$$R_{L_i} = \frac{PipeLength_i}{TotalAssemblyLength} \qquad 3.3.9$$

$$R_{D_i} = \frac{PipeDiameter_i}{MinAssemblyDiameter} \qquad 3.3.10$$

$$R_{I_i} = 1 + \sin(\theta_i) \qquad 3.3.11$$

$$R_i = \frac{R_{L_i} \times R_{D_j} \times R_{I_i}}{\sum_{i=1}^{n} \left(R_{L_i} \times R_{D_j} \times R_{I_i} \right)} \qquad 3.3.12$$

$Friction_i = R_i \times TotalFriction$ yielding friction per element 3.3.13

The index, *i*, specified is the pipe number and "*n*" is the total number of pipes. It could be altered to work over the number of elements but JIFEA will work in conjunction with the Jar placement program previously written, (see Appendix F) so the simplification will be employed. The previous placement software uses a basic summation of forces to provide an operation range. JIFEA is then used to find the optimal location within the range.

In the above formulas, R_L is the length ratio, R_D is the diameter ratio and R_I is the inclination ratio (zero is vertical). The length is a linear distribution of the total hole-drag along the length of the string. The diameter ratio penalizes the pipe for having a large diameter. This concentrates more friction along the larger diameter pipe. The use of the inclination ratio essentially maps some of the directional effects from curved wells onto the 1D model. Intuitively, the pipe lying on its side in a horizontal section will have more friction than a pipe in a straight vertical section of the hole. The ratio used is simplistic but

comparisons between crudely field-measured hole-drag and this distribution indicated reasonable agreement.

The friction can be evenly divided over the elements that make up the pipe. For example, the number of pipes in a 2000 m well is typically 200. If each pipe is divided into 10 elements the friction is first calculated for a specific pipe then evenly distributed over each element. The friction applied in the friction element will encompass half the friction from each adjoining element. Figure 3.4 shows how the friction is taken half from each adjacent element to form the total friction applied to the friction element. The left-leaning hatched (orange) region represents half of the friction on the left element and the right-leaning hatched (green) region is half the friction on the right element. The distribution is left over the pipe length rather than element length since actual Jar placement analysis typically uses very few elements to represent the pipe length.

The model is assembled such that no friction is applied to constrained nodes or to nodes that extend beyond the well (free end).

3.3.4 Axial contact element

The Jar is represented in the model by a simple axial contact element (point-to-point) created using a penalty method (*Ansys theory manual*, 2003). The contact between two nodes is defined as $K_{pipe}/1000$ for out of contact and $1000*K_{pipe}$ when in contact. K_{pipe} is the stiffness of the base pipe where the Jar is placed, such as the drill collar. Using the small stiffness when out of contact reduces the severity of the nonlinearity but also enables this element to be used in static nonlinear analysis. An open gap in a static analysis creates a singular stiffness matrix and leads to rigid body motion. Figure 3.5 indicates the response used to capture the contact behaviour.

The contact element is visualized in Figure 3.6. The difference in the nodal displacement is compared to the specified gap size. When the difference in nodal displacement is less than the gap size the element uses the open stiffness otherwise uses the closed stiffness.

The element is defined such that the gap can open and close as the waves travel through the element but only carries a tensile load (no resistance to opening).

The presence of the contact element allows waves to propagate from the element creating a more natural waveform. The element lengths still dictate the incremental shape of the waves but the use of the contact element will improve the waveform. Many of the previously discussed alternate methods start with a square wave. The contact element enables the comparison between waveforms to test the validity of the square wave approximation.

The stiffness associated with the open and closed state of this element has been chosen somewhat arbitrarily. The magnitude of the stiffness will have an impact on the waveform and amplitude. Some sensitivity tests should be

performed to assess the effects that these stiffness values have on the final results.

3.3.5 Damping element

System damping is provided by an element similar in design to the link element. Rather than a load-displacement relationship it has a load-velocity relationship. The damping element is tied to each pipe node and to ground. Therefore, the relative velocity is that of the pipe node only. The element uses a constant damping coefficient per unit length and the velocity calculated from the numerical methods outlined previously. A brief derivation of the element is in Appendix A. Figure 3.7 shows a depiction of the damping element. The element acts as a dash-pot style damper.

The force generated by the damping element is directly proportional to the nodal velocity by the damping coefficient. Figure 3.8 shows the response curve of the damping element.

Other forms of damping such as material damping could be represented by this element with the appropriate damping coefficient and connecting the element to the appropriate nodes.

3.3.6 Numerical control parameters

The numerical methods presented have several parameters that can be altered to test the performance of JIFEA.

As mentioned in the Central Difference section, this method is usually employed when a lumped mass approximation is used and damping can be neglected. In this implementation the damping also forms a diagonal matrix so the Central Difference method could be efficiently employed to solve the system (Bathe, p771, 1996).

The application-specific FEA program (JIFEA) written for this thesis uses storage and solving systems specific to the 1D wave problem so no further changes were made. The method requiring a small time step size still exists. Since the storage and solver are efficient, the implicit methods actually solve faster because they don't require as small a time step. The time step was 10 times smaller for the Central Difference method to converge for the verification case.

The time step size, in combination with the integration parameters, provides control on the solution. The use of the full or modified Newton iteration provides additional control on the solution.

Sensitivity studies on these parameters and their effect on the wave propagation results will aid in finding the most efficient solution method.

3.4 Verification

Several components were included in JIFEA. Each was verified by comparing results to known solutions. The linear static solver was tested with a basic linear spring assembly and was proven to be correct. It is not discussed in detail because of its simplicity. The time integration schemes represent significantly more effort and were, therefore, evaluated against an analytical solution and two commercial finite element programs, ADINA and ANSYS. The friction and contact elements were compared to an analytical description.

3.4.1 Linear time integration

A basic linear problem was modelled to verify the time integration schemes. The analytical base case use was a vibration example (13.2) taken from "An Introduction to Mechanical Vibrations." (Steidel, p403, 1989). This example is similar to the model being considered in this thesis.

The problem is a rod fixed at one end with an initial strain then released at time t=0. Figure 3.9 shows the model considered in the example problem.

To test the analytical solution the parameters listed in Table 1 were used.

Table 1, Vibration example parameters used for verification model

Parameter	Value
Outside Diameter	0.1524 m
Inside Diameter	0.0508 m
Length	1.0 m
Area	0.0162 m^2
ρ (mass density)	7850 kg/m^2
E (elastic modulus)	2.05 e^{11} Pa
T (time)	.004 seconds
Δt (time step)	.02 milliseconds

The full analytical solution for this problem is in Appendix B. The final solution is repeated here as equation 3.4.1.

$$u(x,t)=\frac{8\varepsilon l}{\pi^2}\sum_{n=1,3,5,\cdots}^{\infty}\frac{(-1)^{\frac{n-1}{2}}}{n^2}\sin\frac{n\pi x}{2l}\cos\omega_n t$$

$$\dot{u}(x,t)=-\omega_n\frac{8\varepsilon l}{\pi^2}\sum_{n=1,3,5,\cdots}^{\infty}\frac{(-1)^{\frac{n-1}{2}}}{n^2}\sin\frac{n\pi x}{2l}\sin\omega_n t \qquad 3.4.1$$

$$\ddot{u}(x,t)=-\omega_n^2\frac{8\varepsilon l}{\pi^2}\sum_{n=1,3,5,\cdots}^{\infty}\frac{(-1)^{\frac{n-1}{2}}}{n^2}\sin\frac{n\pi x}{2l}\cos\omega_n t$$

A minimum of 25 terms was required to return the initially prescribed displacement (strain). For the comparison that follows, 50 terms of the series were used for the displacement, velocity and acceleration. The responses for each are shown for the free end of the bar in Figure 3.10, Figure 3.11 and Figure 3.12 respectively.

The next step is to compare the numerical solutions to those of the analytical solutions. An interesting observation to note is that in all the cases, the displacements agree well with the analytical solution, however, the velocity deviates somewhat and the accelerations are very different. Comparisons were made between solutions generated from ADINA and ANSYS to JIFEA velocity and acceleration results for verification. The solutions are taken from the free end of the model for all of the following comparisons.

The critical time step size and element length were computed in order to compare the results from the different numerical schemes.

Bathe suggests the following method for determining the discretization and time step size (Bathe, p772, 1996).

$$\Delta t \le \Delta t_{cr} = \frac{T_n}{\pi} \qquad 3.4.2$$

$$\Delta t = \frac{t_w}{n}, t_w = \frac{\lambda}{c} \qquad 3.4.3$$

$$L_{element} \le c\Delta t \qquad 3.4.4$$

Using these relationships, the following FEA parameters are calculated:

Table 2, FEA element length and time step size calculated from equations 3.4.4 to 3.4.6

Parameter	Value
Highest Frequency	20,000 Hz
T_n	0.00005 seconds
Δt_{cr}	0.0000159 seconds
λ	0.2555 m
t_w	0.00005 seconds
N	10
Δt	0.000005 seconds
$L_{element}$	0.02555 m

These conditions also produce a ratio between the element length and time step in the order of the wave speed.

$$R_c = \frac{L_{element}}{\Delta t} = \frac{0.02555}{0.000005} = 5110 \text{ m/s} \qquad 3.4.5$$

If we assume 10 steps in time and space are required, then, as the ratio shows, the wave speed relationship is maintained. To ensure accuracy of both time and space, this ratio must be in the order of the wave speed. A course discretization in space (large element size) cannot capture the short wavelengths and similarly, a large time step cannot capture a short period.

The requirement of the "true waveform" shape may not be necessary. What is important to capture in this model is the wave speed, the force amplitude and wavelength. Attempting to capture a true waveform as is reasonably possible should ensure that the speed, force magnitude and length are accurately computed.

3.4.1.1 Central difference verification

Table 3 lists the time step and element length actually used in the analysis.

Table 3, FEA time step size and element length used for the central difference simulation of the vibration example

Parameter	Value
Δt	1.0e-7 seconds
$L_{element}$	0.001 m

Figure 3.13 shows the linear Central Difference FEA results with the displacement analytical results (equation 3.4.1). There is good agreement between the two central difference methods and the analytical response. An interesting effect is the time step required. As listed above, the element size used was considerably smaller than the calculated size. The consequence of making the element size so small was that the time step had to be reduced to 1e-7 s in order to gain convergence. With a time step of 5e-6 s, the solution was very unstable. Based on the ratio in equation 3.4.5, the ideal time step is 1.96e-7 s. This was done to verify that the ratio of element length to time step size is a requirement of the analysis. Due to the smaller time step size, this model was only run to a final time of 0.0008 seconds.

The Central Difference response of the velocity shows reasonable agreement with the analytical response. Figure 3.14 shows the linear and nonlinear central difference results compared to the analytical solution. The nonlinear implementation was used though no nonlinear elements are present to ensure the solution was generated with one equilibrium iteration. The overall solution time had to be reduced to show the results because of the very large number of small time steps.

The accelerations in Figure 3.15 indicate the linear and nonlinear results have a similar trend with the analytical result but the oscillations and amplitude of the numerical results make the analytical solution appear almost flat.

3.4.1.2 Newmark verification

Using the values listed in Table 4, the linear and nonlinear Newmark methods were evaluated. Figure 3.16 shows the Newmark response compared to the analytical results. The figure shows the displacement field is computed accurately. The linear Newmark response curve is completely hidden by the nonlinear curve. The nonlinear version is used to solve a linear system requiring only one equilibrium-iteration as expected.

Table 4, FEA time step size and element length used for Newmark and Wilson simulation of the vibration example

Parameter	Value
Δt	5.0e-6 seconds
$L_{element}$	0.001 m

Figure 3.17 shows the velocity response of the Newmark methods compared to the analytical response. The general trend of the solution seems reasonable but the response was expected to be closer. Comparisons made between ADINA and JIFEA later in the text show good agreement. JIFEA's results are therefore considered correct.
Figure 3.18 shows the acceleration response of the free end using the Newmark method. The trends agree well but the oscillations in the response may require some form of data smoothing or filtering. Later, comparisons between JIFEA and ADINA show good agreement in the response.

3.4.1.3 Wilson Θ verification

The Wilson method was tested using the same parameters as listed in Table 3 and compared to the analytical solution.

Figure 3.19 shows the displacement response of the free end using the Wilson method. Again, good agreement is found between the numerical results and the analytical solution. The response is somewhat different from the Newmark method specifically at the peaks.

Figure 3.20 shows good agreement between the Wilson velocity and the analytical solution.

Figure 3.21 indicates that the acceleration response of the Wilson method matches the analytical response closely with minimal oscillations. However, the peak amplitudes do not match as well. The response seems to exhibit some numerical decay. Different values for the time step or Θ may alter the response and provide a better result.

3.4.1.4 Commercial FEA software comparison

The acceleration results are somewhat questionable in the above results. The implementation of the results is believed to be correct otherwise it is unlikely the displacement and velocity results would be correct. To test the response of the system, additional comparisons between commercial programs ADINA and ANSYS were performed. Figure 3.22 shows the comparison between ANSYS, ADINA and JIFEA results. The responses denoted by "FEA" refer to JIFEA. The ANSYS and JIFEA Newmark and nonlinear Newmark all have very good agreement; however, the ADINA response shows slightly larger peaks. This indicates that JIFEA's implementation is sound.

As a final check, the accelerations between ADINA, ANSYS and JIFEA's Newmark methods (marked FEA) are shown in Figure 3.23.

Clearly, the implemented methods have the same trend as ADINA but the absolute magnitudes are different. ANSYS has the largest variation in response from the group. The problem with the commercial codes is that it may not be possible to completely turn off all the conditioning features. ANSYS does not provide the feature to export the Newmark velocity and acceleration directly. They are numerically calculated derivatives from the displacement field using a simple Newton-forward method. Using the same approach with the application-specific code produces results almost identical to ANSYS.

3.4.2 Friction behaviour

The friction behaviour was defined by the analytical description listed below.

$$\frac{\delta^2 u}{\delta x^2} = \frac{f_r}{AE} \qquad 3.4.6$$

$$\frac{\delta u}{\delta x} = \varepsilon = \frac{f_r}{AE}x + C \qquad 3.4.7$$

$$u = \frac{1}{2}\frac{f_r}{AE}x^2 + Cx + B \qquad 3.4.8$$

Then given the boundary conditions at x = 0, u = 0 and at x = L, $\varepsilon AE = R$.
The final equation for friction can be expressed as:

$$u(x) = \frac{1}{2}\frac{f_r}{AE}x^2 + \frac{R - f_r L}{AE}x \qquad 3.4.9$$

Where f_r is the friction per unit length,
L is the length,
A is the cross sectional area,
E is the elastic modulus,
R is the applied load,

x is the distance along the length and
u is the displacement.

Using this description of friction the analytical force is compared to the FEA results in Figure 3.24. The analytical solution line is hidden behind the FEA results line. A simple four link element model was created with a friction element attached to the middle of the model and tied to ground to further demonstrate the behaviour of the friction element. Figure 3.25 shows the FEA model used to demonstrate the friction element behaviour.

Table 5 lists the results used to generate Figure 3.24. To perform this FEA analysis, a static nonlinear solver with very small increments in load and large equilibrium convergence criteria was used. Tighter convergence criterion would have produced more accurate results.

Table 5, 4 link element distributed friction results

Element	Element Force (N)	Analytical Force (N)
1	44378.3	44822.2
2	177711.5	178155.5
3	311044.1	311488.9
4	444377.7	444822.2

The same FEA model used previously was used to perform a cyclic load friction test. The load R applied is ramped from 0 to 444822.2 N over 25 steps then unloaded to 0 N over the next 25 steps. From there, the load is decreased to -444822.2 N over 25 steps then returns to 0 N over the next 25 steps.

Figure 3.26 shows the response of the friction element (Node 3) over the load steps in black. The red line shows the applied load as a function of load steps as described above. Node 3 remains motionless (stuck) until almost load step 10. Then sufficient force is applied to cause the friction element to slip. At load step 25, the applied load begins to decrease at which point the friction element sticks and remains in this position until the force has changed enough to cause slippage again. The same type of stick-slip behaviour is seen at load step 75 where the applied load reaches -444822.2 N. This load cycle confirms the behaviour of the friction element.

3.4.3 Contact behaviour

A simple 5 node model was built to verify the contact element. The model is shown in Figure 3.27.

Table 6 lists the values used in the contact model. ANSYS was used to verify the response of the element.

Table 6, FEA gap size, tensile load and contact open and closed stiffness used to verify contact

Parameter	Value
Gap	0.25 m
R	444822.2 N
K_{open}	1.0e6
K_{closed}	1.0e16

Figure 3.28 shows the response of the contact elements nodes. The line labelled "Above contact element" indicates the displacement of the node above the gap (free side) and the line labelled "Below contact element" shows the response of the node where the pipe connects to ground (see Figure 3.27). The scale of the displacements for each node is several orders of magnitude apart as the displacement of the lower node (3) is very small. The change in node 4's response is because the gap closing adds significant stiffness to the system. The blue line indicates that the bottom node's displacement is linear with load. This is because of the weak spring used to eliminate rigid body movement. The force applied is transmitted through the contact element to the left part of the model. The remaining elements are linear link elements and therefore displace linearly.

The element agrees with the intended design. The force due to inertia (the wave) is considerably larger than the external force applied therefore the element response is satisfactory.

3.4.4 Damping behaviour

The response produced when using the damping elements showed the characteristic decay typical of dash-pot style damping. Figure 3.29 shows the decay of the free end of a simple 4 link element model with distributed damping. The model represents an assembly of pipe pre-stressed in tension then suddenly released.

3.5 Summary of Solution Strategies for Finite Element Analysis of Nonlinear Wave Propagation

JIFEA has demonstrated that application-specific FEA can be used to effectively and efficiently solve a nonlinear 1D wave propagation problem. Each factor contributing to the solution strategy was evaluated independently and shown to perform well. The matrix storage, the equation solver, the integration techniques and the elements themselves have all been independently evaluated to understand their impact on the solution speed and accuracy.

By using efficient matrix storage and solver, all the methods are very fast to solve the problem. However, because the Central Difference method requires a very small time step size, the Newmark and Wilson methods perform much better. They are just as accurate but do not require as small a step size. The Newmark and Wilson methods' step size was 5 times bigger than the required step size for convergence using the Central Difference method for the verification case.

The Newmark and Wilson methods are very similar in implementation but, for a given step size, the Wilson method was slightly slower with more accurate results. This is attributed to the increased number of vector computations per time step. More extensive testing between these methods varying the integration parameters and time step size is warranted.

All of the integration methods were tested against analytical and commercial packages ANSYS and ADINA and found to exhibit good agreement.

The elements used in the model were tested independently. The link, damping, friction and contact all performed as expected yielding the intended results. The emphasis of the element implementation was efficiency. Computational overhead was reduced as much as possible while maintaining accuracy. For example, the contact uses a weak spring across the gap when the gap is open. This reduces the severity of the nonlinear effects but still maintains accuracy. The friction element was handled similarly with a slight slope in the response rather than a true step function. Damping elements are straightforward to implement and produce the characteristic response decay.

The initial results indicate that with the appropriate choice of step size, element length (number of elements), integration parameters and iteration method, the wave propagation method can be solved directly using application-specific FEA. The performance will be comparable or better than commercial software with reasonable accuracy. Further testing by altering the parameters may indicate that this FEA approach may be even more efficient when the accuracy is allowed to decrease.

3.6 Chapter 3 figures

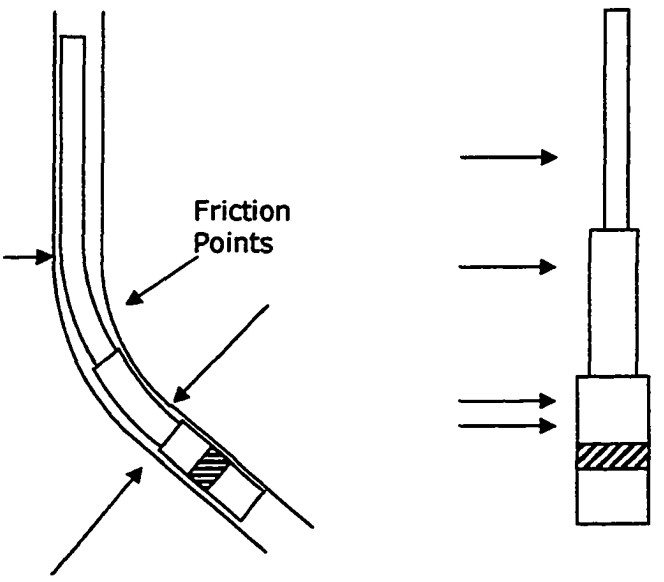

Figure 3.1, One dimensional representation of drilling assembly

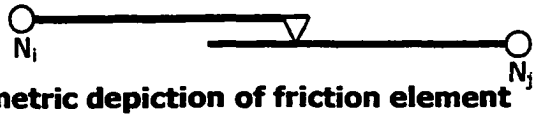

Figure 3.2, Geometric depiction of friction element

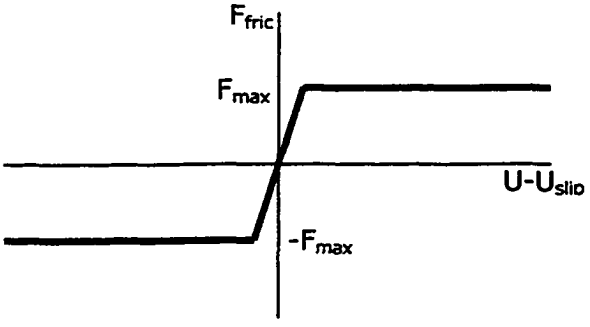

Figure 3.3, Friction force - displacement response curve

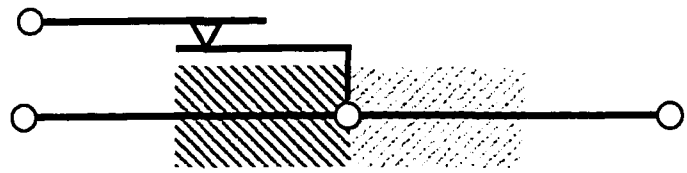

Figure 3.4, Friction distribution of adjacent elements

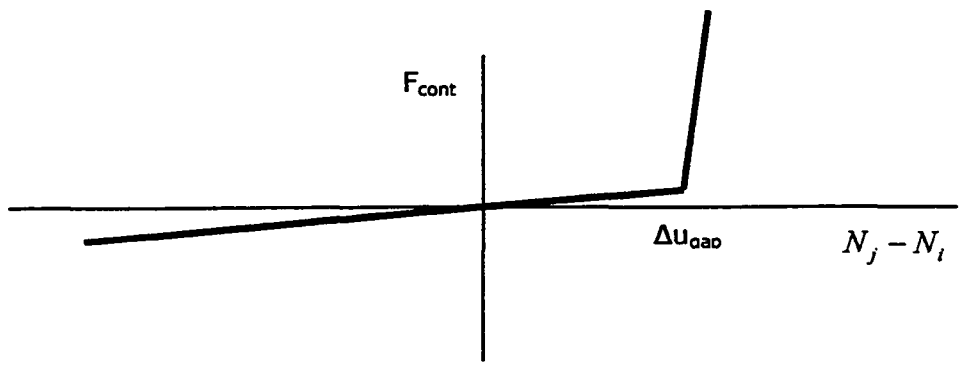

Figure 3.5, Contact element force-displacement response curve

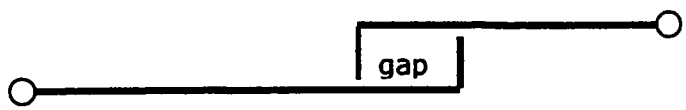

Figure 3.6, Contact element depiction with specified gap size

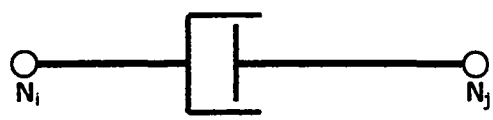

Figure 3.7, Dash-pot style damping element depiction

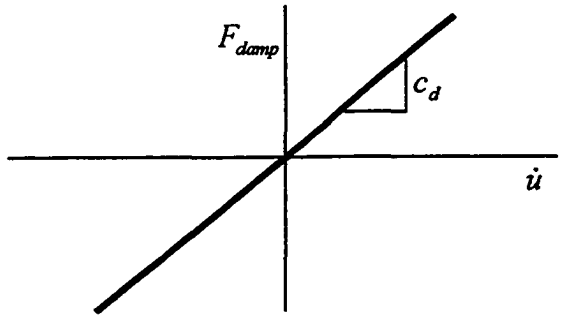

Figure 3.8, Damping element force-velocity response curve

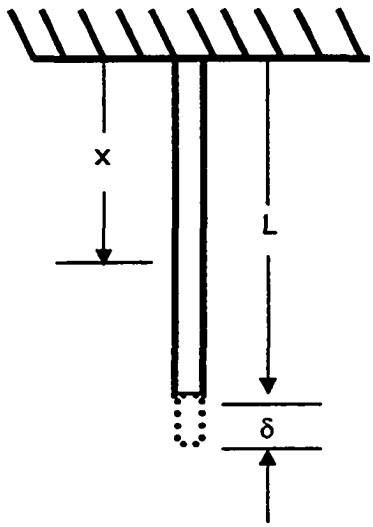

Figure 3.9, Graphical depiction of the example vibration problem (ex13.2)

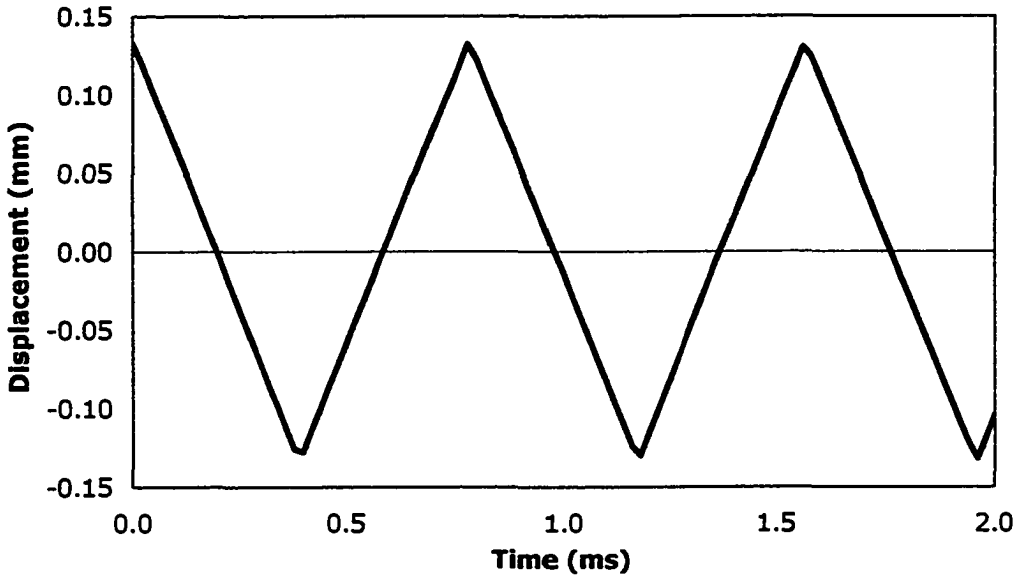

Figure 3.10, Vibration example verification model. Analytical displacement response for free end of bar after pre-stressed tension is released

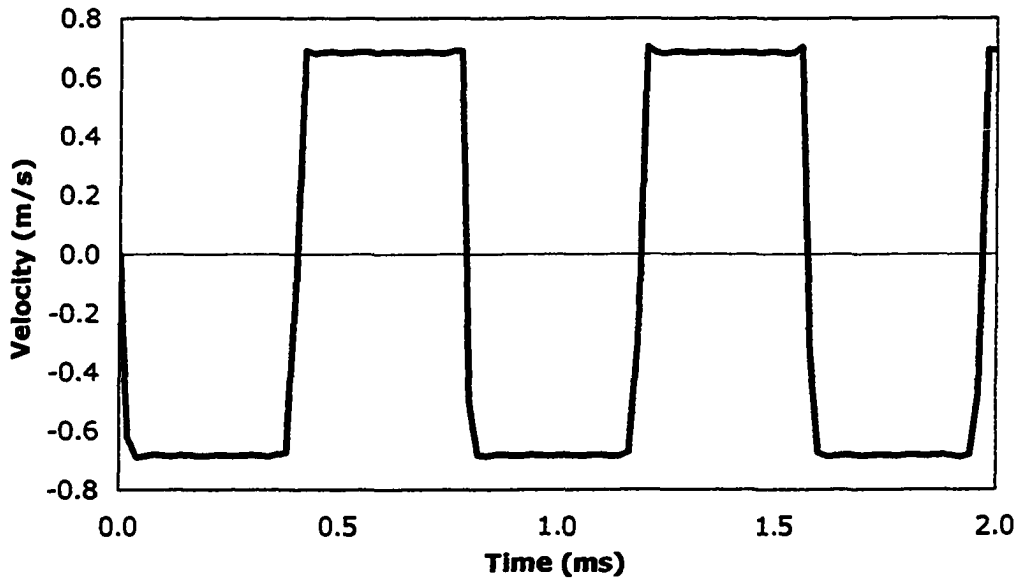

Figure 3.11, Vibration example verification model. Analytical velocity response for free end of bar after pre-stressed tension is released

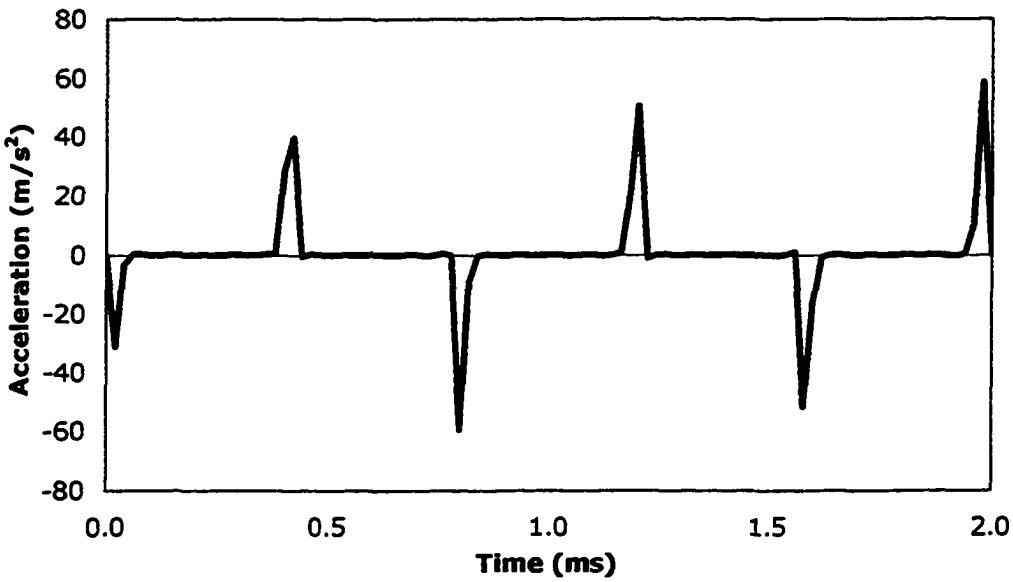

Figure 3.12, Vibration example verification model. Analytical acceleration response for free end of bar after pre-stressed tension is released

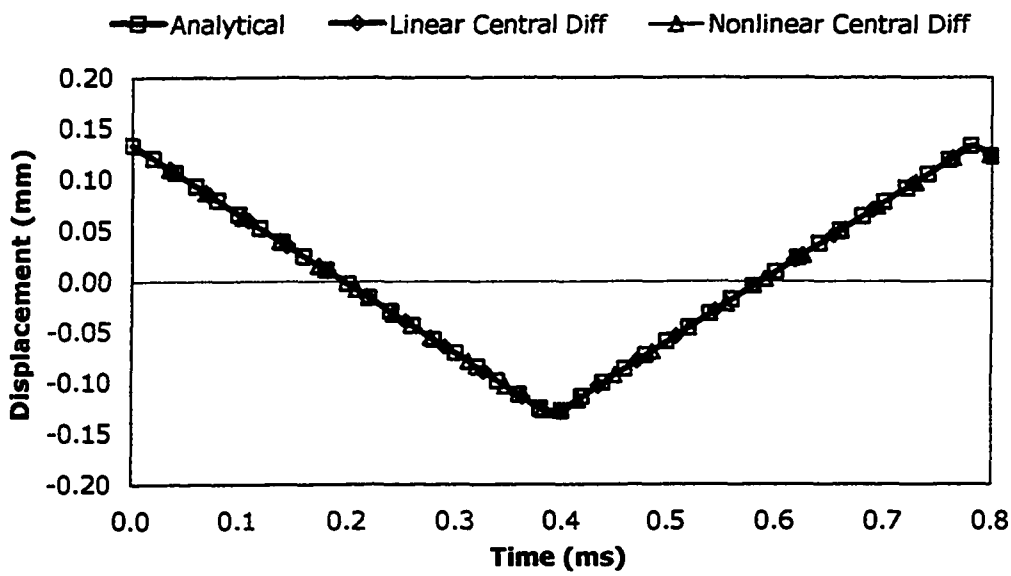

Figure 3.13, Comparison of linear and nonlinear Central difference displacement response to analytical displacement response of free end after release of pre-stressed tension for the vibration example model

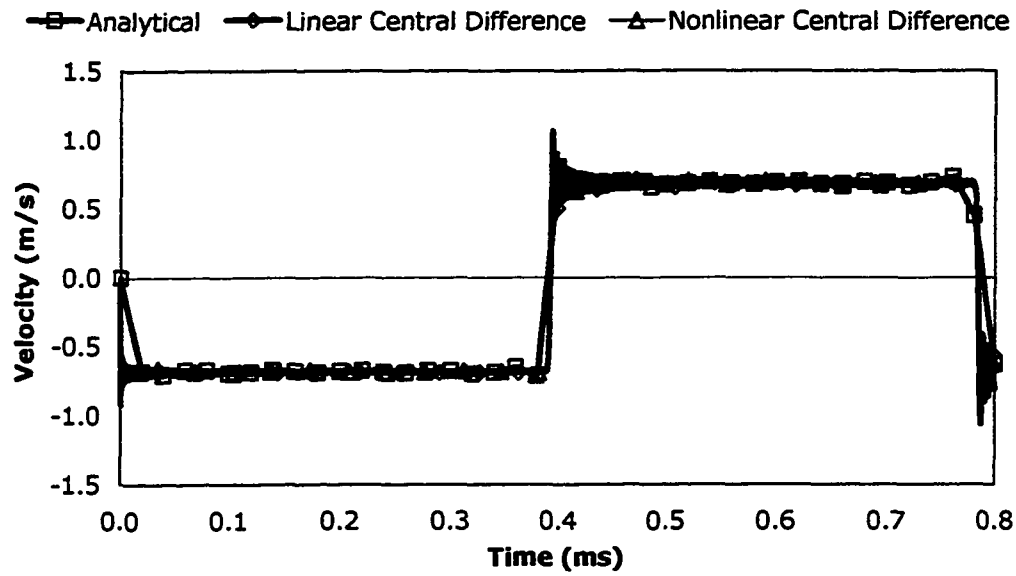

Figure 3.14, Comparison of linear and nonlinear Central difference velocity response to analytical velocity response of free end after release of pre-stressed tension for the vibration example model

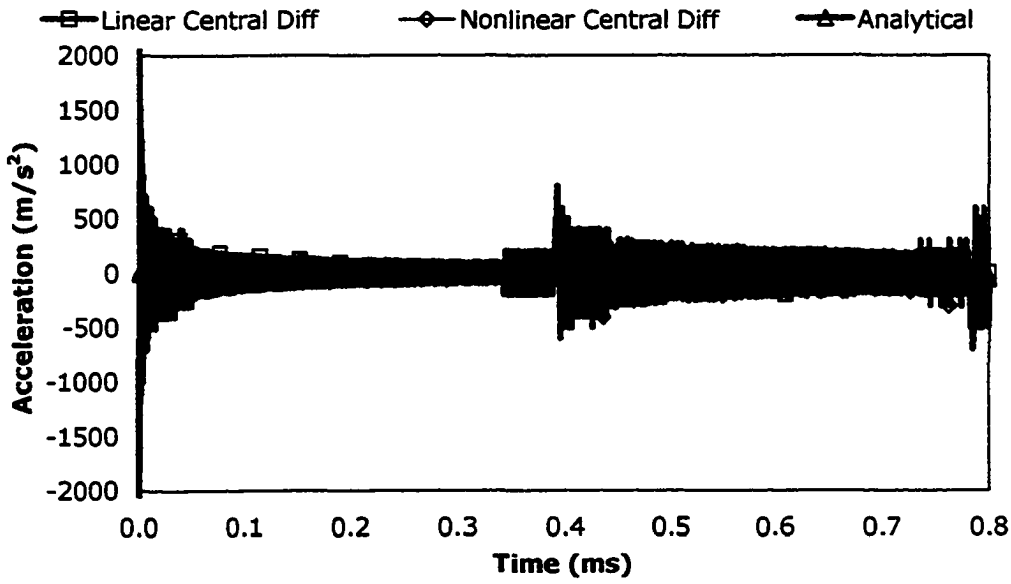

Figure 3.15, Comparison of linear and nonlinear Central difference acceleration response to analytical acceleration response of free end after release of pre-stressed tension for the vibration example model

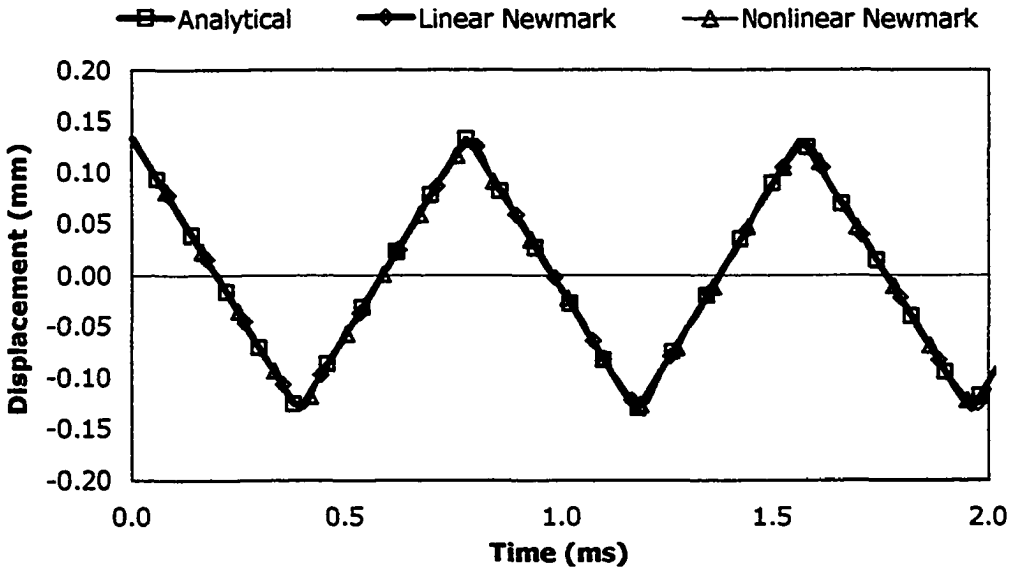

Figure 3.16, Comparison of linear and nonlinear Newmark displacement response to analytical displacement of free end after release of pre-stressed tension for the vibration example model

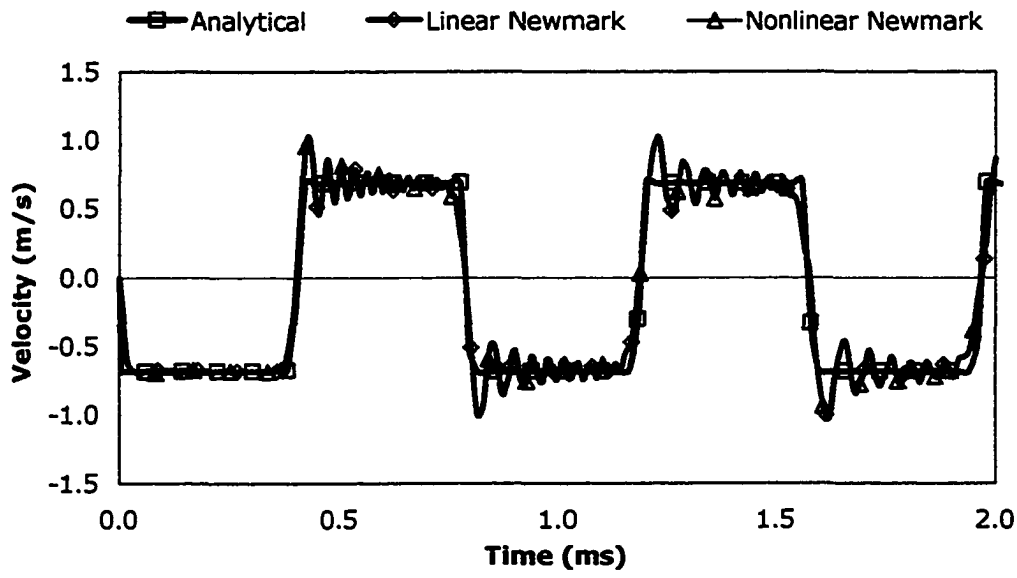

Figure 3.17, Comparison of linear and nonlinear Newmark velocity response to analytical velocity response of free end after release of pre-stressed tension for the vibration example model

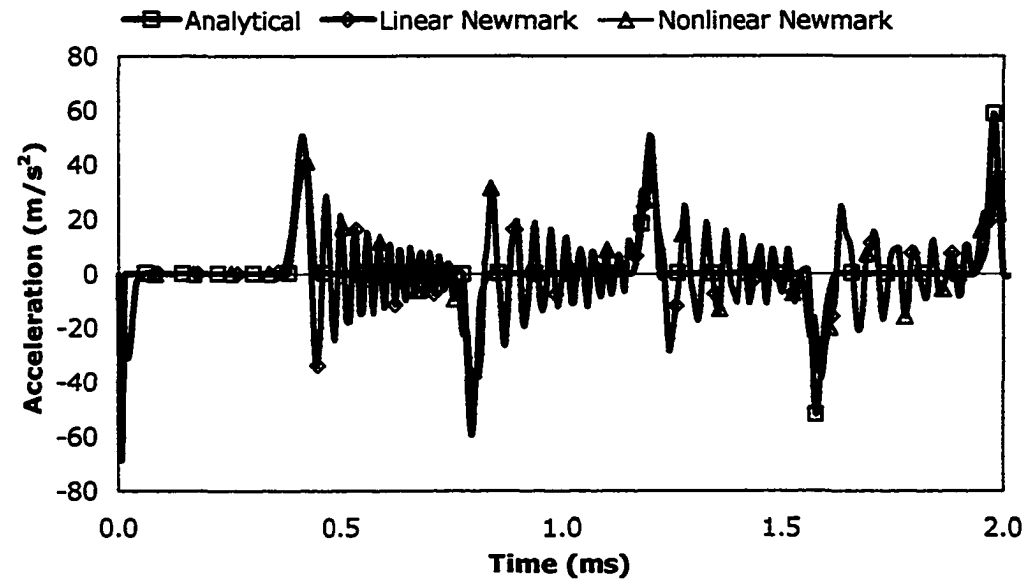

Figure 3.18, Comparison of linear and nonlinear Newmark acceleration response to analytical acceleration response of free end after release of pre-stressed tension for the vibration example model

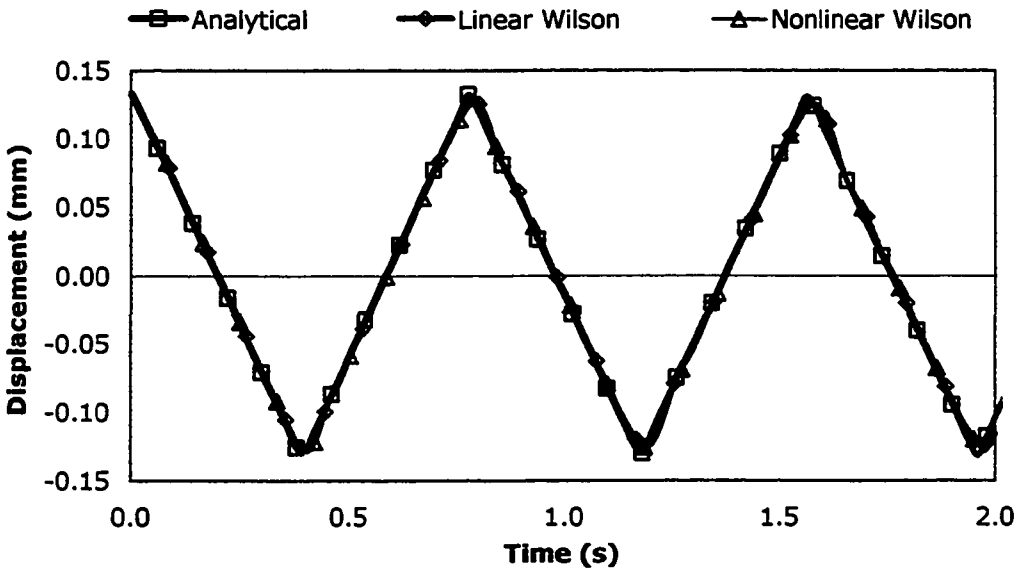

Figure 3.19, Comparison of linear and nonlinear Wilson displacement response to analytical displacement response of free end after release of pre-stressed tension for the vibration example model

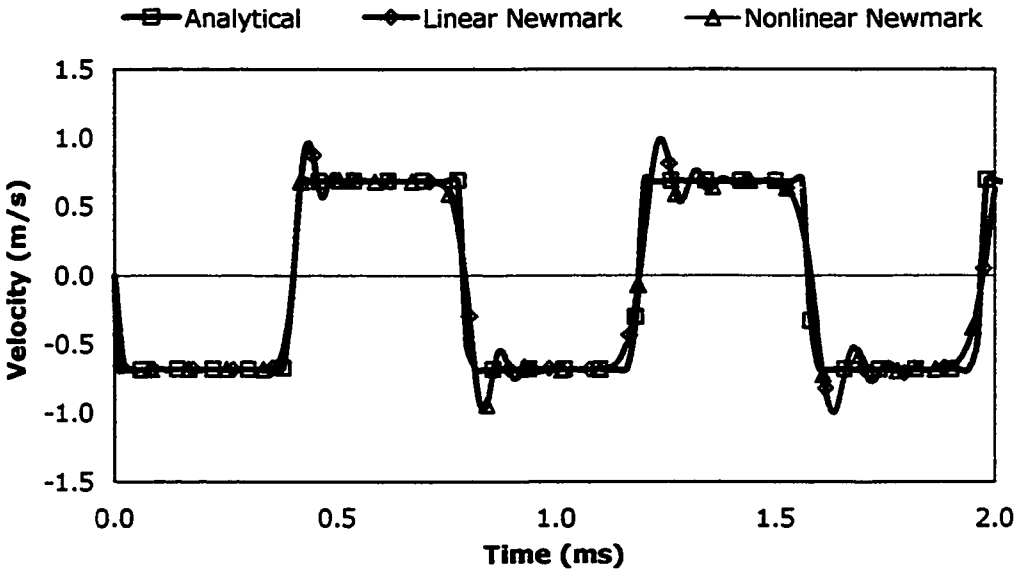

Figure 3.20, Comparison of linear and nonlinear Wilson velocity response to analytical velocity response of free end after release of pre-stressed tension for the vibration example model

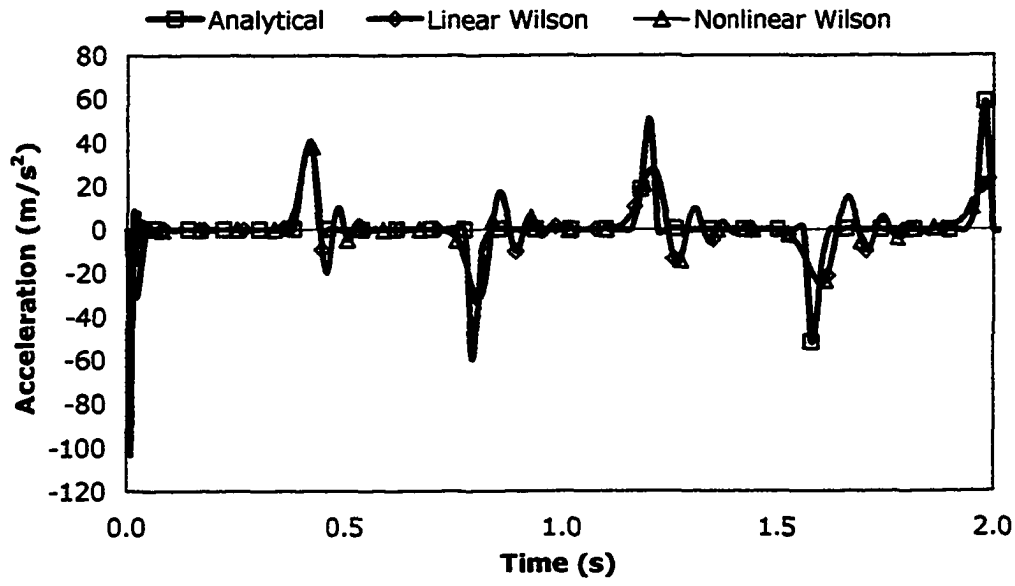

Figure 3.21, Comparison of linear and nonlinear Wilson acceleration response to analytical acceleration response of free end after release of pre-stressed tension for the vibration example model

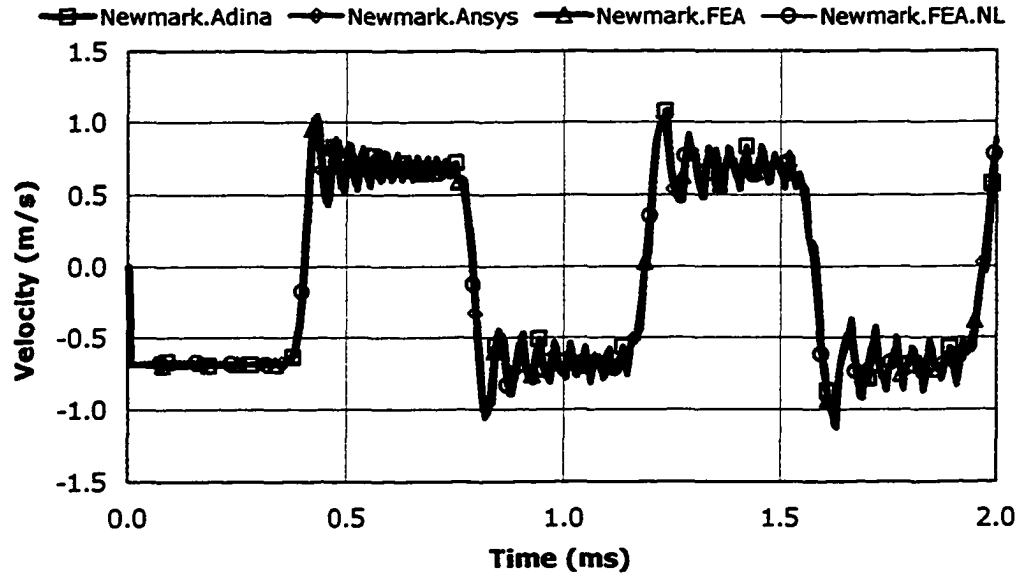

Figure 3.22, Comparison of vibration example model free end velocity response between ADINA, ANSYS and JIFEA

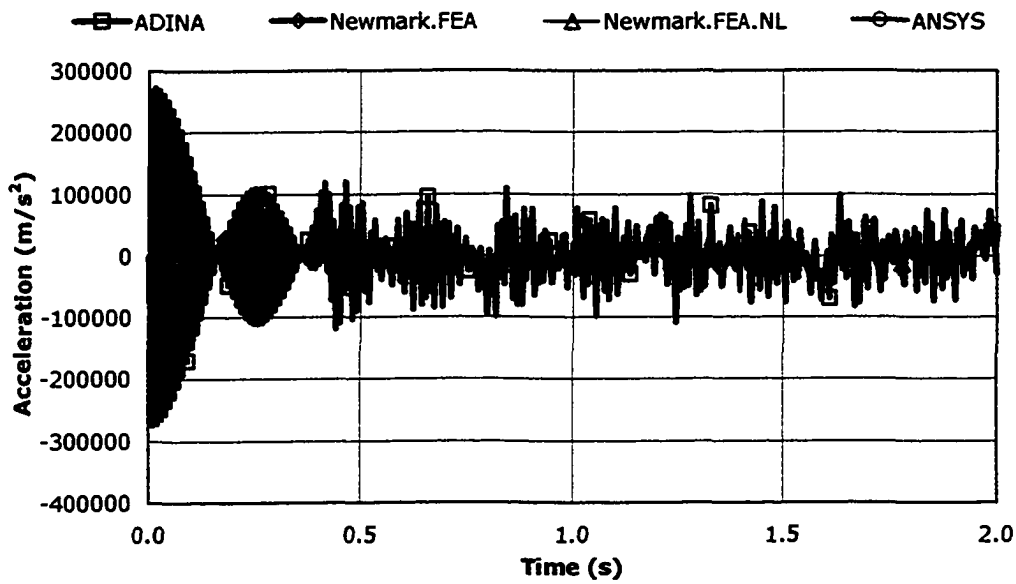

Figure 3.23, Comparison of vibration example model free end acceleration response between ADINA, ANSYS and JIFEA

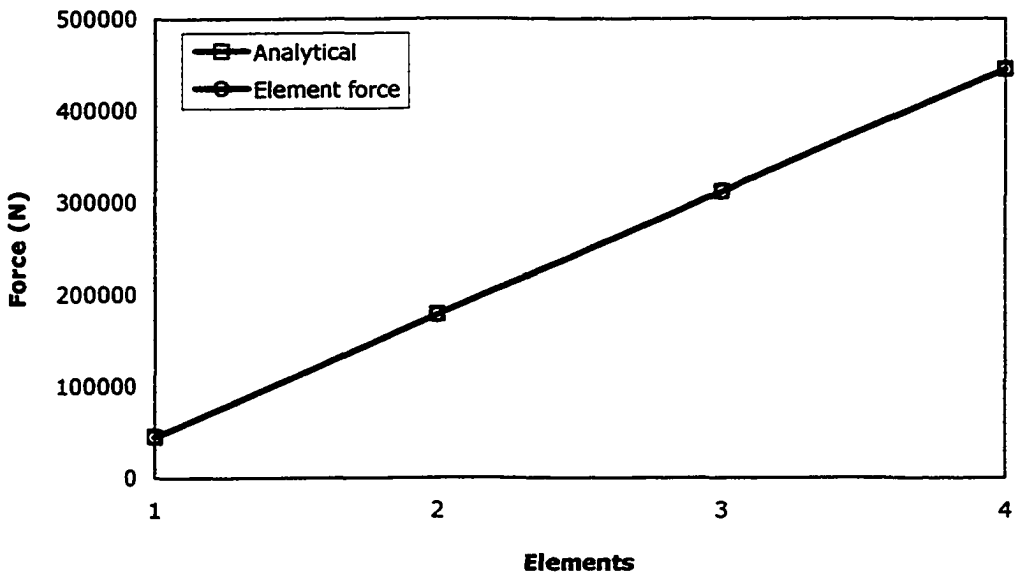

Figure 3.24, Comparison between JIFEA and analytical friction results for a simple 4 link model with distributed friction

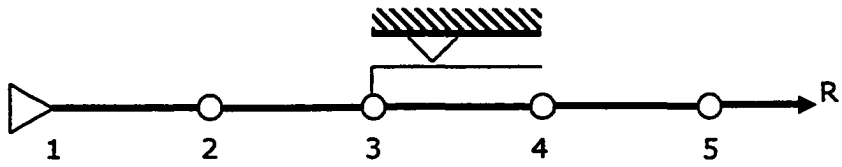

Figure 3.25, Depiction of 4-link element distributed friction model for verification of incremental tensile load

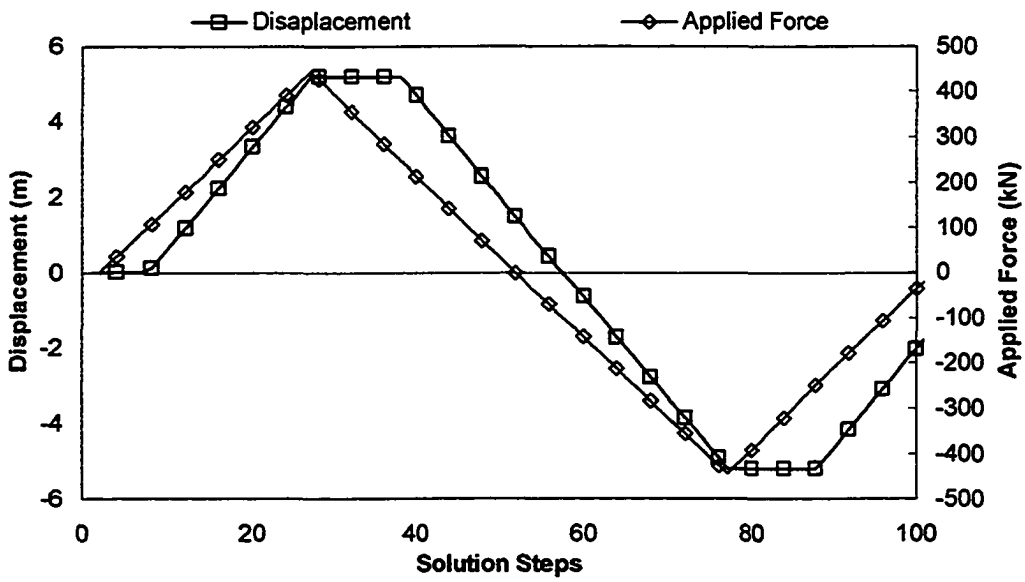

Figure 3.26, Displacement and load response for a single friction element under a single load cycle (Node 3)

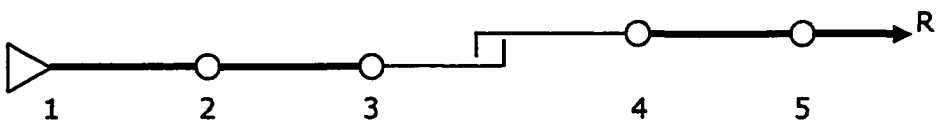

Figure 3.27, Depiction of contact verification model consisting of four link elements and one contact element

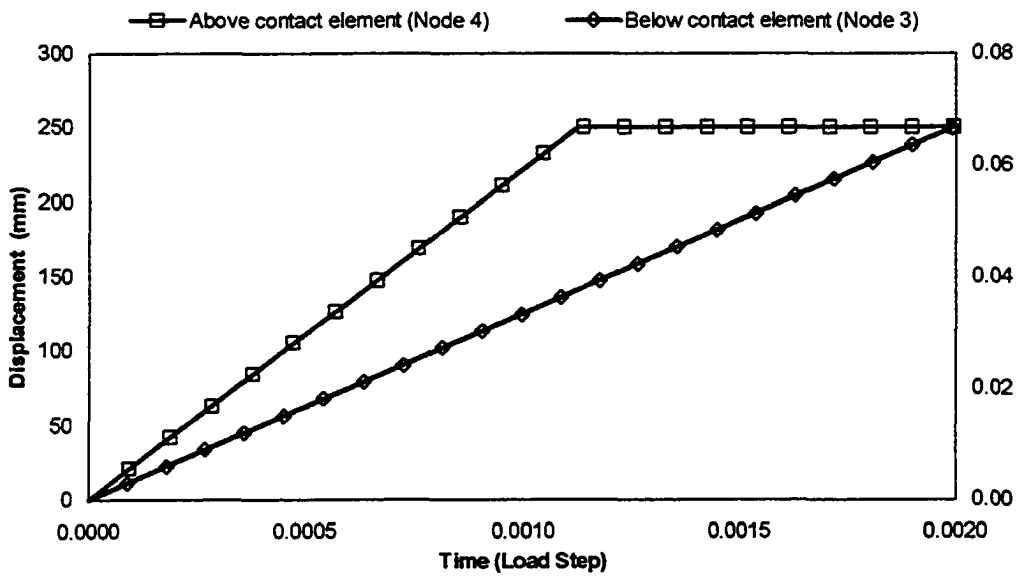

Figure 3.28, Displacement response of contact element for simple contact verification model

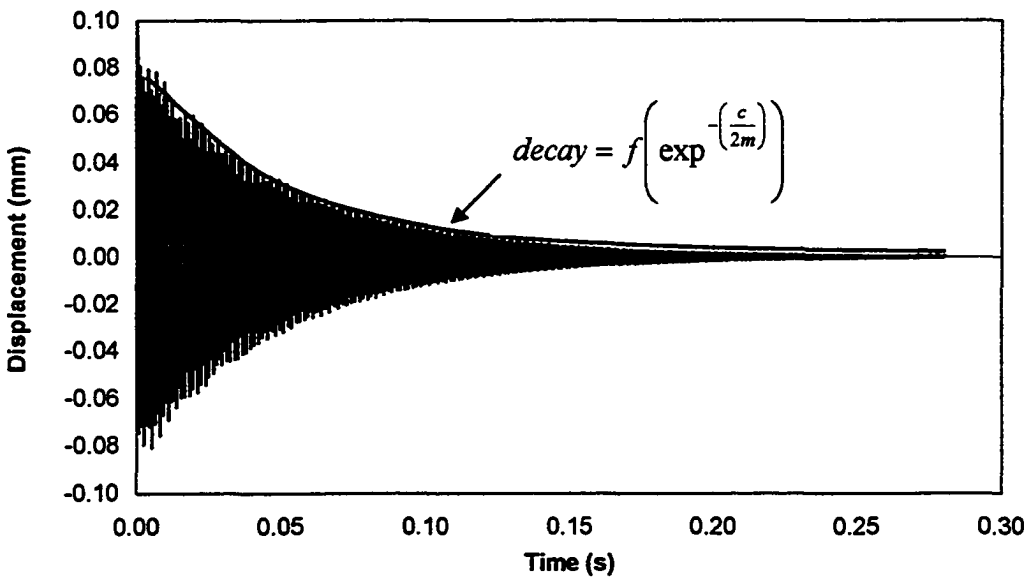

Figure 3.29, Displacement response of distributed damping verification model

Chapter 4

SOLUTION CONTROL VARIABLE SENSITIVITY FOR JAR WAVE PROPAGATION

Creating and using an application-specific finite element analysis (FEA) program to produce results equivalent to commercial FEA software in a fraction of the time is the main objective of this thesis.

Other methods including manual calculations such as impulse-momentum relationships (Skeem et al., 1979), alternate FEA techniques such as application-specific spectral (frequency domain) analysis (Eustes, 1996) and alternate numerical techniques such as wave-tracking (Wang et al., 1990) have been employed to solve the wave propagation problem. These alternate methods were generally sought to reduce the time Jar impact analyses took with commercial FEA aiding determination of "best practice" Jar placement. An additional benefit is the cost advantage in replacing commercial FEA software such as ANSYS.

All the alternate methods found avoided time-history FEA analysis. JIFEA uses many of the same numerical techniques as commercial FEA software but with significantly reduced computational overhead. Solvers and data storage have been streamlined to increase the solution speed and minimize memory requirements.

To achieve the main objective, JIFEA is compared to ANSYS only as many creators of alternate methods used ANSYS to verify, calibrate or study wave propagation. Therefore, being able to replicate the results from ANSYS implies agreement with the alternate methods as well.

The results indicate good agreement between ANSYS and JIFEA with a dramatic increase in speed (30 times faster than ANSYS for the verification model).

Sensitivity to damping and friction are evaluated using JIFEA to determine their effects on the force generated at the stuck point. Also, the numerical integration parameters are studied to assess their influence on the performance (time and accuracy) of the program.

Finally, a few Jar placement impact analyses are evaluated using all the features built into JIFEA to demonstrate the effect Jar location has on stuck point forces and to show where increasing the analysis time may be required to obtain the maximum force.

4.1 Alternate methods

The desire to evaluate drill string dynamics began long before personal computers were available. Various people and companies invested time developing techniques to determine the forces generated from Jars. The force information is used either to improve Jar effectiveness or to assess the load capacity required by other components to sustain Jarring.

The discussion that follows is a very rudimentary overview of some methods that motivated the development of JIFEA and this paper.

4.1.1 Manual calculations

Many hand calculations and manual techniques begin with a basic impulse-momentum approach using the simplified model shown in Figure 4.1. The initial acceleration is computed and the velocity of each mass determined at the point of first contact.
The largest impulse is generated when the greatest relative momentum between the hammer and anvil is achieved. Adjusting both the hammer and anvil mass and stiffness arriving at the greatest momentum is one approach used to gain the largest impulse. This assumes the largest force propagating down the pipe will free the drill string.

Additional factors such as wave speed and wave propagation effects were added by some to increase the accuracy of the computations. The force transferred to the stuck point is a function of the contraction speed (Skeem et al., 1979).

In general these methods are approximations to the complex drilling assembly often omitting damping and hole-drag. They are well documented and fast to compute but are not as accurate as numerical methods analyzing models with more complex details. However, manual methods are reasonable when complex drilling details are unknown.

4.1.2 Wave-tracking method (Wang et al., 1990)

Kalsi, Wang et al developed the wave-tracking method as an alternate approach to FEA (Wang et al., 1990). ANSYS was used with a simple fishing Jar analysis (same as a drilling Jar for all intent and purpose of this discussion) to verify and calibrate the wave-tracking method.

The method uses some of the basic impulse-momentum and wave speed calculations to define the initial wave (impulse). Refractive and reflective wave relationships were implemented in a recursive algorithm to compute the displacements and forces at key points throughout the drilling assembly.

Good agreement was found comparing the results with ANSYS. This led to the development of the JarPRO™ software, which is application-specific software, intended to provide bottom-hole assembly designers a tool to optimize Jar placement ("JarPRO™", 1990).

The wave-tracking method solved much faster than ANSYS making JarPRO™ viable for field use.

4.1.3 Application-specific spectral analysis (Eustes, 1996)

Eustes developed an application-specific spectral (more commonly known as frequency domain analysis) finite element analysis (SFEA) (Eustes, 1996). In part, the effort was motivated by the slow nature of ANSYS when solving a simple wave propagation problem. Eustes also reviewed the work performed by Kalsi and theorized that an alternate numerical method would produce accurate results in a timely fashion.

The SFEA method required a spectral element development. Eustes's spectral element captured the full equation of motion (d'Alembert's principle) with the intent of requiring fewer elements to perform the analysis. The method uses only a few terms of the Fourier series to represent the element and thus is analogous to a time-history analysis with a limited time step size and element length.

Field experience reveals the technique is very sensitive to damping. Small changes to the damping coefficient would cause radical differences in results or cause numerical instabilities preventing a solution. When the damping coefficient was held proportionally constant to the model length, the technique produces results comparable to ANSYS in a fraction of the time.

The method is implemented in several phases. The entire model is built in the time-history domain, converted into the frequency domain using FFT, analyzed, then converted back into the time domain again using IFFT (Inverse Fast Fourier Transforms) for force-time result interpretation. The requirement of the pre- and post-analysis adds additional complexity to the analysis but is a necessary step as interpreting the results is more straight-forward in the time domain.

4.2 Replication of Kalsi model (Kalsi et al., 1985)

The original modelling performed by Kalsi was re-created from the information provided in the SPE paper (Kalsi et al., 1985). It is a model of a partial fishing assembly (similar to a drilling assembly) in a basic vertical well bore with the combination of components as listed in Table 7.

Table 7, Kalsi's FEA model components with length and number of elements

Component	Length (m)	Number of Elements	Element Length (m)
Drill Pipe (link)	609.60	20	30.48
Heavy Weight (link)	91.44	10	9.14
Drill Collar (link)	27.43	10	2.74
Intensifier (spring)	3.05	1	3.05
Drill Collar (link)	54.86	20	2.74
Jar (contact element)	0.165	1	0.165
Drill Collar (link)	45.72	15	3.05
Stuck Point (friction)	0	1	N/A
Drill Collar (link)	45.72	15	3.05
Drill Collar (link)	91.44	15	6.10
Tie down spring	0.0254	1	.0254

Damping elements connect the drill collars from the intensifier to the "tie down" spring to the ground. The damping coefficient specified by both Kalsi and Eustes is 239 N·s/m/m and is used throughout the present paper except in the damping sensitivity cases.

The addition of the intensifier jar above the drilling jar is intended to act as a free-end, reflecting all waves back down towards the stuck point. In practise, intensifiers are rarely used. Basically, an Intensifier Jar is a large spring with stiffness of 2.33 MN/m (much more flexible than the base pipe).

The Kalsi model was reconstructed by interpreting model details from the SPE paper. Since the modelling details are not completely described, variations in the model may exist. However, re-running the analysis in ANSYS version 8.0 produced results very similar to those obtained by Kalsi.

Recreating Kalsi's original work defines a benchmark for JIFEA and verifies the current model. Kalsi chose to model a shortened version of the drilling assembly (609.6 m of drill pipe rather than 3048 m) and included the Intensifier Jar to reflect waves down towards the stuck point. Since the full model was not represented, Kalsi selected an analysis time of 0.14 seconds to limit wave generation. Furthermore, 0.14 seconds only allowed time for the initial wave to reach the stuck point. Running the analysis further into time may show that reflections of subsequent waves produce constructive interference and greater wave amplitude. In the next section, longer times with the full pipe length are modelled without the Intensifier Jar to assess the stuck point force with wave interference effects.

All comparisons between JIFEA and ANSYS for this and the subsequent sections were executed on a computer with the following specifications:

- Dual Pentium III 933
- 1024 Megs SD PC133 RAM
- 1 - 18 Gig 10,000 RPM SCSI drive (boot)
- 2 - 120 Gig 7,200 RPM UlatraDMA100 IDE drives (data/scratch)
- Windows 2000 Professional

The program was written in C++ using object-oriented techniques for all aspects from element implementation to solvers and data storage. Microsoft Visual C++® V6.0 was used with the default compiler optimizations.

4.2.1 Verification / base case

A modified version of the model was defined to benchmark JIFEA with ANSYS, and to establish a base case for the parametric evaluation. It is defined as the original model but with the damping elements and Intensifier Jar omitted. There are slight differences between the ANSYS model and the model built for JIFEA. First, JIFEA is modelled top-down; the top node is node 1, in ANSYS the bottom node is node 1. Second, the Jar is modelled with additional pipe on either side of the contact element to represent the Jar diameter and length. The number and size of elements on each side of the contact element were modified to reflect the modelling techniques employed by JIFEA.

Using the computer described previously, the analysis took 3.5 minutes using ANSYS. Performing the same analysis using JIFEA solved in 7 seconds. Figure 4.2 shows a comparison between the modified Kalsi model solved with ANSYS version 8.0 and JIFEA. It shows good agreement between the Jar (contact element) displacement results. The slight difference is caused by variations between the model definition and the program implementations of both solvers and elements.

Similarly, Figure 4.3, Figure 4.4 and Figure 4.5 show very good agreement between ANSYS and JIFEA for forces calculated at the rig, jar and stuck point. The force calculations include inertia forces indicating the acceleration is also in agreement with ANSYS.

The Jar response is very similar in both programs, however, there is a slight variation in the result magnitude and signature between ANSYS and JIFEA after Jar impact (gap closes). Interestingly, the gap closes at the same time in both responses indicating that the velocity and acceleration in both models agree. The slight variation in response is likely due to the small difference in model description. The JIFEA model has extra pipe on either side of the contact element to represent the Jar. Contact element implementation difference between ANSYS and JIFEA and numerical conditioning preset in ANSYS may also cause some response differences.

The stuck force response exhibits subtle differences but local oscillations are focused around the same mean value. Again, the difference may be due to implementation and model definition.

The forces at these locations are considered paramount in determining best Jar location within the drilling assembly. Given the close agreement between the programs, JIFEA can easily be used to evaluate Jar impact analysis in a fraction of the time of ANSYS. The performance is comparable to the wave-tracking method and the spectral analysis but with the features provided by ANSYS.

4.3 Parametric evaluation

A variety of parameters control the response of the system. These parameters need to be evaluated to assess their affect on the forces generated in the drill string and also how the numerical techniques react. Some parameters damp the response whereas others increase the solution speed but cause numerical instability.

It is convenient to consider three groups of parameters:

1. **External.** External effects are factors that alter the wave propagation by changing the wave form or magnitude independent of integration method. By this description, damping and friction are external parameters. To clarify how these are considered external effects, the basic pipe structure is defined as the reference model and any additional modelling factors that modify the response are external to the base model.
2. **Geometric.** Geometric effects are imposed by modelling artifacts such as element length, time step size (abbreviated as *'its'* for integration time step) and the integration time or duration (hereon in referred to as 'time' or analysis time). Referring to these artifacts as geometric may seem counter-intuitive; however, the wave form is discretized both in space and time. The term geometric is associated with the wave discretization.
3. **Internal.** Internal effects are the integration parameters that directly control the integration process. In the case of both Newmark and Wilson methods, the use of these parameters in effect creates a different integration technique. The Wilson method with $\theta = 1$ becomes the basic linear acceleration method. Similarly the Newmark method with $\alpha = {}^1/_6$ and $\delta = {}^1/_2$ also reduces to linear acceleration method. So by altering the parameters an entire family of integration schemes are possible. These types of parameters are internal to the integration methods and separate from the model.

Combinations of the Geometric and Internal parameters may be required to maximize the performance of JIFEA.

The analysis time and time step size used throughout the parametric study was taken as 0.14 s[1] and 0.2 ms[2] respectively. These values are taken from the Kalsi analysis for comparison purposes.

4.3.1 Nonlinear element sensitivity

Several nonlinear elements are used in the model. The contact element is used to generate the impulse wave and both the damping and friction elements act to reduce the propagating wave energy. This section evaluates the decay sensitivity to damping and friction.

4.3.1.1 Damping coefficient sensitivity

The interest in the damping coefficient stems from the wide spread variation in literature as to how much damping truly exists. The damping coefficient is a function of annulus size, fluid viscosity and density. The coefficient used may vary depending on the literature referenced or the techniques used to measure or calculate it. Evaluating the sensitivity to damping will provide insight as to the importance damping plays in the analysis and the influence it has on the results.

The damping coefficient used by Kalsi et al for the purpose of drilling assembly modelling is 239 N·s/m/m. Furthermore, the Kalsi model only applies the damping to the bottom portion of drill collars from the bit to the intensifier jar (see Table 7). JIFEA was configured to apply the damping to the entire length of the assembly.

Figure 4.6 shows the stuck point force response for a range of damping coefficients. The critical damping lies between 23,900 and 239,000 N·s/m/m. For coefficient values less than and including 1,195 N·s/m/m the stuck point (friction element) slides and is the flat portion of the force response curve above 800 kN. If the stuck point friction is not exceeded then insufficient force has reached the stuck point to free the drill string.

The default damping coefficient of 239 N·s/m/m is somewhat subjective. A value 5 times greater alters the response but still allows the waves to free the stuck point. This indicates the wave propagation is relatively insensitive to the damping coefficient. Therefore, determination of the damping coefficient may not require significant effort.

In this model, the damping elements connect the nodes of the pipe to ground. The spectral analysis model embedded the damping between the nodes of the pipe possibly causing the method's damping sensitivity. Applying damping elements between pipe and ground generates the proper relative velocity for use with the damping coefficient. However, access to the SFEA method was not possible at the time of this writing so no direct comparisons could be

[1] Unless the analysis time is otherwise stated

[2] Unless the time step size is otherwise stated

made. Other forms of damping such as material damping could be employed by connecting the damping elements across the pipe nodes. However, the effects of this type of damping on wave propagation should be explored but are outside the scope of this work.

The dash-pot style damping used in the element derivation is based on equation 4.3.1. It was suggested the damping coefficient generating a force by equation 4.3.1 does not apply to this type of motion. 'c' would be computed from the fluid properties and be representative of the fluid shear in the flow. The wave propagation is a localized effect and as such may not introduce significant motion into the fluid boundary layers. Further work may be required to quantify the localized effects of the damping coefficient on wave propagation.

$$F_D = cv \qquad 4.3.1$$

4.3.1.2 Friction (hole-drag) sensitivity

The hole-drag is the total friction acting on the drilling assembly. It is a single value used to indicate the resistance to movement for inserting (tripping-in) or removing (tripping-out) the drilling assembly from the well bore.

Realistically, the friction is caused by pipe contacting the well bore where localized pipe buckling occurs, global deviations in the well cause pipe bending or inclines where the pipe rests on the well bore. Therefore, friction is unevenly distributed along the length of the pipe.

For the purpose of the sensitivity analysis, the friction is linearly distributed over the length of the pipe. This provides insight as to how the waves behave with friction acting evenly along the length of the pipe.

Figure 4.7 shows the effects increasing hole-drag (friction) has on the force generated at the stuck point. The zero friction case is the base case and the subsequent curves are applied hole-drag. The hole-drag is distributed along the length of the pipe to limit the wave propagation. Clearly, the wave is almost completely suppressed when the drag reaches a total friction of 750 kN (775.7 N/m).

Note: the (*) in the figure indicates that the friction element stiffness had to be revised. The element force-displacement relationship must remain somewhat balanced. If the element stiffness is too high, the critical displacement allowing slippage is too low and oscillations occur. If the stiffness is too low, the element may not slip.

Balancing the friction critical displacement and stiffness can be automated by assuming the friction stiffness is a function of the critical displacement. Equation 4.3.4 shows a possible relationship between the stiffness and the critical displacement.

$$K_{fric} = \frac{1}{u_{crit}^2} \quad 4.3.2$$

$$F_{max} = K_{fric} u_{crit} \quad 4.3.3$$

$$F_{max} = \frac{1}{u_{crit}^2} u_{crit} = \frac{1}{u_{crit}} \quad 4.3.4$$

This keeps the value of K proportional to the critical displacement. Other functions are possible; therefore, further evaluation would be required to ensure the chosen function is appropriate for all common drilling assemblies.

4.3.1.3 Nonlinear element summary

The parametric evaluation has shown that damping exhibits standard decay in the response. However, the default value of 239 N·s/m/m does not generate a significant decay in the response. Increasing the damping coefficient by a factor of 5 increases the decay but still produces a force large enough to free the stuck point. This suggests that when the damping is not close to the critical damping, changes in the damping have minimal effect on the response.

This is easily seen by considering the ratio of damped and natural frequency to the damping ratio. The equation for free damped vibration is given by equation 4.3.5.

$$\left(\frac{\omega_D}{\omega_N}\right)^2 + \zeta^2 = 1 \quad 4.3.5$$

Figure 4.8 shows a plot of equation 4.3.5. When the damping coefficient is very small relative to the system, small changes have little effect on the damped frequency. However, when the damping value is large compared to the system, (right side of figure) a small change in damping produces a significant change in frequency.

As stated previously, the damping causes an exponential decay in the response of the system. Figure 4.9 shows a generic system with modest damping in the system. When the drill string becomes stuck it is desirable to get the maximum force to the stuck point. Viscous damping in the drilling system is caused by fluid between the pipe and annulus. Therefore the further the wave has to travel the more damping decays the magnitude.

The friction sensitivity has shown that distributing friction along the drill string also causes a reduction in the wave magnitude reaching the stuck point similar to viscous damping. However, unlike viscous damping, friction (Coulomb damping) causes a linear decay to the response. Figure 4.10 shows a generic decay to a response when under a distributed friction. Linear decay

is a characteristic of friction being a displacement based phenomenon (Steidel, 1989).

Both forms of damping reduce the magnitude of the wave and lower the likelihood of freeing the stuck point. When both types exist the decay is greatest. In real drilling assemblies, the damping exists along the full string length but may be more concentrated in the lower section where the annulus is smallest. A small annulus also means a concentration of friction may exist. To maximize the force produced at the stuck point, Jars have to be placed as close to the potential stuck point as possible. Since the stuck point is unknown, a general rule of thumb is: place the Jars as low as possible but above any potential sticking location.

4.3.2 Length and time sensitivity

In the cases shown in the damping section, all the models were run to a total time of 0.14 seconds. The modified model described in section 4.3.1.1 is analyzed but with the drill pipe length increased to 3048 meters. Figure 4.11 shows the stuck point force response from the model used in section 4.3.1.1 analyzed for 0.14 second and from a model with the full complement of drill pipe and analyzed for 0.28 seconds. Though the stuck point friction is not exceeded there is significant wave activity taking place after 0.14 seconds. Initially the two curves show the exact same response indicating the increased length had no effect on the response. However, beyond 0.14 seconds, wave interference has caused a change in the response. The encircled point indicates a period change likely caused by interference from reflected or refracted waves. A wave travelling 5135 m/s requires 1.18 seconds to reach the end of the pipe and back (2x3048 meters). Therefore, the change in the response is due to the increased analysis time not the increased model length.

The addition of the full complement of drill pipe increases the number of elements by 80 link elements and 80 damping elements. Furthermore, the analysis time was increased to 0.28 seconds. This increases the model size significantly yet JIFEA solves in 40 seconds, 5 times longer than the original base case model but with twice the elements and twice the time duration.

Stuck point mobilization may only occur as a result of wave interference. Therefore, having the ability to run the analysis for longer durations may be important depending on the parameters and modelling details.

4.3.3 Integration sensitivity

All the integration methods are sensitive to time step size and element length to some degree but certain methods have additional parameters that need to be explored. These parameters control the performance (speed and accuracy) of the results. It is important to determine what specific settings can be used to maximize the speed while retaining reasonable accuracy.

The default values for time step and element length are used as per Kalsi to define the reference response. Results from alterations to the model and/or solution strategy are compared to the reference response to assess accuracy. In cases where the waveform deviates greatly, the modifications to the solution strategy or model are considered a reduction in accuracy.

Acceleration and velocity are not used as a basis for comparison as the forces are representative of the displacement field, which in turn is a function of the velocity and acceleration fields. The force shown in the following analyses is the stuck point force. All of the models used are the modified Kalsi model with no damping.

For the study, the element length will be held constant and only the time step size will be varied.

The Central Difference (CD) method does not have any integration parameters other than the time step size and element length.

The Newmark method (NM) has two additional parameters α and δ. They are used to control the average acceleration and the linear velocity in the method.

Similarly, the Wilson method (WM) has one parameter, Θ, used to control the linear acceleration of the method.

Table 8 lists the default parameters used to define the base cases for each method.

Table 8, Default integration parameters for Central difference, Newmark and Wilson methods

Alpha (NM)	α	0.5050
Delta (NM)	δ	0.25250625
Theta (WM)	Θ	1.40
Time step size	*Its*	0.2 ms
Solution time	time	0.14 s

The Newmark parameters were taken from the ANSYS version 8.0 theory manual since the verification comparisons have been done between JIFEA ANSYS. The Wilson parameter was taken from Bathe (Bathe, p777, 1996) as a common value used for the method.

4.3.3.1 Time step size

The sensitivity to time step size is evaluated for each integration method. This shows how the time step size alters the response produced from each method.

The analysis time and time step size were taken from Kalsi's model as 0.14 s and 0.2 ms respectively[3]. To determine the time step size in advance, the techniques outlined in section 3.2.1.1 are used. Assuming the drilling assembly can be approximated as a continuous length of a uniform cross-section pipe, the time step size and element length can be computed as shown in equation 4.3.6.

$$L_{TotalLength} = 969.45m$$

$$\omega_n = \frac{c_{wavespeed}}{L_{TotalLength}} = \frac{5135}{969.45} = 5.3rad/s$$

$$\Delta t_{crit} = \frac{2}{\omega_n} = \frac{2}{5.3} = 0.378s$$

$$\Delta t = \frac{\Delta t_{crit}}{10} = 0.0378s$$

$$\lambda = c\frac{2\pi}{\omega_n} = 5135\frac{2\pi}{5.3} = 6091.24m$$

$$L_{element} = \frac{\lambda}{20} = \frac{6091.24}{20} = 304.56m \qquad 4.3.6$$

The length and area assumptions produce a time step size and element length larger than that used in the modelling by Kalsi. Realistically, the change in area from section to section makes this model a multi-degree of freedom problem where the natural frequencies are a combination of all pipes present. Bathe suggests calculating the time step based on the desired frequency of interest then use the wave speed to compute the maximum element length as shown in equation 4.3.7.

$$f = 200Hz$$

$$T = \frac{1}{f} = \frac{1}{200} = 5e^{-3}s$$

$$\Delta t = \frac{T}{10} = \frac{5e^{-3}}{10} = 5e^{-4}s$$

$$L_{element} = c\Delta t = 5135 \times 5e^{-4} = 2.56m \qquad 4.3.7$$

With the time step (*its*) of 0.5 ms (0.0005 s) and an element length less than 2.56 meters, the maximum frequency that could be accurately modelled is

[3] Unless the analysis time or time step size is otherwise stated

200 Hz. The longest element in the Kalsi model is longer than this length indicating that the maximum frequency that the analysis can produce is less than 200 Hz. In the region of the stuck point, the element length is 3.05 m, combined with the time step size of 0.0002 s, the maximum frequency is in the order of 168 Hz. However, the ratio of element length to time step does not satisfy the wave speed rule as recommended by Bathe.

For a multi-degree of freedom system, the shortest natural period could be used to ensure that all the frequencies are captured. However, care must be taken when extreme length variations exist in the drill string. These variations may cause a large natural frequency range for the system.

In this work, the analysis time and time step size were taken from the verification models. For field use, the minimum analysis time would be calculated from the wave speed and the model length as shown in equation 4.3.8. This allows time for a single wave to travel the length of the drill string. Also, solving the general eigenvalue problem (equation 4.3.9) (Steidel, Ch. 11, 1989) results in an eigenvector in ω^2. The time step size is then computed from the shortest natural period following the method shown in section 3.2.1.1. The matrix $[A]$ is assembled from the mass and stiffness of the drill string excluding damping, friction and contact.

$$Time_{\min} = \frac{L_{DrillString}}{c_{WaveSpeed}} \qquad 4.3.8$$

$$[A - \omega^2]\{x\} = 0$$

$$Det\left([M]^{-1}[K] - \omega^2\right) = 0 \qquad 4.3.9$$

4.3.3.1.1 Newmark method

The first method evaluated is the Newmark method. Figure 4.12 shows the response at the stuck point of the base case as the time step (*its*) is varied. The default *its* was 0.2 ms. An *its* of 0.02 ms took approximately 68 seconds and does not improve the accuracy enough to warrant the increase in solution time. However, using 2.0 ms decreased the solution time to less than 1 second with a decrease in accuracy. An *its* of less than 2.0 ms produces a very general trend but not sufficient to determine the behaviour of the response. Table 9 lists the solution time for each of the time step analyses.

Table 9, Newmark solution time with time step size

Time Step Size "*its*" (ms)	Solution Time (s)
20	<< 1
2	< 1
0.2 (default)	7
0.02	68

Using an *its* of 2.0 ms may be viable for refining jar placement if maximum values were used to draw comparisons between placements rather than using the analysis results as true forces acting on the drill string. Given the speed in which the analysis can be performed, time step sizes in the order of the default give the best compromise between solution time and accuracy.

4.3.3.1.2 Wilson method

To evaluate the Wilson method the base case is used with varying time step sizes to assess the effects on the stuck point force response.

Figure 4.13 shows how the stuck point response changes as the time step size is varied from the default size. With an *its* of 0.02 ms, the response looks similar to the Newmark response shown in Figure 4.12 but the default *its* of 0.2 ms is much smoother than Newmark. The Wilson method with an *its* of 2.0 ms produces a smooth response with a similar period but with a lower and faster decaying amplitude. An *its* of 20 ms was attempted but the method could not resolve equilibrium.

The response of this system should be essentially a square-like pattern so this suggests that the Wilson method produces accurate results removing the local oscillations if the time step size is suitable for the model in question. Clough and Penzien claim that the linear acceleration method is one of the most accurate methods; the Wilson method is derived from the linear acceleration method.

In general the Wilson method is slightly slower than the Newmark method due to an extra set of operations per time step. The difference in solution times becomes more prevalent at smaller time step sizes. Table 10 lists the analysis times for the Wilson method for the various time step sizes.

Table 10, Wilson solution time with time step size

Time Step Size (s)	Solution Time (s)
0.02	no convergence
0.002	< 2
0.0002 (default)	7
0.00002	75

Similar to the Newmark method, an *its* of 2.0 ms could be used if the absolute results are not considered important but rather as a comparison between Jar locations.

4.3.3.1.3 Central Difference method

The evaluation of the Central Difference method was chosen due to its common use in commercial finite element analysis and dynamics. This method requires a smaller time step size than those of the other methods but with the proper choice of time step size and element length produces an exact solution to the linear wave propagation method (Bathe, p815, 1996).

Figure 4.14 shows the response at the stuck point when the central difference method is used. The largest time step size (*its*) that could be used for convergence was 0.03 ms, a factor of 6.67 times smaller than the default *its* used for the Newmark or Wilson methods. However, the response using this increment oscillates once the stuck point slips. Using a time step size of 0.02 ms generates a flat response for the stuck point slippage consistent with the previous methods. Further refinement to the time step size (0.002 ms) does not increase the response accuracy for this model but increases the solution time to 114 s.

Central Difference required a smaller time step than the implicit methods. Table 11 shows a list of the solution times with respect to the time step size. With the default time step size of 0.2 ms, the Central difference method is unstable and does not produce a result. The central difference method required at least a time step of approximately 0.03 ms before a solution could be obtained. However, the solution at an *its* of 0.03 ms has severe oscillations in the response indicating that a finer time step is required.

Table 11, Central difference solution time with time step size

Time Step Size (ms)	Solution Time (s)
0.2	no solution
0.03	8 (oscillation)
0.02	12
0.002	114

The central difference method has fewer operations per time step than the other methods but requires a time step approximately 10 times smaller for this model. The danger is that a small change in time step can make the difference between a valid and invalid result, i.e. as in the 0.03 ms to 0.02 ms case (factor of 1.5). Use of the other methods would still produce reliable results even if the time step was varied within a factor of 2. The difficulty in determining the time step size for implicit methods a priori is that the time step is largely dependent on the severity of the nonlinearities present (*Ansys theory manual*, 2003). However, in general, the time step required for implicit methods is larger than for explicit methods so the techniques shown in section 3.2.1.1 can be used to calculate the time step size.

4.3.3.2 Integration parameter variation

The implicit methods used in JIFEA have parameters that alter the performance of the method. These parameters are evaluated for their effect on the solution time and results generated. The explicit method only has the time step size and element length and is therefore not present in this section.

4.3.3.2.1 Newmark method

There are two parameters in the Newmark method, α and δ. ANSYS uses the relationships shown in equations 4.3.10 and 4.3.11 for α and δ to cast the Newmark parameters in terms of a new variable γ that must be greater than or equal to zero for unconditional stability. Note: the function response can be nonlinear but must be continuous for unconditional stability. Newmark will be conditionally stable for discontinuous responses from plasticity, friction or contact. The ANSYS theory manual describes the effect of a non-zero γ as adding numerical damping to the method. ANSYS uses a default of γ = 0.005. Using γ = 0 makes Newmark equivalent to the Trapezoid rule.

$$\alpha = \frac{1}{4}(1+\gamma)^2 \qquad 4.3.10$$

$$\delta = \frac{1}{2}+\gamma \qquad 4.3.11$$

Figure 4.15 shows the stuck point force response with changing γ. The response does not begin to show the numerical damping effects until γ = 0.05 and greater. Notice that for values of γ greater than 0.1 the response becomes similar to those of the Wilson method.

In all of the cases the solution took 7 seconds to complete. Initially it was expected that different values for γ would cause convergence problems and increase solution time but it is likely that for the simple base case with minimal nonlinear effects, the model is still well behaved.

4.3.3.2.2 Wilson method

The Wilson method uses Θ as the integration parameter. It can be shown mathematically that values of 1.37 or greater are required for unconditional stability (Bathe, 1996; Clough & Penzien, 1993). The default for the analyses performed is 1.40. Figure 4.16 shows the response of the stuck point force as Θ is varied. Θ = 2.0 begins to show the local oscillations but these are more likely present due to the decrease in the time step size. Only Θ = 1.37 and 1.40 could be solved with the default *its* of 0.2 ms. The remaining analyses required smaller time step sizes. Table 12 lists the required time step size to gain convergence for a given value of Θ. Also, the table lists the solution time for each analysis.

Table 12, Wilson solution time with time step size

Theta (Θ)	Time Step Size (ms)	Solution Time (s)
1.37	0.2	8
1.40	0.2	8
1.50	0.1	13
1.75	0.08	16
2.00	0.02	61

The method is slightly slower than Newmark which was expected as it has a greater number of operations to perform per time step. Wilson method uses a linear assumption between the current acceleration and the future acceleration. Θ = 2.0 uses more of the future acceleration than the current hence the time step must be smaller. This indicates that unconditional stability may not apply when the nonlinearity is discontinuous.

4.3.3.2.3 Newmark and Wilson as linear acceleration

To test other possibilities, the Newmark and Wilson methods were configured to simulate the linear acceleration method. I.e. α =1/6, δ =1/2 and Θ =1.0. With these integration parameters and time step size of 0.2 ms, the methods should be identical. Figure 4.17 shows that the response of the two methods is identical as expected. The linear acceleration method is not unconditionally stable and therefore will not be used for general purpose analysis.

4.3.3.3 Integration sensitivity summary

The Newmark method provides reasonable results even with larger time steps sizes and with the fastest solution times. The integration parameter had minimal affects on the results produced. Theoretically, adding numerical damping smoothes the response of the system simplifying the nonlinear equilibrium iterations. However, the nonlinearities are discontinuities and are minimally affected by numerical damping.

Wilson provides a more accurate solution but with a slight increase in solution time. Wilson is more sensitive to the integration parameter and time step size. The study revealed that for the same model Wilson could not produce results with the same time step range as Newmark and showed greater variation in the response as the integration parameter was varied.

The Central Difference method was generally slower requiring 12 seconds producing similar results to Newmark and Wilson with a smaller time step of 0.02 ms, 10 times smaller than the default (0.2 ms).

It could be argued that Newmark be used for "quick and dirty" solutions and stable field use reserving Wilson for refined analyses. Table 13 shows a summary comparison between integration methods. Either the Wilson or Newmark methods with a time step size of 0.2 ms could be used. However, the Wilson method is more sensitive to time step size and integration parameter modifications loosing convergence under some circumstances. The Central Difference method does not provide more accuracy than the implicit methods, however, it is generally slower and very sensitive to step size. Therefore, the best option is to use the Newmark method unless strict computational rules were implemented in JIFEA to ensure the time step size and element length will produce a valid solution using the Wilson method.

Table 13, Solution times comparison for accuracy and performance

Method	Accuracy	Time Step Size "*its*" (ms)	Solution Time (s)
Newmark	moderate	2	< 1
Newmark	Good	0.2 (default)	7
Wilson	very good	0.2 (default)	7
Wilson	Good	0.02	75
Central Difference	Good	0.02	12

Central Difference	Good	0.002	114

4.4 Combined modelling effects

Several cases were run to benchmark JIFEA and evaluate the external, geometric and internal parameters. For practical and complete Jar placement analysis, adjustments in all these components may be required.

The parametric evaluation indicated the Newmark method was the most reliable integration method. All the cases analyzed in this section were done with the Newmark method configured with an *its* of 0.2 ms and the default integration parameters of α =0.25250625 and δ =0.505 (γ = 0.005).

A full model is defined to assess the performance of the model. Several changes were made to the original Kalsi model.

1. A full complement of drill pipe to represent the entire length of the drilling assembly. (3048 m rather than 609.6 m)
2. Damping is distributed along the entire length of the drilling assembly using the default damping coefficient of 239 N·s/m/m. Currently, a single damping coefficient is used but different values could be used to represent the varying annulus size.
3. Hole-drag distributed along the length of the pipe. Distributed by the following factors:
    a. Length
    b. Outside diameter
    c. Inclination

    The effect of using this distribution is to concentrate the hole-drag in locations where the drag is expected to be highest.

Reference to the Jar position is made with respect to the Jar location of the original Kalsi model. +1 collar means one collar is moved from above the Jar to below it. This effectively moves the Jar up in the drilling assembly by one collar. The placement is similar for the -1 and -2 collar(s) cases.

The full model has approximately 80 more link elements, 80 more damping elements and 160 friction elements that the original Kalsi model did not possess. The extra elements were added to the drill pipe section using the same element length as in the original Kalsi model. Despite the increase in model size and complexity, the solution times ranged from 16 to 18 seconds.

4.4.1 Jar position +1 collar

The Jar position within the drilling assembly was moved up by one collar. Figure 4.18 shows the force response at the stuck point over a range of hole-drag values.

Only the 200 kN hole-drag case shows that the friction of the stuck point is exceeded within the time frame of the analysis. As suggested earlier, performing the analysis to a time further than 0.14 seconds may show that wave interference produces forces great enough to free the drill string. The stuck point slips at approximately t=0.13 seconds. The sliding distance was not determined as the analysis was not run past 0.14 seconds.

4.4.2 Jar position – original position

The original position case is the original Kalsi model description but with the full complement of drill pipe, distributed friction and damping. Figure 4.19 shows the force response at the stuck point for the Jar in the original location. The stuck point friction is exceeded at approximately t=0.123 seconds. Moving the Jar up the drill string by one collar caused a delay in the wave reaching the stuck point. With the distributed damping and friction, the further the Jar is placed from the stuck point, the less likely the wave will reach it.

4.4.3 Jar position -1 collar

By moving the Jar down one collar in the drill string the stuck point slips at approximately t=0.135 seconds. Figure 4.20 shows the stuck point force response at various hole-drag values and indicates that the period of the wave decreases as the Jar approaches the stuck point. The reduced length of pipe between the Jar and the stuck point changes the frequency of the wave, hence the period change. Again nothing can be inferred about the amount of stuck point slip beyond the extent of the analysis.

4.4.4 Jar position -2 collars

Finally a model where the Jar is moved down by two collars is analyzed. As Figure 4.21 shows, the stuck point never slips within the analysis time for any of the friction values. The period gets considerably shorter due to the short distance between the Jar and the stuck point. This may suggest that the Jar should not be placed too close to the stuck point. However, without running the analysis beyond 0.14 seconds such a judgement may be premature. It is possible that with the higher frequency waves, subsequent wave reflections may cause constructive interference increasing the force to free the stuck point.

The 200 kN -2 collar case was re-run with an analysis time of 0.28 seconds, double the default, to show the stuck point response beyond 0.14 seconds. As Figure 4.22 shows, the waves free the stuck point an instant after 0.14 seconds. Given the history up to 0.14 seconds, the interpretation could easily have been that the force response would decay, looking similar to the response from 0 to 0.06 seconds. This is a good example of why running the analysis further in time may make the difference between a good Jar placement decision and a poor one.

4.4.5 Combined modelling effects summary

During discussion of the alternate methods it was mentioned that to get the maximum force to the stuck point the largest impulse must be generated. It was stated that the maximum impulse occurs as a result of the maximum relative momentum between hammer and anvil. Moving the Jar location effectively changes the stiffness and mass of the hammer and anvil, thus altering the relative momentum.

The mass-stiffness relationship of the system changes as the Jar is moved within the drill string. This causes the period and the amplitude of the force response to change. Ideally, to free the stuck point, the largest force with minimal damping and friction is desired. Since damping and friction are fixed parameters, Jar placement is the only remaining parameter the driller has to control the force generation.

The analyses performed do not show the maximum force produced at the stuck point. As the force wave hits the stuck point, if the maximum prescribed friction force is reached, then the element slips. To determine the maximum force, the friction element could be defined with a larger friction force. Alternately, the stuck point could be constrained and the maximum reaction force computed as a function of time.

Best placement can be viewed two ways: as the maximum force produced at the stuck point or as a function of the stuck point slip. The slippage can also be viewed in two ways: the total distance the stuck point moves or as the slip time duration. The analysis time would have to be increased to determine the amount of slip or the total time of slip of the stuck point. In either case, to arrive at a best-placement scenario multiple iterations with longer times may

be required. Since JIFEA solves the system so much faster and with the nonlinear complexities included, neither the multiple iterations nor the longer time duration is a problem. The analysis(es) can be solved in a timely and accurate manner.

4.5 Summary of Solution Control Variable Sensitivity for Jar Wave Propagation

The primary conclusion is, JIFEA and ANSYS generate consistent results but the former 30 times faster in the sample problems.

Kalsi, Eustes et al, have made use of ANSYS to verify and calibrate the results of their methods. JIFEA has been shown to agree very well with ANSYS. Therefore, it can be stated that JIFEA provides the accuracy of ANSYS but with the speed advantage sought by Kalsi or Eustes in developing their methods. Wave-tracking or SFEA may still run faster than JIFEA but the speed, accuracy and flexibility demonstrated by JIFEA makes it the best overall.

The damping sensitivity revealed the model results are somewhat insensitive to damping for the initial value used. Doubling the coefficient had a fairly small effect on the forces generated at the stuck point. A factor over 5 times the original damping was required before the decay became appreciable. Since damping was applied over the entire length of the drill string, 5 times the damping is a significant increase. The change in damping is relative to the initial value and how close the system is to being critically damped. It seems for the models used, a damping coefficient of 239 N·s/m/m is far enough from the critical damping that doubling the damping has minimal effect. Nevertheless, damping reduces the wave amplitude preventing the force from freeing the stuck point.

Friction showed similar results to that of damping. Friction acting at the nodes along the drill string length impeded the wave travel and caused the wave to lose energy (force) at every node. Therefore, high friction may prevent the wave from freeing the stuck point.

The Newmark method was shown to be the most versatile of the integration methods. It was relatively insensitive to time step size so even crude calculations could be used to determine the time step size with less convergence issues. It was insensitive to the integration parameters so no modifications would be warranted between placements. The Newmark method is fast and requires minimal prior calculations or monitoring making it a good choice for field use. If more refined analysis is required, the Wilson method produced the most accurate result. However, this method requires more care in determining the time step size and integration parameters. Therefore, its use is geared more towards research rather than "quick and dirty" field use.

Both Newmark and Wilson are deemed unconditionally stable for specific integration parameter values. The Wilson method proved to be time-step size

dependent despite the integration parameter chosen to be unconditionally stable. This suggests stability requires a continuous nonlinear function.

4.6 Chapter 4 figures

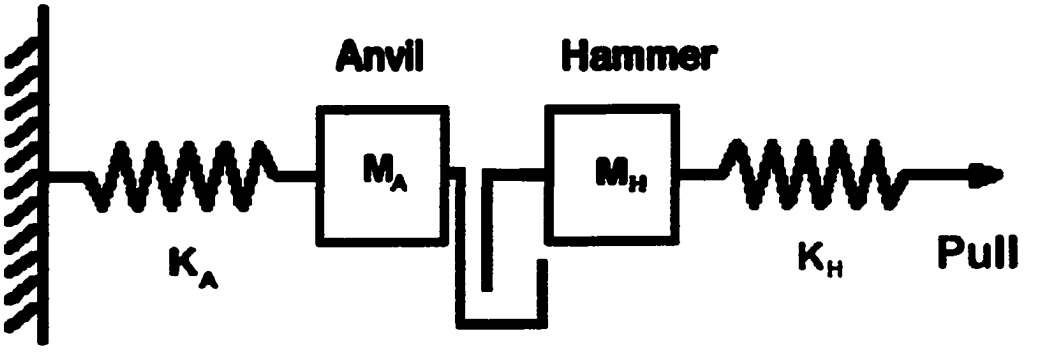

Figure 4.1 Depiction of simplified linear drill string spring-mass system

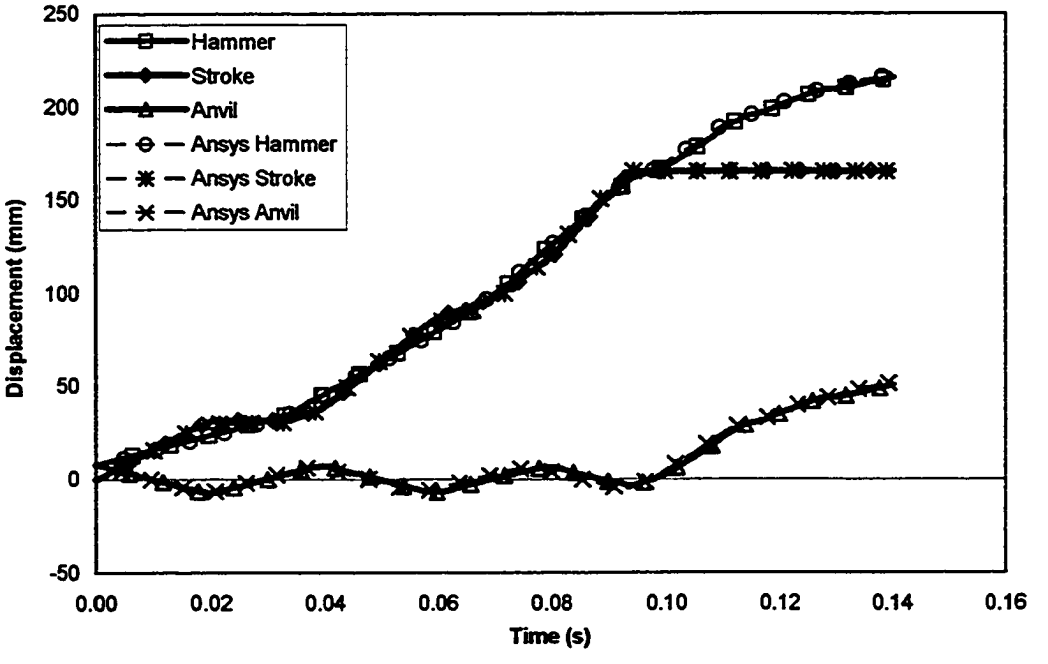

Figure 4.2, Comparison between contact displacement results between JIFEA and ANSYS of the modified Kalsi model

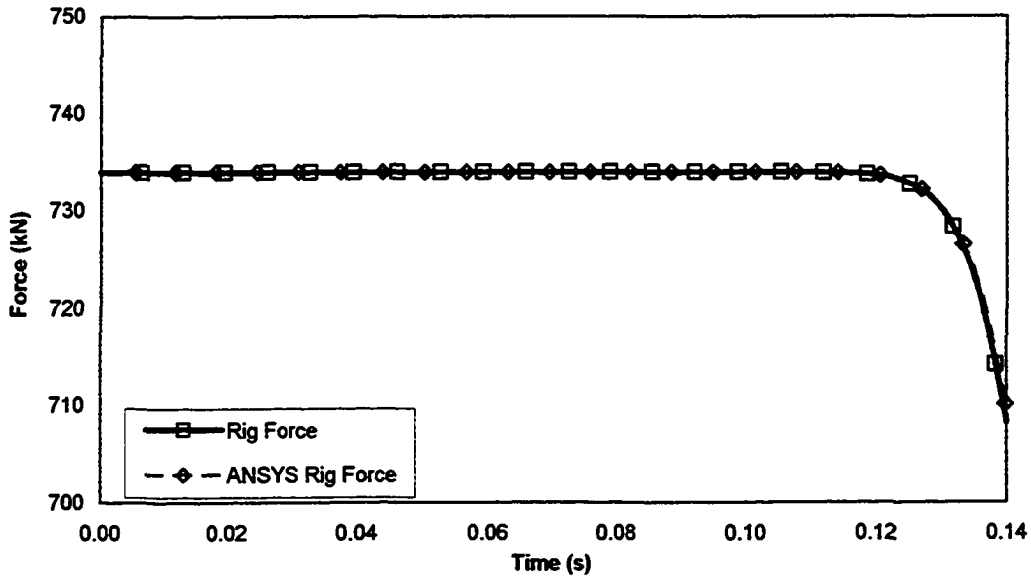

Figure 4.3, Rig force response comparison between JIFEA and ANSYS for the modified Kalsi model

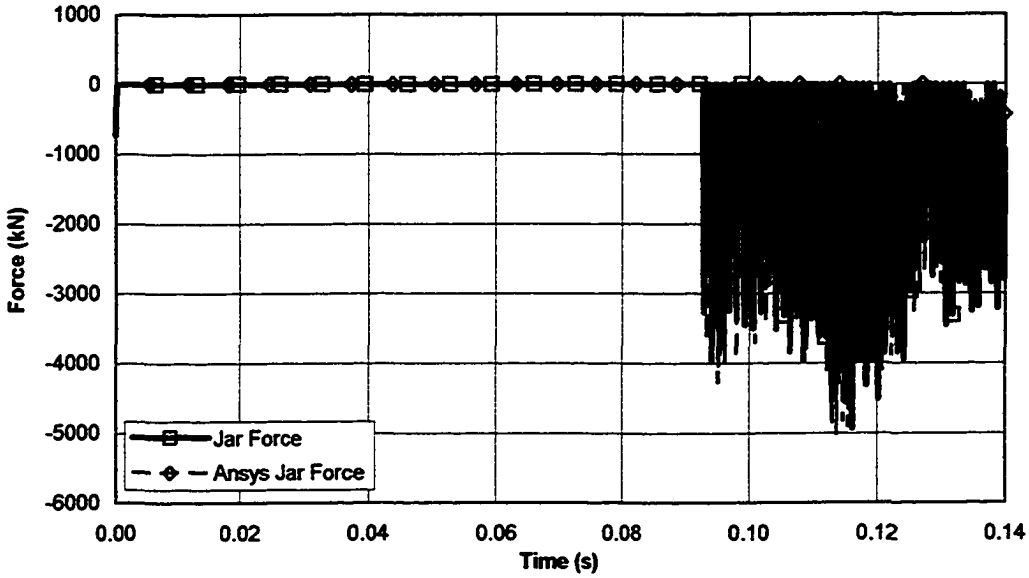

Figure 4.4, Jar force comparison between JIFEA and ANSYS for the modified Kalsi model

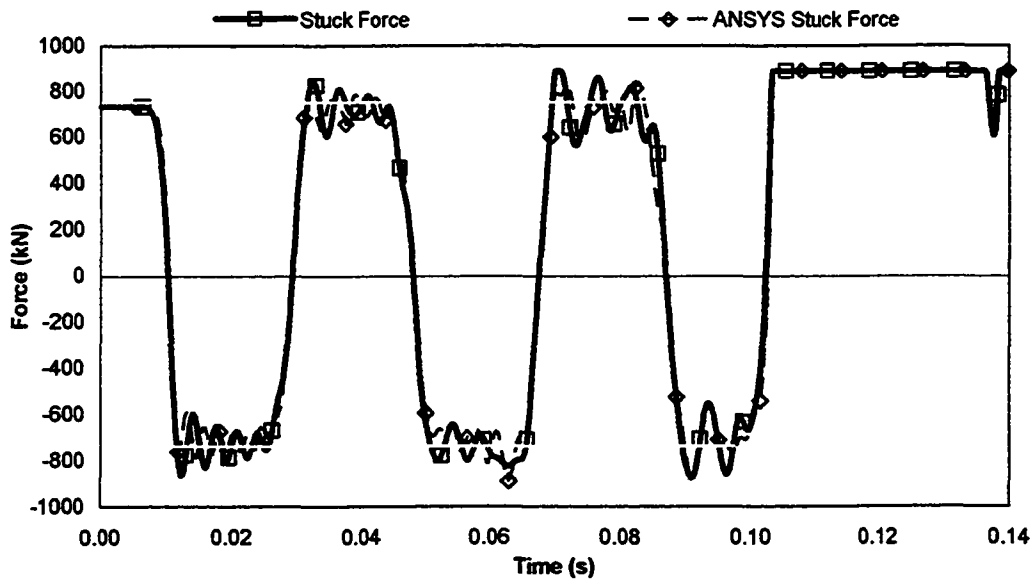

Figure 4.5, Stuck force comparison between JIFEA and ANSYS for the modified Kalsi model

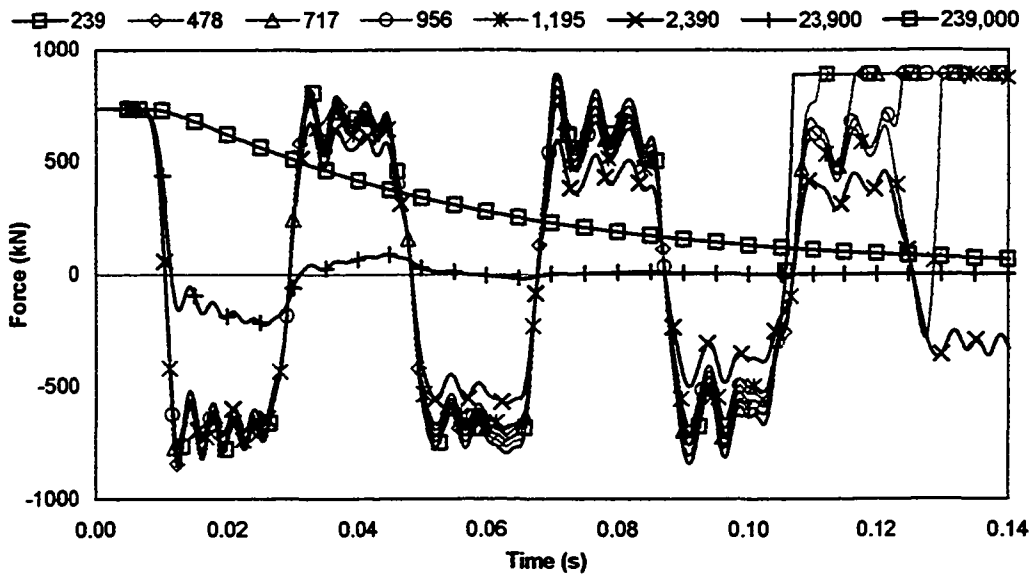

Figure 4.6, Stuck point force comparison with varying damping coefficients (time=0.14 seconds) using JIFEA

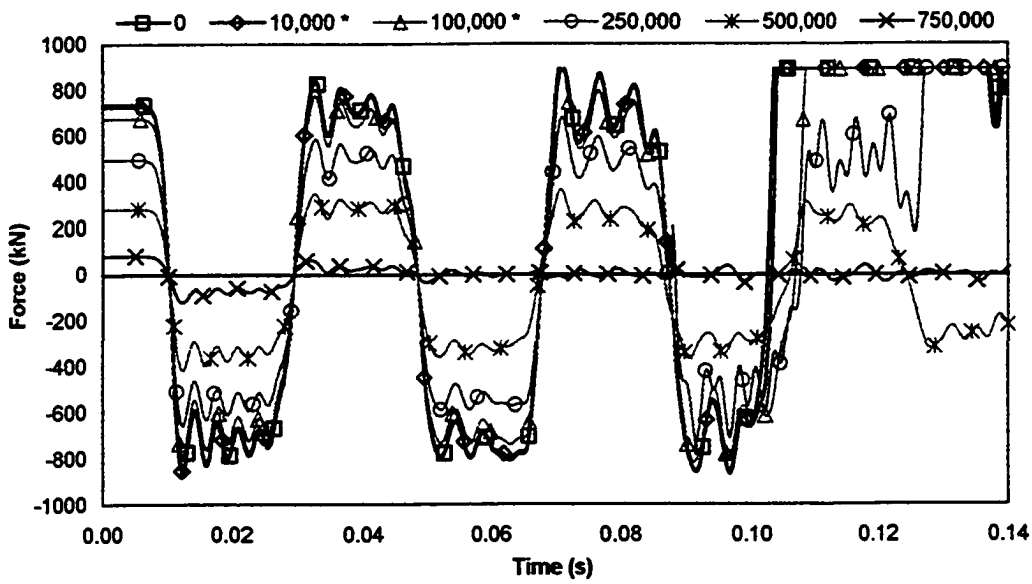

Figure 4.7, Stuck point force comparison with linear friction distribution using JIFEA

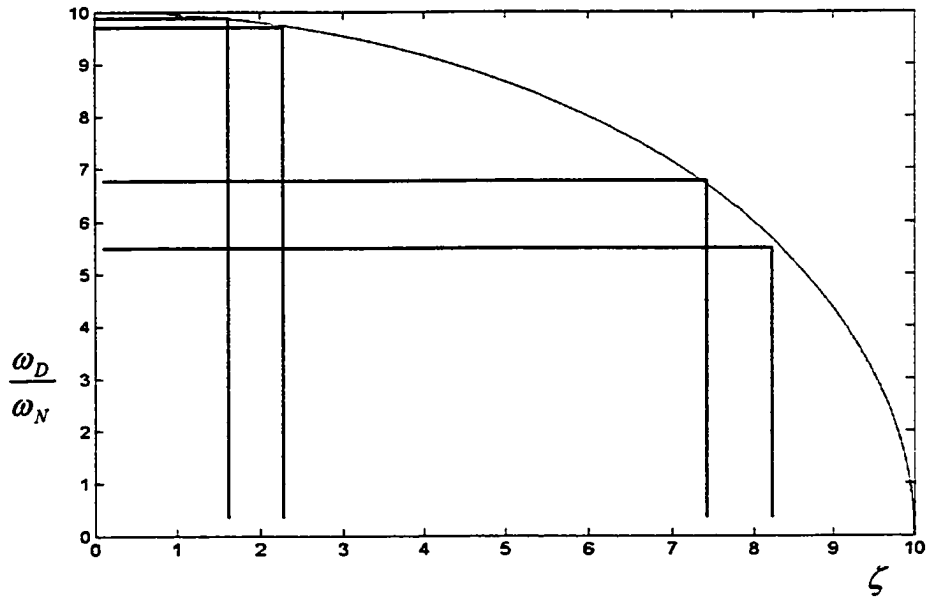

Figure 4.8, Damped circular natural frequency as a function of damping coefficient

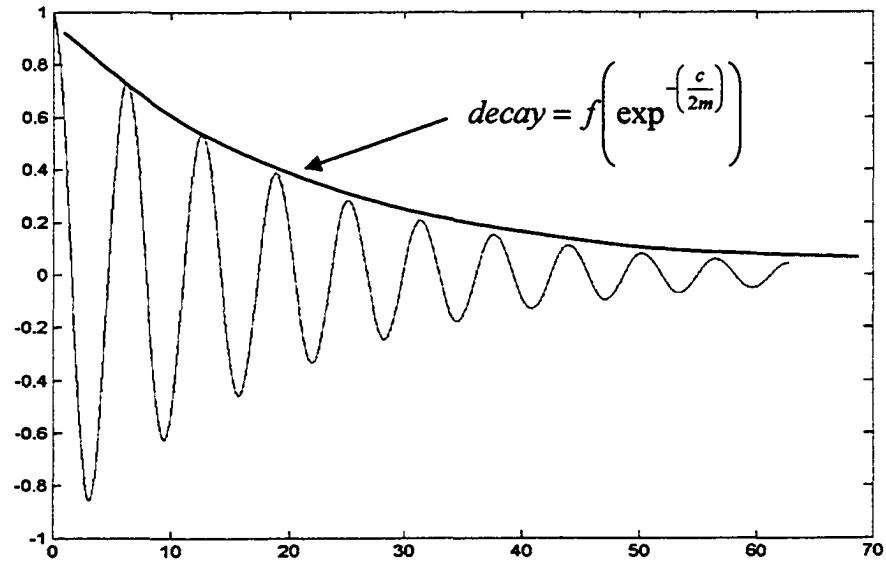

Figure 4.9, Generic damped response depicting exponential decay

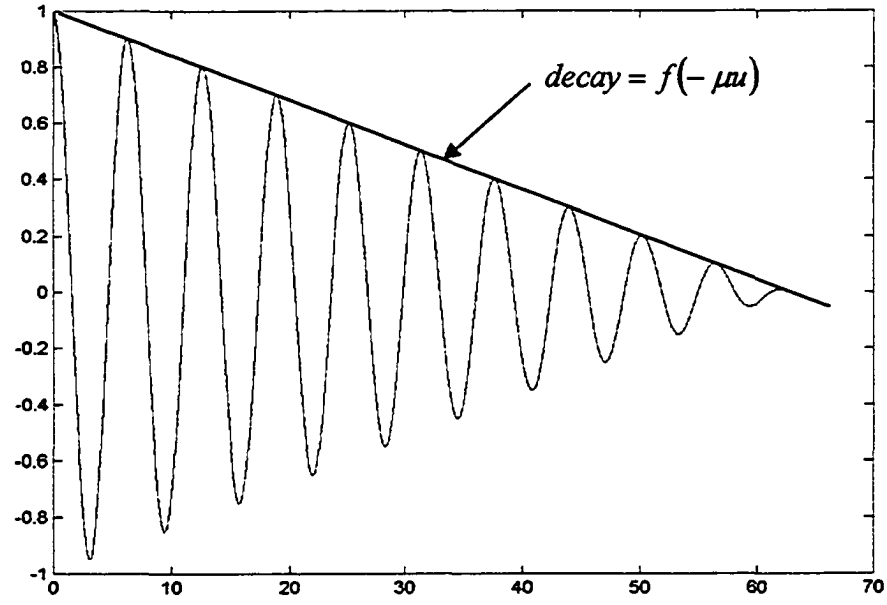

Figure 4.10, Generic frictional response depicting linear decay

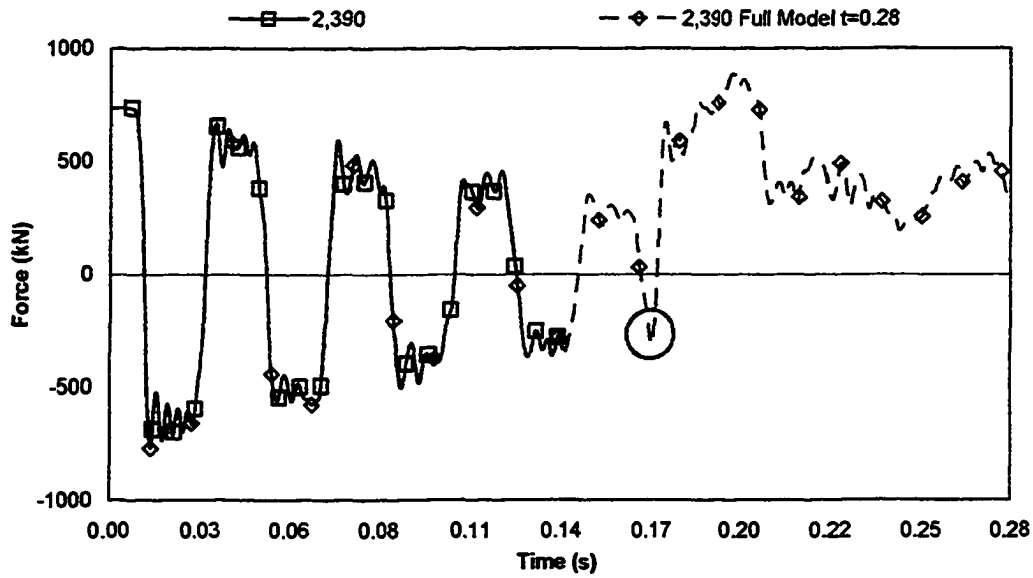

Figure 4.11, Comparison between reduced drill pipe model and full complement drill pipe models (*its*=0.2ms)

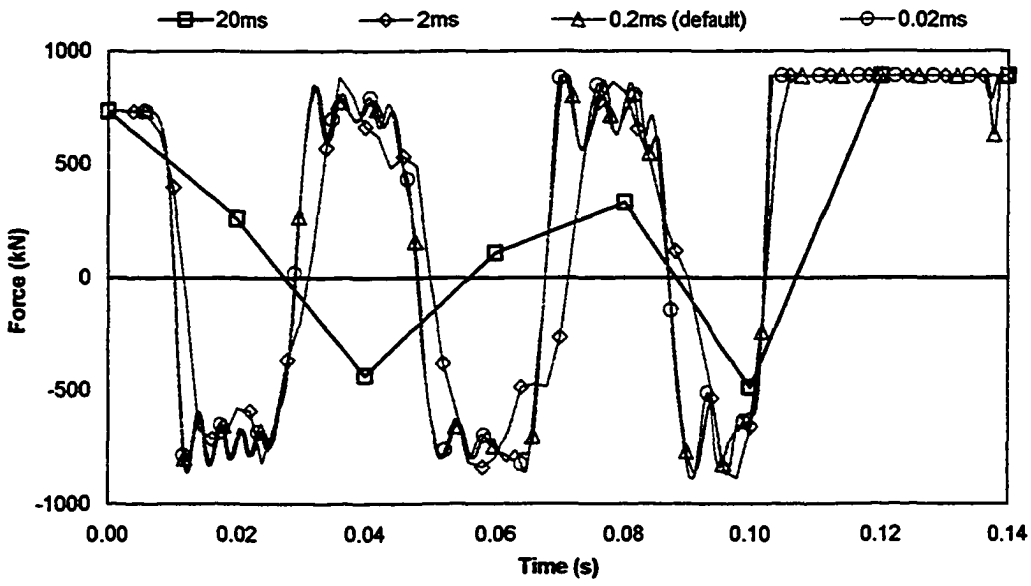

Figure 4.12, Comparison of stuck force reaction with various time step size using the Newmark method

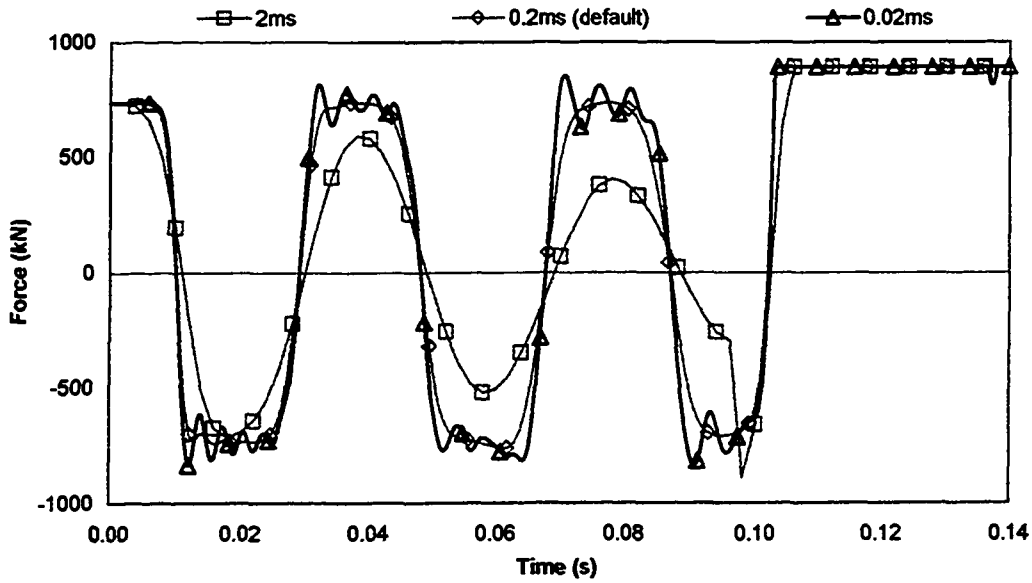

Figure 4.13, Comparison of stuck force reaction with various time step size using the Wilson method

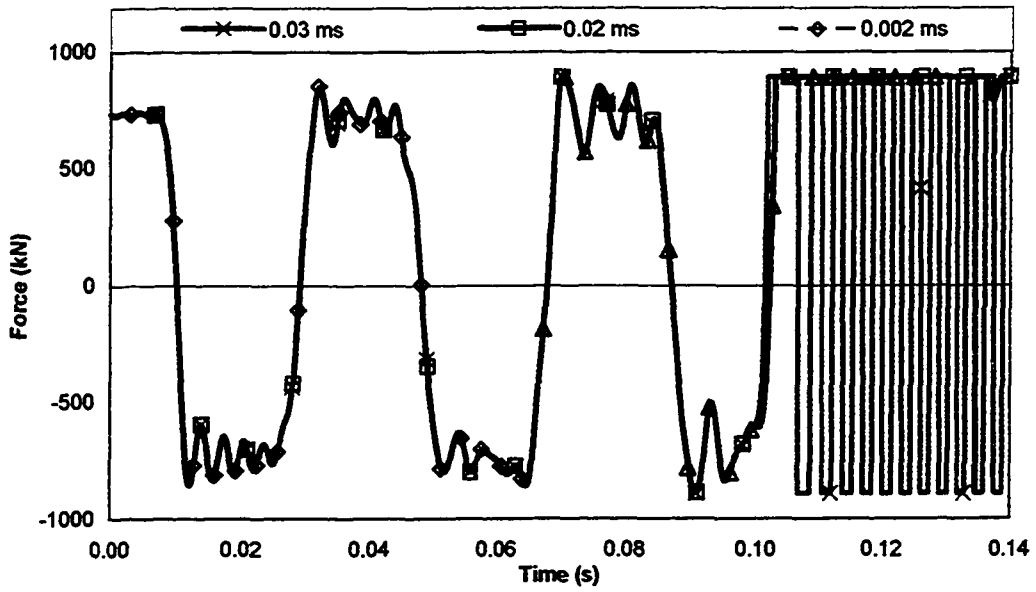

Figure 4.14, Comparison of stuck force reaction with various time step size using the Central Difference method

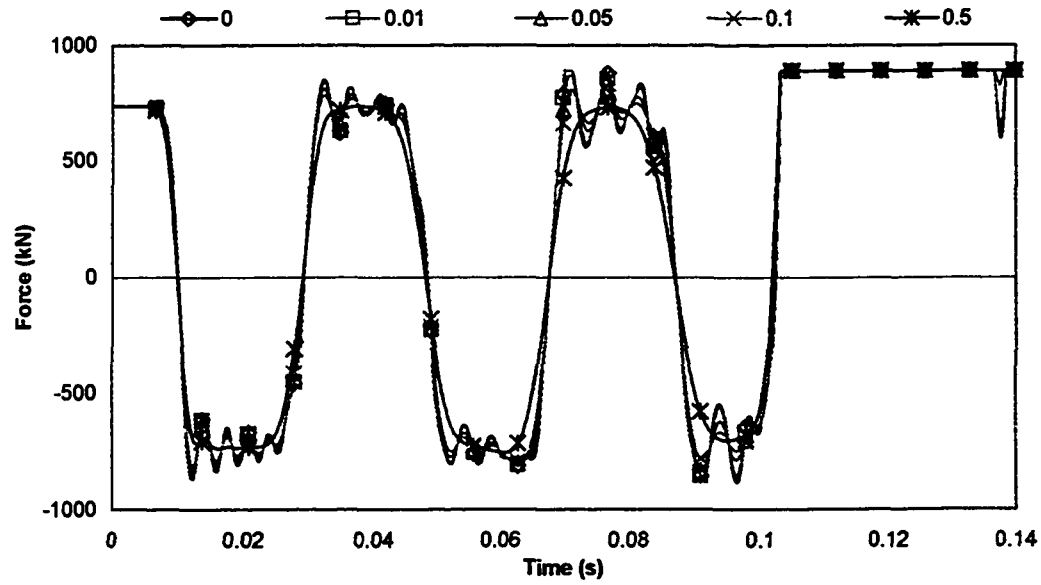

Figure 4.15, Comparison of stuck force reaction for various integration parameter (γ) for the Newmark method (t=0.14s *its*=0.0002s)

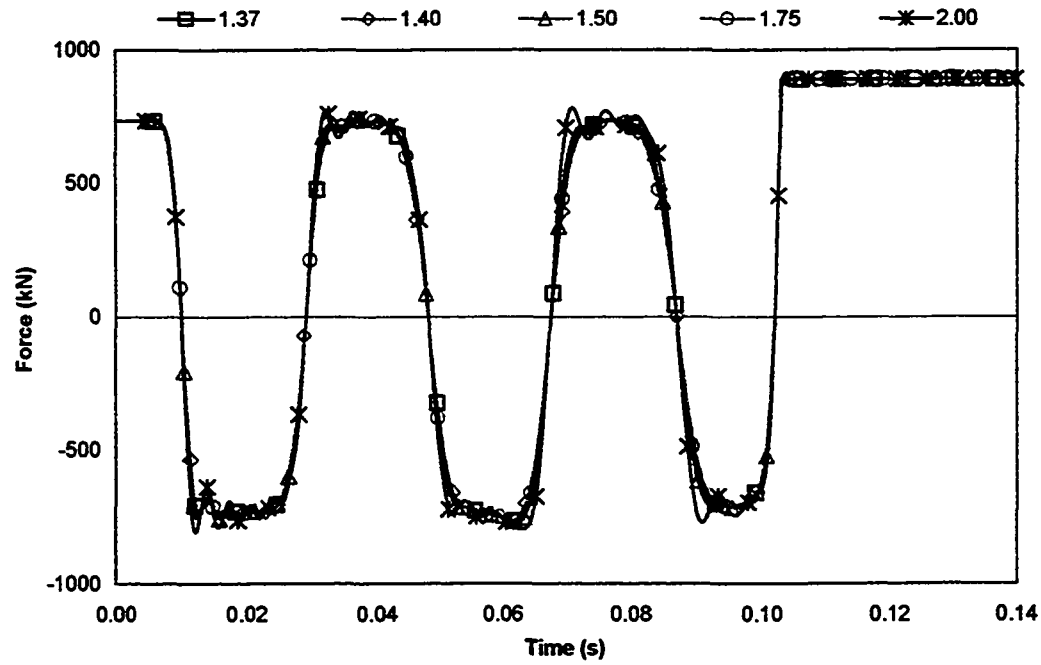

Figure 4.16, Comparison of stuck force reaction for various integration parameter (Θ) for the Wilson method (t=0.14s *its*=0.0002s)

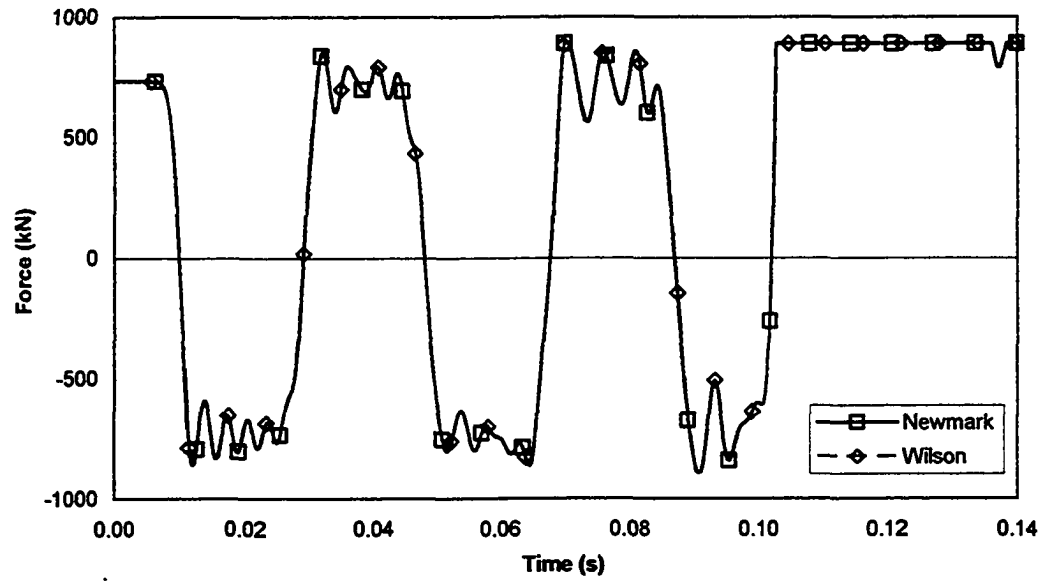

Figure 4.17, Comparison of stuck force reaction using linear acceleration configuration with Newmark and Wilson (*its* = 0.2 ms)

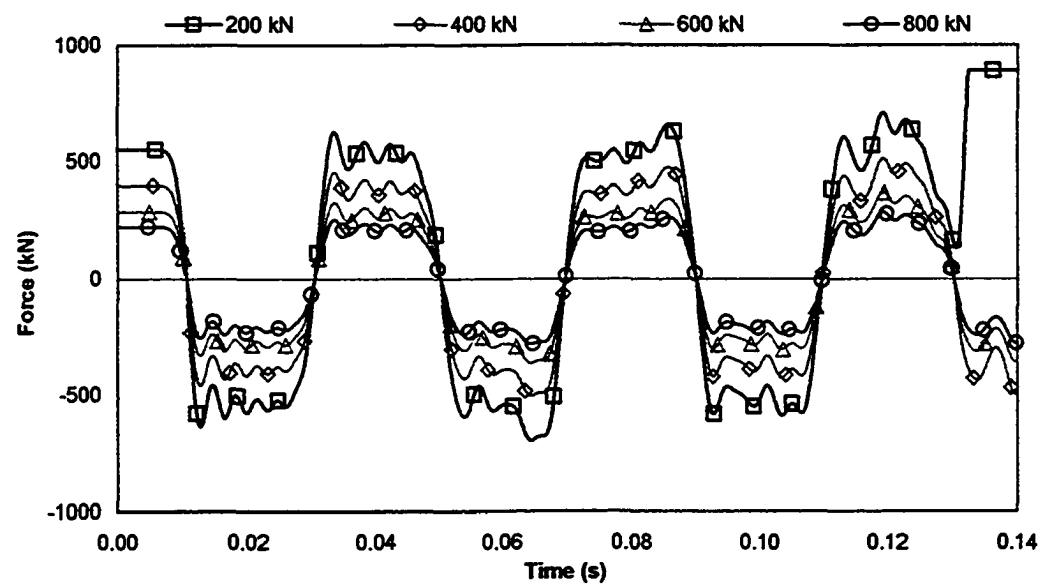

Figure 4.18, Comparison of stuck force reaction with various total friction and Jar position moved up one collar in the drilling assembly from the base case (Kalsi model)

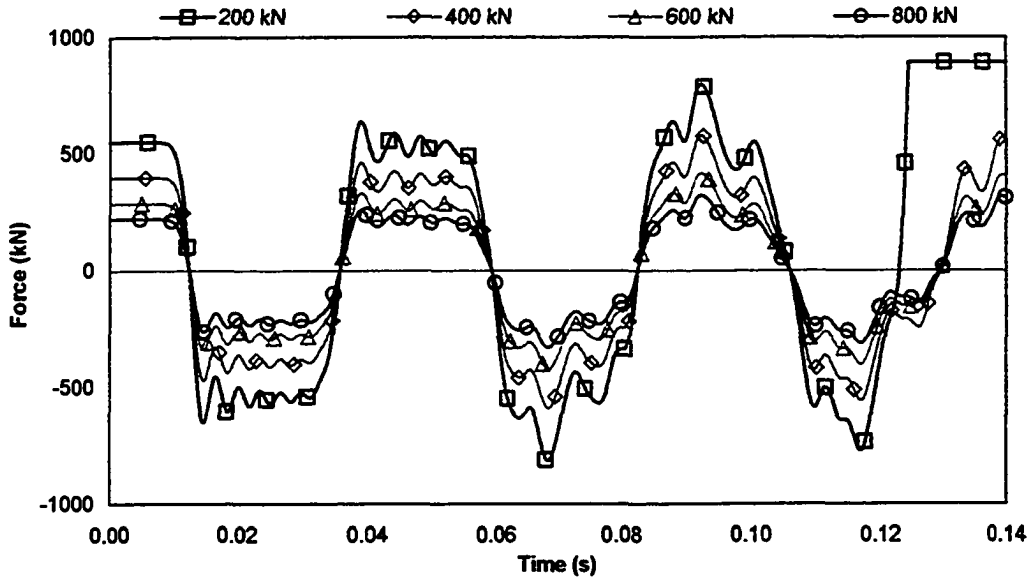

Figure 4.19, Comparison of stuck force reaction with various total friction and Jar in original position (Kalsi model)

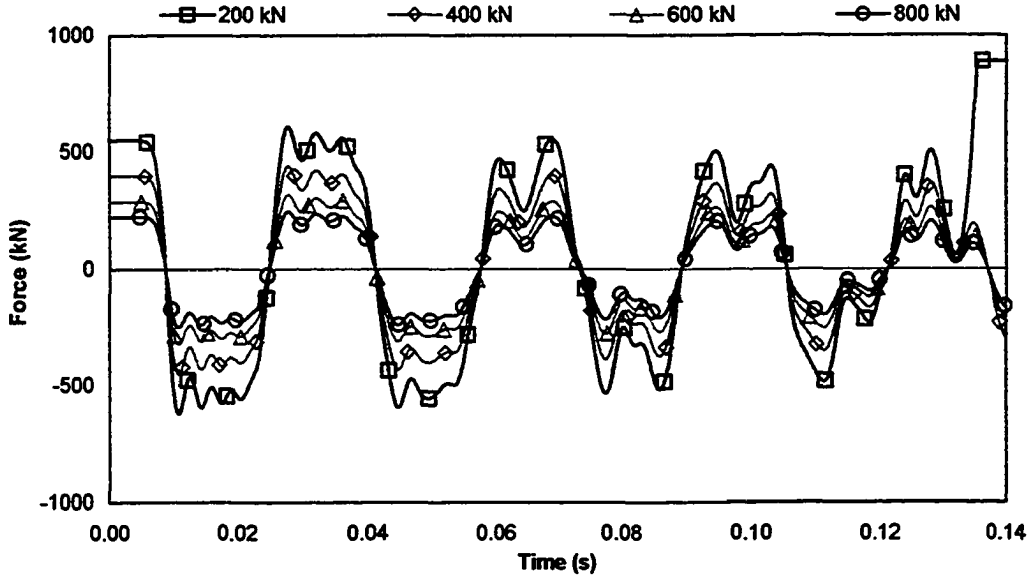

Figure 4.20, Comparison of stuck force reaction with various total friction and Jar position moved down by one collar in the drilling assembly from the base case (Kalsi model)

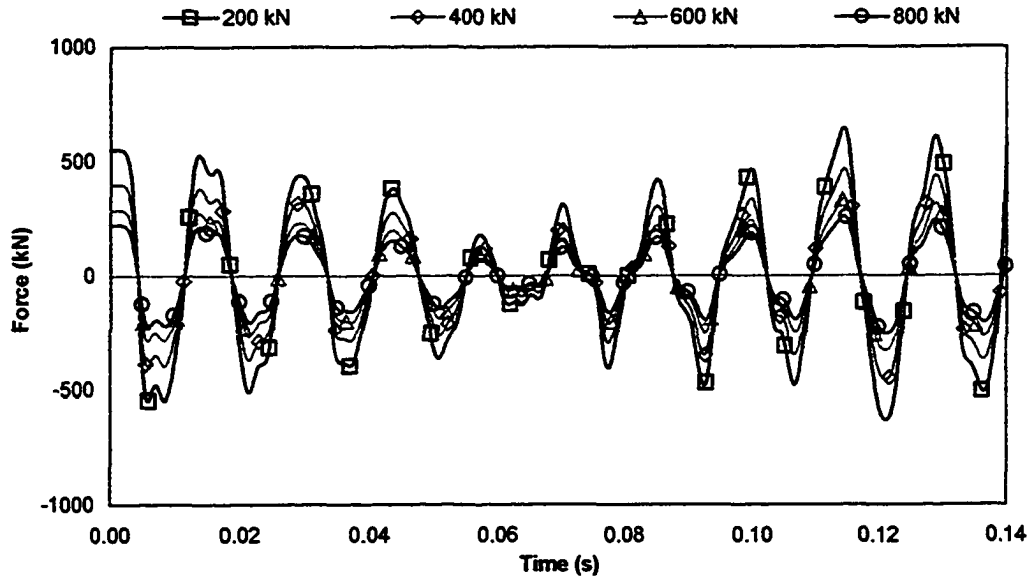

Figure 4.21, Comparison of stuck force reaction with various total friction and Jar position moved down by two collar in the drilling assembly from the base case (Kalsi model)

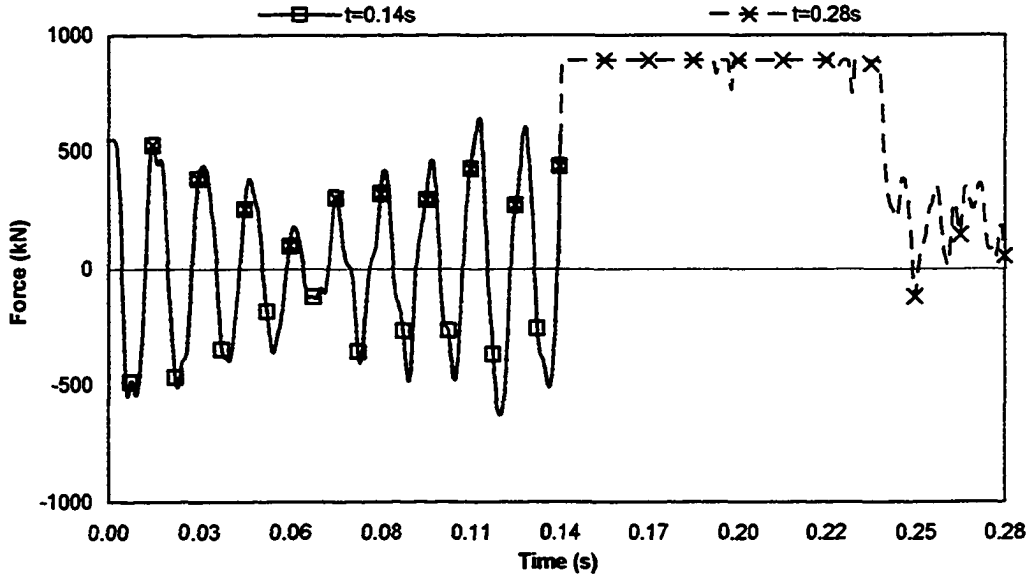

Figure 4.22, Comparison of stuck force reaction between the standard run time and an extended run time for the Jar position down two collars case (200 kN total friction)

Chapter 5

CONCLUSION

The thesis was presented in two parts; first, the numerical methods were evaluated piecewise, and second, the combined pieces used to study the results when analyzing a well-documented wave propagation problem.

Chapter 3 considered the components required to perform nonlinear finite element analysis of wave propagation. The components consisted of elements, time-integrators and the nonlinear incremental solver.

To improve solution efficiency, all components in JIFEA were implemented focusing on performance. Each component was compared to either analytical solutions or results from commercial FEA software ANSYS and ADINA.

Central Difference, Newmark and Wilson time integration methods were evaluated for accuracy against text book examples and both commercial FEA programs. JIFEA's implementation agreed well with the results produced from ANSYS and ADINA. The Central Difference method required a time-step size 10 times smaller than the implicit methods, Newmark and Wilson, for the sample problem.

The Wilson method is similar to Newmark in implementation but requires a few extra vector computations per time step. Therefore, Wilson is slightly slower than Newmark for the same time step size.

The link, damping, friction and contact elements were all verified using analytical methods or compared using ANSYS and ADINA. In all cases, good agreement was found between the JIFEA implementation and the verification cases. Differences found in the friction and contact responses were primarily attributed to slight modelling details and to element and/or solution strategy implementation discrepancies between programs.

JIFEA has demonstrated good efficiency and accuracy performing nonlinear one dimensional wave propagation analysis.

Chapter 4 demonstrates JIFEA used to solve real drill string problems and evaluates the effects various parameters have on the results. This section presented several comparisons between JIFEA and various other results. First, Kalsi's model was re-created using ANSYS to ensure the results could be reproduced, which was confirmed. The model was modified slightly to match the JIFEA model description. JIFEA produced similar results to ANSYS but 30 times faster[1].

[1] On the same computer system

The performance suggests that JIFEA performs as well as the wave-tracking or SFEA methods. Both the wave-tracking and SFEA methods were verified using ANSYS and JIFEA produces comparable results. Therefore, JIFEA provides the performance and accuracy of other technologies complete with multiple solvers and nonlinear elements for extensive Jar placement analysis.

Factors such as integration technique, integration parameters, friction and damping were tested to determine solution effects.

Modest variation in viscous damping coefficient had some effect on the response but still freed the stuck point. Increasing the damping by a factor of five times the original value was required before the waves were insufficient to free the stuck point. The stuck point force is somewhat insensitive to damping coefficient. However, the sensitivity depends on how relatively close the system is to being critically damped.

In general, damping and friction reduce the magnitude of the wave reaching the stuck point. Therefore, generating the largest force possible may be the best practice for selecting Jar placement.

The most robust integration technique was the Newmark method. It produced accurate results and showed little deviation in results from modifying time step or integration parameters. In fact, Newmark proved to be more reliable than the other methods if unrealistic time step sizes are used. This makes Newmark a good choice for field use.

The Wilson method was more accurate but demonstrated convergence difficulties for large integration parameter values despite the value chosen for unconditional stability. Two thoughts arise from this; first, the Wilson method may not be suitable for "quick and dirty" field use and second, the concept of unconditional stability may not apply to discontinuous nonlinearities.

Literature has indicated need for dynamic analysis, specifically wave propagation, when evaluating drill string behaviour. The use of wave propagation to understand the forces produced from Jarring and the effect on the stuck point has grown over the years. FEA has been used to refine Jar placement and increase the understanding of how the force is transmitted to the stuck point and even to the rig. JIFEA uses techniques common to commercial software, generates fast, accurate solutions comparable to alternate methods and can easily produce force, stress or kinematics at any point in the model with a simple user interface. In short, the program can be used in commercial applications, field use and research without compromise.

There are several benefits of JIFEA.

1. **Performance.** The accuracy is comparable to ANSYS with a speed in the order of the alternate methods such as Kalsi's Wave-tracking method or Eustes's spectral analysis. Even with the full complement of elements including the distributed friction, the model still solved in 17 seconds.

2. **Efficient.** The storage and solvers have been specifically written to solve only this problem. The final executable (program file) used to generate the results is only 212 kilobytes. Even a minimum installation of ANSYS is in the order of Gigabytes. This makes the possibility of running the program on a pocket PC, handheld or a website plausible.
3. **Cost.** Commercial FEA software such as ANSYS is expensive, typically greater than $20,000 USD with high annual maintenance costs. Licensing on such software is typically very restrictive and third party distribution is essentially impossible. The application-specific code can be used as a FEA engine in software that companies could sell very inexpensively or even give away with tool rentals.
4. **Longer analysis.** Since the application-specific program runs so much faster, the analysis can be allowed to run for longer times to assess the force response of constructively interfering waves.
5. **More Jar placement variations.** With only 17 seconds for a fairly long drilling assembly analysis, more variations on Jar placement may be evaluated. Ignoring model setup time, in theory, 30 times more placements could be evaluated within the same time than ANSYS.
6. **Element Library.** With the element library present, other tools can be modelled in the drilling assembly. Shock tools, stabilizers or other friction and/or damping distributions are all possible with minimal incremental effort to solve the system.

5.1 Recommended Future Research

When undertaking a project of this magnitude it is often difficult to keep the scope under control. Producing the work contained within this thesis raised as many questions as it answered. Future considerations for this type of analysis follow.

5.1.1 Determination of viscous damping coefficient

Typically the damping coefficient is determined by a simple correlation between the moving pipe and the force required to maintain motion. Fluid properties such as viscosity and density enter the damping coefficient.

Obviously if the pipe is stuck then there is no global pipe motion. However, in many cases the drilling fluid circulation is maintained.

Stress waves propagating through the pipe produce a very small disturbance in the surface. The strains in the axial and radial directions are small compared to the length and diameter of the pipe. The no-slip condition requires boundary layers to form on the surface of the pipe. Considering small perturbations of the pipe and the size of the boundary layers, does determination of the damping coefficient lend itself to this type of motion?

In cases where the formation has caved in around the pipe, there may be a loss of circulation so the only the localized pipe velocity contributes to viscous damping forces. This produces a similar concept but with a very short length of pipe affected.

Further research and scale testing may provide a different damping value than used in this thesis. I.e. damping more suitable to the localized effects stress waves have on the pipe.

5.1.2 Multi-dimensional effects imposed on 1D model

The friction distribution system used in this thesis is based on an intuitive rationalization of hole-drag characteristics. Keeping the model symmetric and banded keeps the matrix size small and simplifies the solvers. The structure of the model used in JIFEA forms a tri-diagonal matrix. Both the damping and friction elements are tied to ground so using matrix portioning also helps to reduce the matrix size.

An interesting concept is the creation of a one dimensional element capable of storing pre-stress information. If lateral deformations are not of interest it may be possible to develop an element and process that enables 3D effects to be imposed on this 1D model and compute the longitudinal displacement more accurately.

Effects such as buckling, helical buckling and bending due to key-seat or well deviation could be included and imposed on the 1D model to better calculate the friction at well-contact points and the stresses in the pipe with pre-stress conditions.

Using these effects, the analysis may be faster and as accurate as performing a full 3D analysis.

5.1.3 Advanced FEA techniques

Throughout this thesis the performance, being speed and accuracy, is the driving force behind the development of the application-specific program. It has been well documented that in order to generate accurate results using FEA, the element size must be small enough with a small enough time step. There are two possibilities for an advanced approach that would produce similar or improved accuracy at the same or increased speed.

5.1.3.1 Adaptive meshing

Along a long section of drill pipe, the stress waves that travel are very short respectively. The waveform then could be captured by a very fine element mesh localized to the location of the wave. As the wave is constantly moving, this requires the mesh to move as well. By having a region of fine mesh density that follows the wave the rest of the pipe may be meshed with very coarse density.

Consideration for velocity and acceleration may be required to ensure continuity between models.

It is uncertain if the extra computing required to perform the re-meshing at every time step would counteract the speed increase from the reduced model size or if the effort would warrant an increase in accuracy.

5.1.3.2 Temporal/Spatial adaptive meshing

Another requirement of time-history wave propagation is a suitable time step size. Stiff differential equations require a smaller time step size than non-stiff equations. Another way to think of this is: systems that have modest responses can be integrated with simple methods and large time steps. In regions where the model has a rapid response, the time step must be smaller and the use of more complex integration schemes may be required.

This suggests that regions where little is happening, i.e. no waves are present, the time step size could be large with a simple integration technique. Where waves are travelling, a small time step could be used with a more sophisticated integration method.

Combining a temporal adaptive technique in conjunction with the adaptive meshing strategy may produce far too much complexity to warrant the effort but, in theory, would have similar benefits to that of adaptive meshing alone but with increased accuracy.

5.1.4 Tool Modelling

The Jar in the Kalsi model was represented as a gap within the drill collar. To better capture the behaviour of a Jar, a combination of elements could be used; Contact to represent the gap, specialized friction to represent the locking mechanism, standard friction to represent the internal tool friction and link elements to represent the tool body. Shock Tools could be modelled in a similar fashion by using link and damping elements. Even stabilizers could be modelled in greater detail.

Better representation of each tool could be useful in determining stress wave amplitude at the stuck point or in the various tools. Tool forces may provide insight for placing other tools in Jar proximity.

Note: Shock tools placed close (typically under) Jars usual sustain severe damage from Jar impulse waves.

5.1.5 Lateral Wave Propagation

The majority of the papers reviewed consider longitudinal wave propagation only. These waves cause localized length variation in the presence of the stress waves. In conjunction with these waves lateral waves are also produced. Little reference is made to the effects these wave have on the friction distribution, the damping or the stuck point.

It could be argued that lateral waves cause cross-section expansion or contraction localized in the region of the waves. In full 3D, these waves may cause localized ovalization in the cross-section rather than uniform expansion or contraction.

Cross-section area changes may affect the hole-drag or the viscous damping acting at that region. As stated previously, the damping may be minimally affected by the waves as the disturbance in the pipe is localized.

Appendix A – Elements

Link Element Description

The internal force is calculated from the internal stresses found in the element. In this case, the element is a simple link or truss in the elastic material regime, therefore, the element force calculation is straightforward.

The force-displacement relationship for the link element is:

$$F_1 = k_e x_1 - k_e x_2 \quad \text{A.1}$$

$$F_2 = -k_e x_1 + k_e x_2 \quad \text{A.2}$$

$$k_e = \frac{AE}{L} \quad \text{A.3}$$

Since the material modelled is elastic, the iso-parametric nodal element force can be computed directly using F_1 and F_2.

Damping Element

The damping coefficient c_d could be a function of viscosity, surface area of the pipe, length of the pipe or annular width, etc. To provide a consistent damping, c_{eff}, the effective damping coefficient is defined as a function of pipe surface area and length.

The force-velocity relationship for the damping element is:

$$F_1 = c_{eff}\dot{x}_1 - c_{eff}\dot{x}_2 \quad \text{A.4}$$

$$F_2 = -c_{eff}\dot{x}_1 + c_{eff}\dot{x}_2 \quad \text{A.5}$$

$$c_d = damping\ coefficient$$

$$c_{eff} = c_d \pi D L \quad \text{A.6}$$

The damping element is based on the damping component of the ANSYS Spring-Damping element Combin14.

Friction Element

The force-displacement relationship for the friction element is:

$$F_1 = k(x_1 - x_2 - x_{slip}) \quad \text{A.7}$$

$$F_2 = -k(x_1 - x_2 - x_{slip}) \quad \text{A.8}$$

$$k = k_{fric}, 0 \quad \text{A.9}$$

As implemented, x_2 is always tied to ground, therefore, F_1 is the force at the node connected to the pipe and F_2 is the friction element ground reaction. The determination of the amount of slip is equivalent to the behaviour of an elastic-perfectly plastic material but expressed in terms of force and displacement rather than stress and strain.

Contact Element

The force-displacement relationship for the contact element is:

$$F_1 = k_{open}(x_1 - x_2) \quad \text{A.10}$$

$$F_2 = -k_{open}(x_1 - x_2) \quad \text{A.11}$$

$$F_1 = k_{closed}(x_1 - x_2 - x_{gap}) + k_{open} x_{gap} \quad \text{A.12}$$

$$F_2 = -(k_{closed}(x_1 - x_2 - x_{gap}) + k_{open} x_{gap}) \quad \text{A.13}$$

F_1 is the force at node 1 and F_2 is the force at node 2. To reduce the nonlinear effects, the element is described with a very low stiffness when the gap is open. The element is intended to only carry a tensile load. If the gap opens, it is free to continue to open. It is modelled after the description of the point to point contact element (Contac12) in ANSYS.

Appendix B – Linear Vibration Problem

Linear Vibration Problem

In general the wave equation is:

$$c^2 \frac{\partial^2 u}{\partial x^2} = \frac{\partial^2 u}{\partial t^2} \qquad \text{B.1}$$

From which the general solution is:

$$u(x,t) = \left(A\cos\omega_n t + B\sin\omega_n t\right)\left(C\cos\frac{\omega_n x}{c} + D\sin\frac{\omega_n x}{c}\right) \qquad \text{B.2}$$

For longitudinal waves the wave speed (speed of sound in medium) is:

$$c = \sqrt{\frac{Eg}{\mu}} = \sqrt{\frac{E}{\rho}} \qquad \text{B.3}$$

where μ is the weight density and ρ is the mass density.

Boundary conditions

The fixed end of the rod can never have any displacement. Therefore, the following can be written:

$$u(0,t) = \left(A\cos\omega_n t + B\sin\omega_n t\right)\left(C\cos\frac{\omega_n(0)}{c} + D\sin\frac{\omega_n(0)}{c}\right) \qquad \text{B.4}$$

$$u(0,t) = \left(A\cos\omega_n t + B\sin\omega_n t\right)C, \quad \therefore C = 0 \qquad \text{B.5}$$

To determine the natural circular frequency, the rod is assumed to be free of forces or initial strains. This provides the condition for the free end that no forces are applied. This can be expressed as:

$$EA\frac{\partial u}{\partial x} = 0 \qquad \text{B.6}$$

$$0 = \left(A\cos\omega_n t + B\sin\omega_n t\right)\left(D\frac{\omega_n}{c}\cos\frac{\omega_n(l)}{c}\right) \qquad \text{B.7}$$

$$\therefore \cos\frac{\omega_n l}{c} = 0 \qquad \text{B.8}$$

$$\frac{\omega_n l}{c} = \frac{\pi}{2}, \frac{3\pi}{2}, \frac{5\pi}{2}, \ldots \quad \text{B.9}$$

$$\omega_n = \frac{n\pi}{2l}\sqrt{\frac{E}{\rho}} \quad \text{B.10}$$

Therefore, the displacement for the principle mode can be expressed as:

$$u(x,t) = \sin\frac{n\pi x}{2l}\left(A\cos\omega_n t + B\sin\omega_n t\right) \quad \text{B.11}$$

This indicates that there are several modes that form the displacement. The total displacement then is the sum of all the modes.

$$u(x,t) = \sum_{n=1,3,5,\cdots}^{\infty} \sin\frac{n\pi x}{2l}\left(A_n\cos\omega_n t + B_n\sin\omega_n t\right) \quad \text{B.12}$$

Since the complete dynamic response is sought, equation B.12 can be differentiated to determine the velocity and acceleration as:

$$\dot{u}(x,t) = \sum_{n=1,3,5,\cdots}^{\infty} \omega_n \sin\frac{n\pi x}{2l}\left(-A_n\sin\omega_n t + B_n\cos\omega_n t\right) \quad \text{B.13}$$

and

$$\ddot{u}(x,t) = \sum_{n=1,3,5,\cdots}^{\infty} \omega_n^2 \sin\frac{n\pi x}{2l}\left(-A_n\cos\omega_n t - B_n\sin\omega_n t\right) \quad \text{B.14}$$

The prescribed strain is now applied since the natural frequency and total displacement was determined.

The strain at any point in the rod is described by:

$$\varepsilon = \frac{\Delta x}{x} = \frac{\Delta l}{l} = \frac{\delta}{l} \quad \text{B.15}$$

The prescribed strain is an initial condition as it occurs at t=0 and is only known to be true at t=0. In addition, since the rod is "pulled" and allowed to come to equilibrium there is no initial velocity at t=0. Therefore:

$$u(x,0) = \varepsilon x \quad \text{B.16}$$

$$\dot{u}(x,0) = 0 \quad \text{B.17}$$

$$\varepsilon x = \sum_{n=1,3,5,\cdots}^{\infty} \sin\frac{n\pi x}{2l}\left(A_n \cos\omega_n(0) + B_n \sin\omega_n(0)\right) \qquad \text{B.18}$$

$$\varepsilon x = \sum_{n=1,3,5,\cdots}^{\infty} \sin\frac{n\pi x}{2l} A_n \qquad \text{B.19}$$

$$0 = \sum_{n=1,3,5,\cdots}^{\infty} \omega_n \sin\frac{n\pi x}{2l}\left(-A_n \sin\omega_n(0) + B_n \cos\omega_n(0)\right) \qquad \text{B.20}$$

$$0 = \sum_{n=1,3,5,\cdots}^{\infty} \omega_n \sin\frac{n\pi x}{2l} B_n \qquad \text{B.21}$$

Solving for the coefficients requires recalling knowledge of Fourier coefficients.

$$A_n = \frac{8\varepsilon l}{n^2\pi^2}(-1)^{\frac{n-1}{2}} \qquad \text{B.22}$$

$$B_n = 0 \qquad \text{B.23}$$

So finally, the displacement, velocity and acceleration are:

$$u(x,t) = \frac{8\varepsilon l}{\pi^2} \sum_{n=1,3,5,\cdots}^{\infty} \frac{(-1)^{\frac{n-1}{2}}}{n^2} \sin\frac{n\pi x}{2l} \cos\omega_n t \qquad \text{B.24}$$

$$\dot{u}(x,t) = -\omega_n \frac{8\varepsilon l}{\pi^2} \sum_{n=1,3,5,\cdots}^{\infty} \frac{(-1)^{\frac{n-1}{2}}}{n^2} \sin\frac{n\pi x}{2l} \sin\omega_n t \qquad \text{B.25}$$

$$\ddot{u}(x,t) = -\omega_n^2 \frac{8\varepsilon l}{\pi^2} \sum_{n=1,3,5,\cdots}^{\infty} \frac{(-1)^{\frac{n-1}{2}}}{n^2} \sin\frac{n\pi x}{2l} \cos\omega_n t \qquad \text{B.26}$$

Appendix C – Central Difference Derivation

Central Difference Derivation

The second derivative approximation can be expressed as:

$$\{\ddot{x}\}^t = \frac{\left(\{x\}^{t+\Delta t} - 2\{x\}^t + \{x\}^{t-\Delta t}\right)}{\Delta t^2} \qquad \text{C.1}$$

The first derivative approximation can be expressed as:

$$\{\dot{x}\}^t = \frac{\left(\{x\}^{t+\Delta t} - \{x\}^{t-\Delta t}\right)}{2\Delta t} \qquad \text{C.2}$$

Using this formulation, both approximations have the same error of order $O(\Delta t)^2$ (for more information on Newton forward, backward or central methods refer to an intermediate or advanced numerical text).

Using these approximations, the equation of motion can be re-written as:

$$[M]\{\ddot{x}\}^t + [C]\{\dot{x}\}^t + [K]\{x\}^t = \{R\}^t \qquad \text{C.3}$$

$$[M]\left(\frac{\left(\{x\}^{t+\Delta t} - 2\{x\}^t + \{x\}^{t-\Delta t}\right)}{\Delta t^2}\right) + [C]\left(\frac{\left(\{x\}^{t+\Delta t} - \{x\}^{t-\Delta t}\right)}{2\Delta t}\right) + [K]\{x\}^t = \{R\}^t \qquad \text{C.4}$$

Grouping the known values on the right and the unknowns on the left produces:

$$\left(\frac{[M]}{\Delta t^2} + \frac{[C]}{2\Delta t}\right)\{x\}^{t+\Delta t} = \{R\}^t - \left([K] - \frac{2[M]}{\Delta t^2}\right)\{x\}^t - \left(\frac{[M]}{\Delta t^2} - \frac{[C]}{2\Delta t}\right)\{x\}^{t-\Delta t} \qquad \text{C.5}$$

The only remaining factor is that of determining a starting procedure. Since this is a multi-step method, at time $t = 0$ there is a requirement of knowing $\{x\}$ at $t = -\Delta t$. For this the initial conditions can be used to determine the displacement at $t = -\Delta t$. If the entire body is at rest, the initial condition is:

$$\left(\{\dot{x}\}=0\right) \text{ then } \{^{-\Delta t}x\}=\{^{0}x\}-\Delta t\{^{0}\dot{x}\}+\frac{\Delta t^2}{2}\{^{0}\ddot{x}\} \qquad \text{C.6}$$

The main difference between the linear and nonlinear derivation is the calculation of the stiffness. For a linear system, $[K]\{x\}=\{F\}$, but in a nonlinear analysis this linear relationship does not exist. Therefore, C.5 can be re-written in terms of the element's internal forces. Otherwise the method is treated the same as the linear method.

$$\left(\frac{[M]}{\Delta t^2}+\frac{[C]}{2\Delta t}\right)\{^{t+\Delta t}x\}= \qquad \text{C.7}$$
$$\{^{t}R\}+\frac{2[M]}{\Delta t^2}\{^{t}x\}-\left(\frac{[M]}{\Delta t^2}-\frac{[C]}{2\Delta t}\right)\{^{t-\Delta t}x\}-\{^{t}F\}$$

Appendix D – Newmark Method

Newmark Derivation

$$\{^{t+\Delta t}\dot{x}\}=\{^{t}\dot{x}\}+[(1-\delta)\{^{t}\ddot{x}\}+\delta\{^{t+\Delta t}\ddot{x}\}]\Delta t \quad \text{D.1}$$

$$\{^{t+\Delta t}x\}=\{^{t}x\}+\{^{t}\dot{x}\}\Delta t+\left[\left(\frac{1}{2}-\alpha\right)\{^{t}\ddot{x}\}+\alpha\{^{t+\Delta t}\ddot{x}\}\right]\Delta t \quad \text{D.2}$$

When δ = $^1/_2$ and α = $^1/_6$ the above equations produce the linear acceleration method and when δ = $^1/_2$ and α = $^1/_4$ the above equations produce the trapezoidal rule. The parameters are to be chosen for speed, accuracy and stability of the integration method. They are often set for specific types or classes of problems. In the 1D wave propagation, the method will start using the constant-average-acceleration (trapezoidal) values. Considering the equations of motion at the desired time, the equation takes the following form:

$$[M]\{^{t+\Delta t}\ddot{x}\}+[C]\{^{t+\Delta t}\dot{x}\}+[K]\{^{t+\Delta t}x\}=\{^{t+\Delta t}R\} \quad \text{D.3}$$

Rewriting equations D.1 and D.2 in terms of the unknown displacements at $t+\Delta t$ yields equations D.4 and D.5 respectively

$$\{^{t+\Delta t}\ddot{x}\}=\frac{1}{\alpha\Delta t^2}(\{^{t+\Delta t}x\}-\{^{t}x\})-\frac{1}{\alpha\Delta t}\{^{t}\dot{x}\}-\left(\frac{1}{2\alpha}-1\right)\{^{t}\ddot{x}\} \quad \text{D.4}$$

$$\{^{t+\Delta t}\dot{x}\}=\{^{t}\dot{x}\}+\Delta t(1-\delta)\{^{t}\ddot{x}\}+\delta\Delta t\{^{t+\Delta t}\ddot{x}\} \quad \text{D.5}$$

and imposing the following conditions on the two parameters:

$$\delta\geq\frac{1}{2} \text{ and } \alpha\geq\frac{1}{4}\left(\frac{1}{2}-\delta\right)^2 \quad \text{D.6}$$

Substituting equations D.4 and D.5 into equation D.3 puts the equation of motion in terms of known displacements, velocities and accelerations.

$$[M]\left(\frac{1}{\alpha\Delta t^2}\left(\{^{t+\Delta t}x\}-\{^{t}x\}\right)-\frac{1}{\alpha\Delta t}\{^{t}\dot{x}\}-\left(\frac{1}{2\alpha}-1\right)\{^{t}\ddot{x}\}\right)+ \quad \text{D.7}$$
$$[C]\left(\{^{t}\dot{x}\}+\Delta t(1-\delta)\{^{t}\ddot{x}\}+\delta\Delta t\{^{t+\Delta t}\ddot{x}\}\right)+[K]\{^{t+\Delta t}x\}=\{^{t+\Delta t}R\}$$

$$[M]\frac{1}{\alpha\Delta t^2}\{^{t+\Delta t}x\}+[C]\frac{\delta}{\alpha\Delta t}\{^{t+\Delta t}x\}+[K]\{^{t+\Delta t}x\}=$$
$$\{^{t+\Delta t}R\}+$$
$$[M]\left(\frac{1}{\alpha\Delta t^2}\{^{t}x\}+\frac{1}{\alpha\Delta t}\{^{t}\dot{x}\}+\left(\frac{1}{2\alpha}-1\right)\{^{t}\ddot{x}\}\right)+ \quad \text{D.8}$$
$$[C]\left(\frac{\delta}{\alpha\Delta t}\{^{t}x\}+\left(\frac{\delta}{\alpha}-1\right)\{^{t}\dot{x}\}+\frac{\Delta t}{2}\left(\frac{\delta}{\alpha}-2\right)\{^{t}\ddot{x}\}\right)$$

Equation D.8 can be simplified by considering the matrices on the left side as the effective stiffness matrix and the right side as the effective load vector.

$$[K_{eff}]=[M]\frac{1}{\alpha\Delta t^2}+[C]\frac{\delta}{\alpha\Delta t}+[K] \quad \text{D.9}$$

$$\{^{t+\Delta t}R_{eff}\}=\{^{t+\Delta t}R\}+$$
$$[M]\left(\frac{1}{\alpha\Delta t^2}\{^{t}x\}+\frac{1}{\alpha\Delta t}\{^{t}\dot{x}\}+\left(\frac{1}{2\alpha}-1\right)\{^{t}\ddot{x}\}\right)+ \quad \text{D.10}$$
$$[C]\left(\frac{\delta}{\alpha\Delta t}\{^{t}x\}+\left(\frac{\delta}{\alpha}-1\right)\{^{t}\dot{x}\}+\frac{\Delta t}{2}\left(\frac{\delta}{\alpha}-2\right)\{^{t}\ddot{x}\}\right)$$

So finally the equation being solved is

$$[K_{eff}]\{^{t+\Delta t}x\}=\{^{t+\Delta t}R_{eff}\} \quad \text{D.11}$$

Nonlinear Derivation

Equation D.3 can be modified to allow for an iterative approach necessary for implementing the full Newton-Raphson iteration technique.

$$[M]\{^{t+\Delta t}\ddot{x}\}+[C]\{^{t+\Delta t}\dot{x}\}+\left[^{t+\Delta t}K^{(k-1)}\right]\{\Delta x^{(k)}\}=\{^{t+\Delta t}R\}-\{^{t+\Delta t}F^{(k-1)}\} \quad \text{D.12}$$

And with the relationship:

$$\left\{{}^{t+\Delta t}x^{(k)}\right\}=\left\{{}^{t+\Delta t}x^{(k-1)}\right\}+\left\{\Delta x^{(k)}\right\} \qquad \text{D.13}$$

At this point several texts including Bathe take $\alpha=\frac{1}{4}$ and $\delta=\frac{1}{2}$. By using these values, the terms in the equations simplify yielding the constant-average acceleration method. Furthermore, Bathe's derivation of the nonlinear Newmark method uses the modified Newton–Raphson method (Newton method). To keep the general format using the full Newton method, the following are used.

$$\left\{{}^{t+\Delta t}\ddot{x}^{(k)}\right\}=a_0\left(\left\{{}^{t+\Delta t}x^{(k-1)}\right\}-\left\{{}^{t}x\right\}+\left\{\Delta x^{(k)}\right\}\right)-a_2\left\{{}^{t}\dot{x}\right\}-a_3\left\{{}^{t}\ddot{x}\right\} \qquad \text{D.14}$$

$$\left\{{}^{t+\Delta t}\dot{x}^{(k)}\right\}=\left\{{}^{t}\dot{x}\right\}+a_6\left\{{}^{t}\ddot{x}\right\}+a_7\left\{{}^{t+\Delta t}\ddot{x}^{(k)}\right\} \qquad \text{D.15}$$

Using these relationships and equation D.12, the general nonlinear form of Newmarks equations are:

$$\begin{aligned}&[M]\left(a_0\left(\left\{{}^{t+\Delta t}x^{(k-1)}\right\}-\left\{{}^{t}x\right\}+\left\{\Delta x^{(k)}\right\}\right)-a_2\left\{{}^{t}\dot{x}\right\}-a_3\left\{{}^{t}\ddot{x}\right\}\right)+\\&[C]\left(\left\{{}^{t}\dot{x}\right\}+a_6\left\{{}^{t}\ddot{x}\right\}+a_7\left\{{}^{t+\Delta t}\ddot{x}^{(k)}\right\}\right)+\\&\left[{}^{t+\Delta t}K^{(k-1)}\right]\left\{\Delta x^{(k)}\right\}=\left\{{}^{t+\Delta t}R\right\}-\left\{{}^{t+\Delta t}F^{(k-1)}\right\}\end{aligned} \qquad \text{D.16}$$

$$\begin{aligned}&[M]\left(a_0\left(\left\{{}^{t+\Delta t}x^{(k-1)}\right\}-\left\{{}^{t}x\right\}+\left\{\Delta x^{(k)}\right\}\right)-a_2\left\{{}^{t}\dot{x}\right\}-a_3\left\{{}^{t}\ddot{x}\right\}\right)+\\&[C]\begin{pmatrix}\left\{{}^{t}\dot{x}\right\}+a_6\left\{{}^{t}\ddot{x}\right\}-a_7a_2\left\{{}^{t}\dot{x}\right\}-a_7a_3\left\{{}^{t}\ddot{x}\right\}+\\a_7\left(a_0\left(\left\{{}^{t+\Delta t}x^{(k-1)}\right\}-\left\{{}^{t}x\right\}+\left\{\Delta x^{(k)}\right\}\right)\right)\end{pmatrix}+\\&\left[{}^{t+\Delta t}K^{(k-1)}\right]\left\{\Delta x^{(k)}\right\}=\left\{{}^{t+\Delta t}R\right\}-\left\{{}^{t+\Delta t}F^{(k-1)}\right\}\end{aligned} \qquad \text{D.17}$$

$$\begin{aligned}&[M]a_0\left(\left\{{}^{t+\Delta t}x^{(k-1)}\right\}-\left\{{}^{t}x\right\}\right)+[M]a_0\left\{\Delta x^{(k)}\right\}-[M]a_2\left\{{}^{t}\dot{x}\right\}-[M]a_3\left\{{}^{t}\ddot{x}\right\}+\\&[C]\left\{{}^{t}\dot{x}\right\}+[C]a_6\left\{{}^{t}\ddot{x}\right\}+[C]a_7a_0\left(\left\{{}^{t+\Delta t}x^{(k-1)}\right\}-\left\{{}^{t}x\right\}\right)+[C]a_7a_0\left\{\Delta x^{(k)}\right\}-\\&[C]a_7a_2\left\{{}^{t}\dot{x}\right\}-[C]a_7a_3\left\{{}^{t}\ddot{x}\right\}+\left[{}^{t+\Delta t}K^{(k-1)}\right]\left\{\Delta x^{(k)}\right\}=\left\{{}^{t+\Delta t}R\right\}-\left\{{}^{t+\Delta t}F^{(k-1)}\right\}\end{aligned} \qquad \text{D.18}$$

$$\begin{aligned}&\left([M]a_0+[C]a_7a_0+\left[{}^{t+\Delta t}K^{(k-1)}\right]\right)\left\{\Delta x^{(k)}\right\}=\left\{{}^{t+\Delta t}R\right\}-\left\{{}^{t+\Delta t}F^{(k-1)}\right\}-\\&[M]\left[a_0\left(\left\{{}^{t+\Delta t}x^{(k-1)}\right\}-\left\{{}^{t}x\right\}\right)-a_2\left\{{}^{t}\dot{x}\right\}+a_3\left\{{}^{t}\ddot{x}\right\}\right]-\\&[C]\left[a_7a_0\left(\left\{{}^{t+\Delta t}x^{(k-1)}\right\}-\left\{{}^{t}x\right\}\right)-(a_7a_2-1)\left\{{}^{t}\dot{x}\right\}-(a_7a_3-a_6)\left\{{}^{t}\ddot{x}\right\}\right]\end{aligned} \qquad \text{D.19}$$

Rewriting the equation of motion using the Newmark approximation for velocity and acceleration enables the solution of the incremental displacement. The equation still takes the form:

$$[K_{eff}]\{\Delta x^{(k)}\}=\{{}^{t+\Delta t}R_{eff}\} \qquad \text{D.20}$$

Where,

$$[K_{eff}]=a_0[M]+a_7a_0[C]+[{}^{t+\Delta t}K^{(k-1)}] \qquad \text{D.21}$$

and

$$\begin{aligned}\{{}^{t+\Delta t}R_{eff}\}&=\{{}^{t+\Delta t}R\}-\{{}^{t+\Delta t}F^{(k-1)}\}-\\ &[M]\left(a_0\left(\{{}^{t+\Delta t}x^{(k-1)}\}-\{{}^{t}x\}\right)-a_2\{{}^{t}\dot{x}\}+a_3\{{}^{t}\ddot{x}\}\right)-\\ &[C]\left(a_7a_0\left(\{{}^{t+\Delta t}x^{(k-1)}\}-\{{}^{t}x\}\right)-(a_7a_2-1)\{{}^{t}\dot{x}\}-(a_7a_3-a_6)\{{}^{t}\ddot{x}\}\right)\end{aligned} \qquad \text{D.22}$$

The following coefficients have been specified to simplify the equations.

$$\begin{aligned}a_0&=\frac{1}{\alpha\Delta t^2}\\ a_1&=\frac{\delta}{\alpha\Delta t}\\ a_2&=\frac{1}{\alpha\Delta t}\\ a_3&=\frac{1}{2\alpha}-1\\ a_4&=\frac{\delta}{\alpha}-1\\ a_5&=\frac{\Delta t}{2}\left(\frac{\delta}{\alpha}-2\right)\\ a_6&=\Delta t(1-\delta)\\ a_7&=\Delta t\delta\end{aligned} \qquad \text{D.23}$$

Using these coefficients, the final form of equations D.21 and D.22 are:

$$\left[K_{eff}\right] = a_0\left[M\right] + a_1\left[C\right] + \left[{}^{t+\Delta t}K^{(k-1)}\right] \qquad \text{D.24}$$

$$\begin{aligned}\left\{{}^{t+\Delta t}R_{eff}\right\} = {} & \left\{{}^{t+\Delta t}R\right\} - \left\{{}^{t+\Delta t}F^{(k-1)}\right\} - \\ & \left[M\right]\left(a_0\left(\left\{{}^{t+\Delta t}x^{(k-1)}\right\} - \left\{{}^{t}x\right\}\right) - a_2\left\{{}^{t}\dot{x}\right\} + a_3\left\{{}^{t}\ddot{x}\right\}\right) - \\ & \left[C\right]\left[a_1\left(\left\{{}^{t+\Delta t}x^{(k-1)}\right\} - \left\{{}^{t}x\right\}\right) - a_4\left\{{}^{t}\dot{x}\right\} - a_5\left\{{}^{t}\ddot{x}\right\}\right]\end{aligned} \qquad \text{D.25}$$

Note that these equations are very similar to the linear counterpart except that the displacement is in terms of the incremental displacement and the internal element force, $\{F\}$, has been added to resolve equilibrium. This describes the full Newton-Raphson technique. Several modified or quasi-Newton methods could be employed to reduce computation overhead.

The process for performing the incremental solution requires the following conditions:

$$\left\{{}^{t+\Delta t}x^{(0)}\right\} = \left\{{}^{t}x\right\} \qquad \text{D.26}$$

$$\left[{}^{t+\Delta t}K^{(0)}\right] = \left[{}^{t}K\right] \qquad \text{D.27}$$

$$\left\{{}^{t+\Delta t}F^{(0)}\right\} = \left\{{}^{t}F\right\} \qquad \text{D.28}$$

Appendix E – Wilson Θ Derivation

Wilson Θ Derivation

The following derivation is taken from Bathe

$$\{^{t+\tau}\ddot{x}\} = \{^{t}\ddot{x}\} + \frac{\tau}{\theta\Delta t}\left(\{^{t+\theta\Delta t}\ddot{x}\} - \{^{t}\ddot{x}\}\right) \quad \text{E.1}$$

$$\{^{t+\tau}\dot{x}\} = \{^{t}\dot{x}\} + \{^{t}\ddot{x}\}\tau + \frac{\tau^2}{2\theta\Delta t}\left(\{^{t+\theta\Delta t}\ddot{x}\} - \{^{t}\ddot{x}\}\right) \quad \text{E.2}$$

$$\{^{t+\tau}x\} = \{^{t}x\} + \{^{t}\dot{x}\}\tau + \frac{1}{2}\{^{t}\ddot{x}\}\tau^2 + \frac{\tau^3}{6\theta\Delta t}\left(\{^{t+\theta\Delta t}\ddot{x}\} - \{^{t}\ddot{x}\}\right) \quad \text{E.3}$$

Equations E.1 to E.3 form the basis of the Wilson method. When θ is 1 then these equations reduce to the linear acceleration method. Rewriting equations E.2 and E.3 with $\tau = \theta\Delta t$ we obtain:

$$\{^{t+\theta\Delta t}\dot{x}\} = \{^{t}\dot{x}\} + \frac{\theta\Delta t}{2}\left(\{^{t+\theta\Delta t}\ddot{x}\} + \{^{t}\ddot{x}\}\right) \quad \text{E.4}$$

and

$$\{^{t+\theta\Delta t}x\} = \{^{t}x\} + \theta\Delta t\{^{t}\dot{x}\} + \frac{\theta^2\Delta t^2}{6}\left(\{^{t+\theta\Delta t}\ddot{x}\} + 2\{^{t}\ddot{x}\}\right) \quad \text{E.5}$$

From which the acceleration and velocity can be expressed in terms of the displacement.

$$\{^{t+\theta\Delta t}\ddot{x}\} = \frac{6}{\theta^2\Delta t^2}\left(\{^{t+\theta\Delta t}x\} - \{^{t}x\}\right) - \frac{6}{\theta\Delta t}\{^{t}\dot{x}\} - 2\{^{t}\ddot{x}\} \quad \text{E.6}$$

$$\{^{t+\theta\Delta t}\dot{x}\} = \frac{3}{\theta\Delta t}\left(\{^{t+\theta\Delta t}x\} - \{^{t}x\}\right) - 2\{^{t}\dot{x}\} - \frac{\theta\Delta t}{2}\{^{t}\ddot{x}\} \quad \text{E.7}$$

With the acceleration and velocity known at $t+\theta\Delta t$, the equation of motion can be solved at time $t+\theta\Delta t$. Because we are solving at $t+\theta\Delta t$ the load vector at that time is required. Since the acceleration is assumed to vary linearly, the load vector can be linearly extrapolated.

$$[M]\{{}^{t+\theta\Delta t}\ddot{x}\}+[C]\{{}^{t+\theta\Delta t}\dot{x}\}+[K]\{{}^{t+\theta\Delta t}x\}=\{{}^{t+\theta\Delta t}\overline{R}\} \quad \text{E.8}$$

$$\{{}^{t+\theta\Delta t}\overline{R}\}=\{{}^{t}R\}+\theta(\{{}^{t+\Delta t}R\}-\{{}^{t}R\}) \quad \text{E.9}$$

Substituting equations E.6 and E.7 into equation E.8 expresses the equation of motion in terms of the unknown displacement and all the known quantities.

$$\begin{aligned}&[M]\left(\frac{6}{\theta^2\Delta t^2}(\{{}^{t+\theta\Delta t}x\}-\{{}^{t}x\})-\frac{6}{\theta\Delta t}\{{}^{t}\dot{x}\}-2\{{}^{t}\ddot{x}\}\right)+\\&[C]\left[\frac{3}{\theta\Delta t}(\{{}^{t+\theta\Delta t}x\}-\{{}^{t}x\})-2\{{}^{t}\dot{x}\}-\frac{\theta\Delta t}{2}\{{}^{t}\ddot{x}\}\right]+\\&[K]\{{}^{t+\theta\Delta t}x\}=\{{}^{t+\theta\Delta t}\overline{R}\}\end{aligned} \quad \text{E.10}$$

Grouping the known and unknown values, equation E.10 in the final form is:

$$[K_{eff}]=[K]+a_0[M]+a_1[C] \quad \text{E.11}$$

$$\begin{aligned}&\{{}^{t+\theta\Delta t}R_{eff}\}=\{{}^{t}R\}+\theta(\{{}^{t+\Delta t}R\}-\{{}^{t}R\})+\\&[M](a_0\{{}^{t}x\}+a_2\{{}^{t}\dot{x}\}+2\{{}^{t}\ddot{x}\})+[C](a_1\{{}^{t}\dot{x}\}+2\{{}^{t}\dot{x}\}+a_3\{{}^{t}\ddot{x}\})\end{aligned} \quad \text{E.12}$$

$$[K_{eff}]\{{}^{t+\theta\Delta t}x\}=\{{}^{t+\theta\Delta t}R_{eff}\} \quad \text{E.13}$$

Once the displacements at $t+\theta\Delta t$ are determined the displacement, velocity and acceleration at $t+\Delta t$ can be computed from:

$$\{{}^{t+\Delta t}\ddot{x}\}=a_4(\{{}^{t+\theta\Delta t}x\}-\{{}^{t}x\})+a_5\{{}^{t}\dot{x}\}+a_6\{{}^{t}\ddot{x}\} \quad \text{E.14}$$

$$\{{}^{t+\Delta t}\dot{x}\}=\{{}^{t}\dot{x}\}+a_7(\{{}^{t+\Delta t}\ddot{x}\}-\{{}^{t}\ddot{x}\}) \quad \text{E.15}$$

$$\{{}^{t+\Delta t}\dot{x}\}=\{{}^{t}x\}+\Delta t\{{}^{t}\dot{x}\}+a_8(\{{}^{t+\Delta t}\ddot{x}\}-2\{{}^{t}\ddot{x}\}) \quad \text{E.16}$$

Where the coefficients are defined as:

$$a_0 = \frac{6}{(\theta \Delta t)^2}$$

$$a_1 = \frac{3}{\theta \Delta t}$$

$$a_2 = \frac{6}{\theta \Delta t}$$

$$a_3 = \frac{\theta \Delta t}{2}$$

$$a_4 = \frac{6}{\theta^3 \Delta t^2} \qquad \text{E.17}$$

$$a_5 = \frac{-6}{\theta^2 \Delta t}$$

$$a_6 = 1 - \frac{3}{\theta}$$

$$a_7 = \frac{\Delta t}{2}$$

$$a_8 = \frac{\Delta t^2}{6}$$

This derivation is the linear method presented by Bathe. For the nonlinear derivation, no specific formulation is provided. In order to show the nonlinear derivation the linear equations and background is required.

The main difference in the nonlinear derivation is the use of the incremental displacement. Using equation E.18 and assuming that the acceleration and velocity in equations E.6 and E.7 are at iteration *k*, then:

$$\left\{{}^{t+\theta\Delta t}x^{(k)}\right\} = \left\{{}^{t+\theta\Delta t}x^{(k-1)}\right\} + \left\{\Delta x^{(k)}\right\} \qquad \text{E.18}$$

$$\left\{{}^{t+\theta\Delta t}\ddot{x}^{(k)}\right\} = \frac{6}{\theta^2 \Delta t^2}\left(\left\{{}^{t+\theta\Delta t}x^{(k)}\right\} - \left\{{}^{t}x\right\}\right) - \frac{6}{\theta \Delta t}\left\{{}^{t}\dot{x}\right\} - 2\left\{{}^{t}\ddot{x}\right\} \qquad \text{E.19}$$

$$\left\{{}^{t+\theta\Delta t}\ddot{x}^{(k)}\right\} = \frac{6}{\theta^2 \Delta t^2}\left(\left\{{}^{t+\theta\Delta t}x^{(k-1)}\right\} + \left\{\Delta x^{(k)}\right\} - \left\{{}^{t}x\right\}\right) - \frac{6}{\theta \Delta t}\left\{{}^{t}\dot{x}\right\} - 2\left\{{}^{t}\ddot{x}\right\} \qquad \text{E.20}$$

$$\left\{{}^{t+\theta\Delta t}\dot{x}^{(k)}\right\} = \frac{3}{\theta \Delta t}\left(\left\{{}^{t+\theta\Delta t}x^{(k)}\right\} - \left\{{}^{t}x\right\}\right) - 2\left\{{}^{t}\dot{x}\right\} - \frac{\theta \Delta t}{2}\left\{{}^{t}\ddot{x}\right\} \qquad \text{E.21}$$

$$\left\{{}^{t+\theta\Delta t}\dot{x}^{(k)}\right\}=\frac{3}{\theta\Delta t}\left(\left\{{}^{t+\theta\Delta t}x^{(k-1)}\right\}+\left\{\Delta x^{(k)}\right\}-\left\{{}^{t}x\right\}\right)-2\left\{{}^{t}\dot{x}\right\}-\frac{\theta\Delta t}{2}\left\{{}^{t}\ddot{x}\right\} \qquad \text{E.22}$$

Then equations E.20 and E.22 can be substituted into the full Newton-Raphson implementation of Wilson, equations E.23 and E.24.

$$\left[M\right]\left\{{}^{t+\theta\Delta t}\ddot{x}^{(k)}\right\}+\left[C\right]\left\{{}^{t+\theta\Delta t}\dot{x}^{(k)}\right\}+\left[{}^{t+\theta\Delta t}K^{(k-1)}\right]\left\{\Delta x^{(k)}\right\}= \left\{{}^{t+\theta\Delta t}\overline{R}\right\}-\left\{{}^{t+\theta\Delta t}F^{(k-1)}\right\} \qquad \text{E.23}$$

$$\left\{{}^{t+\theta\Delta t}\overline{R}\right\}=\left\{{}^{t}R\right\}+\theta\left(\left\{{}^{t+\Delta t}R\right\}-\left\{{}^{t}R\right\}\right) \qquad \text{E.24}$$

Expanding yields:

$$\left[M\right]\left(\frac{6}{\theta^2\Delta t^2}\left(\left\{{}^{t+\theta\Delta t}x^{(k-1)}\right\}+\left\{\Delta x^{(k)}\right\}-\left\{{}^{t}x\right\}\right)-\frac{6}{\theta\Delta t}\left\{{}^{t}\dot{x}\right\}-2\left\{{}^{t}\ddot{x}\right\}\right)+$$

$$\left[C\right]\left(\frac{3}{\theta\Delta t}\left(\left\{{}^{t+\theta\Delta t}x^{(k-1)}\right\}+\left\{\Delta x^{(k)}\right\}-\left\{{}^{t}x\right\}\right)-2\left\{{}^{t}\dot{x}\right\}-\frac{\theta\Delta t}{2}\left\{{}^{t}\ddot{x}\right\}\right)+ \qquad \text{E.25}$$

$$\left[{}^{t+\theta\Delta t}K^{(k-1)}\right]\left\{\Delta x^{(k)}\right\}=\left\{{}^{t}R\right\}+\theta\left(\left\{{}^{t+\Delta t}R\right\}-\left\{{}^{t}R\right\}\right)-\left\{{}^{t+\theta\Delta t}F^{(k-1)}\right\}$$

$$\left[M\right]\frac{6}{\theta^2\Delta t^2}\left\{\Delta x^{(k)}\right\}+\left[C\right]\frac{3}{\theta\Delta t}\left\{\Delta x^{(k)}\right\}+\left[{}^{t+\theta\Delta t}K^{(k-1)}\right]\left\{\Delta x^{(k)}\right\}=$$

$$\left\{{}^{t}R\right\}+\theta\left(\left\{{}^{t+\Delta t}R\right\}-\left\{{}^{t}R\right\}\right)-\left\{{}^{t+\theta\Delta t}F^{(k-1)}\right\}-$$

$$\left[M\right]\left(\frac{6}{\theta^2\Delta t^2}\left(\left\{{}^{t+\theta\Delta t}x^{(k-1)}\right\}-\left\{{}^{t}x\right\}\right)-\frac{6}{\theta\Delta t}\left\{{}^{t}\dot{x}\right\}-2\left\{{}^{t}\ddot{x}\right\}\right)- \qquad \text{E.26}$$

$$\left[C\right]\left(\frac{3}{\theta\Delta t}\left(\left\{{}^{t+\theta\Delta t}x^{(k-1)}\right\}-\left\{{}^{t}x\right\}\right)-2\left\{{}^{t}\dot{x}\right\}-\frac{\theta\Delta t}{2}\left\{{}^{t}\ddot{x}\right\}\right)$$

Equation E.26 is expressed in terms of the effective stiffness, effective load vector and coefficients, similar to the linear derivation.

$$\left[{}^{t+\theta\Delta t}K_{eff}\right]=\left[{}^{t+\theta\Delta t}K^{(k-1)}\right]+a_0\left[M\right]+a_1\left[C\right] \qquad \text{E.27}$$

$$\left\{{}^{t+\theta\Delta t}R_{eff}\right\}=\left\{{}^{t}R\right\}+\theta\left(\left\{{}^{t+\Delta t}R\right\}-\left\{{}^{t}R\right\}\right)-$$

$$\left[M\right]\left(a_0\left(\left\{{}^{t+\theta\Delta t}x^{(k-1)}\right\}-\left\{{}^{t}x\right\}\right)-a_2\left\{{}^{t}\dot{x}\right\}-2\left\{{}^{t}\ddot{x}\right\}\right)- \qquad \text{E.28}$$

$$\left[C\right]\left(a_1\left(\left\{{}^{t+\theta\Delta t}x^{(k-1)}\right\}-\left\{{}^{t}x\right\}\right)-2\left\{{}^{t}\dot{x}\right\}-a_3\left\{{}^{t}\ddot{x}\right\}\right)$$

Such that the final form is

$$\left[{}^{t+\theta\Delta t}K_{eff}\right]\left\{\Delta x^{(k)}\right\}=\left\{{}^{t+\theta\Delta t}R_{eff}\right\}-\left\{{}^{t+\theta\Delta t}F^{(k-1)}\right\} \qquad \text{E.29}$$

Once the incremental displacement is computed, the total displacement is updated using E.18 then the following equations are used to obtain the solution at $t+\Delta t$. Note that these equations are very similar to the linear derivation if the overall implementation and use of E.18 are handled properly.

$$\left\{{}^{t+\Delta t}\ddot{x}\right\}=a_4\left(\left\{{}^{t+\theta\Delta t}x^{(k)}\right\}-\left\{{}^{t}x\right\}\right)+a_5\left\{{}^{t}\dot{x}\right\}+a_6\left\{{}^{t}\ddot{x}\right\} \qquad \text{E.30}$$

$$\left\{{}^{t+\Delta t}\dot{x}\right\}=\left\{{}^{t}\dot{x}\right\}+a_7\left(\left\{{}^{t+\Delta t}\ddot{x}\right\}-\left\{{}^{t}\ddot{x}\right\}\right) \qquad \text{E.31}$$

$$\left\{{}^{t+\Delta t}\dot{x}\right\}=\left\{{}^{t}x\right\}+\Delta t\left\{{}^{t}\dot{x}\right\}+a_8\left(\left\{{}^{t+\Delta t}\ddot{x}\right\}-2\left\{{}^{t}\ddot{x}\right\}\right) \qquad \text{E.32}$$

Appendix F – Jar Placement Software

The creation of Jar Placement software initially led to this thesis. Companies that provide Jar placements to customers generally performed a basic force analysis (summation of forces) on the drill string. The Jar placements were performed by hand using an approximation to the drilling assembly. To aid in this process software was created to perform force calculations on the drilling assembly. As the program advanced, the interface was enhanced so more complicated drilling assemblies could be built and analyzed. The program generated a range of viable locations where a Jar could be placed. The results produced a wide range of placement possibilities.

The software was expanded by including various well geometries with distributed friction. The rationalization presented in this thesis was originally developed for the Jar placement software to distribute the friction.

To refine the placement wave analysis was sometimes employed using commercial FEA. The time to perform a wave analysis generally was too long for most customers and therefore rarely done.

The next step in the program's evolution was to add Jar placement refinement, thus work on the wave propagation was initiated. The problem was commercial programs solved the problem too slowly and cost too much to be of any practical field use. This prompted work into coding the application-specific FEA based wave propagation solution and ultimately this thesis. The FEA code written could be added to the Jar placement software to refine the placement. Therefore much of the code structure has been done with the Jar placement software in mind.

Appendix G – ANSYS Input Code

ANSYS input code for Kalsi model.

```
PI=2*ASIN(1)

RunTime=.14/.0002+10
gosolve=1          ! 0- don't solve, 1- solve
gopost=1           ! 0- don't post, 1- post
dampon=0           ! 0 - no damping 1 - damping
inton=0            ! Turn on Intensifier Jar
dofxon=0           ! Turn on ux constraints

/Title, Vertical Jar Impact Analysis -- IMP001

!!! Parametric Parameters !!!

PullLoad=733956.6
FForce=1779289

! Drill Pipe Area
DSArea=PI/4*(0.1143**2-0.094742**2)
! Srill Collar Area
DCArea=PI/4*(0.18415**2-0.0714248**2)
! Heavy Weight Drill Pipe Area
HWArea=PI/4*(0.1143**2-0.070104**2)
! Intensifier Jar Stiffness (N/m)
IntK=2330006

! Damping coefficient ((N sec/m) / m)
Damp=239

! Drill String length
DSl=609.6
dsel=20

! Heavy Weight Length
HWl=91.44
hwel=10

! Drill Collar Length (above intensifier)
DCl1=27.432
dc1el=10

! Intensifier Length
intl=3.048
```

```
! Drill Collar Length (below intensifier above jar)
DCl2=54.864
dc2el=20

! Drill Collar length (below jar above stuck point)
dcl3=45.72
dc3el=15

! Drill Collar length (below stuck point)
dcl4=45.72
dc4el=15

! More DC.
dcl5=91.44
dc5el=15

! Total number of elements
tot=dsel+hwel+dc1el+dc2el+dc3el+dc4el+dc5el
! Total length of string
totl=dsl+hwl+intl+dcl1+dcl2+dcl3+dcl4+dcl5

!!!!! Determine Integration Time Step as per Ansys 5.5 Dynamics manual.
!!!!!

! Wave Speed
ws=(2.068427e+011/(7850))**.5
! Integration Time Step (instead of .0002)
! its= .0002 !totl/tot/3/ws*.9


/PREP7
!!! Basic Steel Properties !!!

mp,ex,1,2.068427e+011    ! Modulas of Elasticity
mp,nuxy,1,.3             ! Poison's Ratio
mp,mu,1,.5               ! Coulomb Friction coefficient
                         (used to create stuck point)

mp,dens,1,7850           ! Density of Steel (lb mass / cu. in.)

!!! Define Elements !!!

et,1,link1               !Element to represent Drill String
R,1,DSArea

et,2,link1               !Element to represent Heavy Weight Drill String
r,2,HWArea
```

```
et,3,link1                    !Element to represent Drill Collar
r,3,DCArea

*if,inton,eq,1,then
  et,4,combin14               !Element to represent an Intensifier Jar
  r,4,IntK
  keyopt,4,2,2
*endif

*if,dampon,eq,1,then
  et,17,14                    !Element to represent string damping.
  r,17,,Damp*dc2el
  keyopt,17,2,2

  et,18,14                    !Element to represent string damping.
  r,18,,Damp*dc3el
  keyopt,18,2,2

  et,19,14                    !Element to represent string damping.
  r,19,,Damp*dc4el
  keyopt,19,2,2

  et,20,14                    !Element to represent string damping.
  r,20,,Damp*dc5el
  keyopt,20,2,2

*endif

et,8,contac12                 !Element to represent Stuck Point by applying
                              Normal load and friction coefficient
r,8,90,1.751885e+009,,2

! Theta  = 90   - interface surface 90 degrees from global x axis
! KN     = 10e6 - Normal Stiffness of Contact surface
! INTF   = 0    - initial Gap size
! Start  = 2    - node J slides to the right of node I
! KS     = 0    - Surface Stiffness "Sticking" force
! Redfact = 0    - Weak spring between gap Reduction Factor of KN (default
1e-6)

et,9,combin14                 ! Element to remove rigid body motion from
                              model
r,9,26278.27                  ! Weak spring to promote fast solution
keyopt,9,2,2                  ! uy only. added Apr 20, 2000
et,10,12                      ! Element to represent jar stroke and impact
r,10,180,1.751885e+010,-0.1651,,,
```

```
!keyopt,10,3,1

et,11,link1                    ! Tie element for holding the gap open during
                               static step
r,11,17518.85

!!!!!!!!!!!!!!!!!!!!!!!!!!!!!!!!!!!!!!!!!!!!
!!!                            !!!
!!!     Build The Model        !!!
!!!                            !!!
!!!!!!!!!!!!!!!!!!!!!!!!!!!!!!!!!!!!!!!!!!!!

! Tie Down Spring

n,1

type,9
real,9
n,2,0,2.54
e,1,2

TieNod=2
! Lower Section of Drill Collar

kk=2
jj=2.54
*do,ii,kk+1,kk+dc5el
  type,3
  real,3
  jj=jj+dcl5/dc5el
  n,ii,0,jj
  e,ii-1,ii

  *if,dofxon,eq,1,then
    d,ii,ux,0
  *endif

  *if,dampon,eq,1,then
    dn=ii+5000
    n,dn,0,jj!-1
    d,dn,all,0
    type,20
    real,20
    e,ii,dn
  *endif
*enddo
```

```
! Lower Section of Drill Collar
kk=ii
LoDCNod=kk

*do,ii,kk+1,kk+dc4el
 type,3
 real,3
 jj=jj+dcl4/dc4el
 n,ii,0,jj
 e,ii-1,ii

 *if,dofxon,eq,1,then
  d,ii,ux,0
 *endif

 *if,dampon,eq,1,then
  dn=ii+5000
  n,dn,0,jj!-1
  d,dn,all,0
  type,19
  real,19
  e,ii,dn
 *endif

*enddo

! Stuck Point (Arbitrarily set 0.1 m x axis)
type,8
real,8

kk=ii
n,1000,0.0254,jj          ! 0.1 m to the right (positive x axis) of y=0 axis
e,1000,kk                 ! node i at 1000 node j at kk

! Add Force and constraint to Stuck Point

d,1000,all,0
FricNode = kk

! Upper Drill Collar

*do,ii,kk+1,kk+dc3el
 type,3
 real,3
 jj=jj+dcl3/dc3el
 n,ii,0,jj
```

```
  e,ii-1,ii

  *if,dofxon,eq,1,then
    d,ii,ux,0
  *endif

  *if,dampon,eq,1,then
    dn=ii+5000
    n,dn,0,jj!-1
    d,dn,all,0
    type,18
    real,18
    e,ii,dn
  *endif

*enddo

! Jar
jj=jj+6.5

kk=ii
UpDCNod=kk

type,11                              ! Tie Element
real,11
kk=kk+1
n,kk,0,jj
e,kk-1,kk

type,10
real,10

e,kk-1,kk
*get,Jarelem,elem,,num,max
Linkelem=Jarelem-1
JarNodej=kk
JarNodei=kk-1

!  Upper Drill Collar

*do,ii,kk+1,kk+dc2el
  type,3
  real,3
  jj=jj+dcl2/dc2el
  n,ii,0,jj
  e,ii-1,ii
```

```
  *if,dofxon,eq,1,then
    d,ii,ux,0
  *endif

  *if,dampon,eq,1,then
    dn=ii+5000
    n,dn,0,jj-1
    d,dn,all,0
    type,17
    real,17
    e,ii,dn
  *endif

*enddo

! Intensifier jar
kk=ii
Up2DCNod=kk

*if,inton,eq,1,then
  type,4
  real,4

  jj=jj+intl
  kk=kk+1
  n,kk,0,jj
  e,kk-1,kk
*endif

! Upper Drill Collar 9' sections

*do,ii,kk+1,kk+dc1el
  type,3
  real,3
  jj=jj+dcl1/dc1el
  n,ii,0,jj
  e,ii-1,ii

  *if,dofxon,eq,1,then
    d,ii,ux,0
  *endif

  !*if,dampon,eq,1,then
    !dn=ii+5000
    !n,dn,0,jj!-1
    !d,dn,all,0
    !type,7
```

```
   !real,7
   !e,ii,dn
  !*endif

*enddo

! Heavy Weight Pipe 30' sections

kk=ii
DcHwNode=kk

*do,ii,kk+1,kk+hwel
  type,2
  real,2
  jj=jj+hwl/hwel
  n,ii,0,jj
  e,ii-1,ii

  *if,dofxon,eq,1,then
    d,ii,ux,0
  *endif

  !*if,dampon,eq,1,then
    !dn=ii+5000
    !n,dn,0,jj!-1
    !d,dn,all,0
    !type,7
    !real,7
    !e,ii,dn
  !*endif

*enddo

! Drill String 100' sections

kk=ii
HwDsNode=kk

*do,ii,kk+1,kk+dsel
  type,1
  real,1
  jj=jj+dsl/dsel
  n,ii,0,jj
  e,ii-1,ii

  *if,dofxon,eq,1,then
    d,ii,ux,0
```

```
  *endif

  !*if,dampon,eq,1,then
    !dn=ii+5000
    !n,dn,0,jj!-1
    !d,dn,all,0
    !type,7
    !real,7
    !e,ii,dn
  !*endif

*enddo

kk=ii

! Add Constraint to fixed end (bottom end)

d,1,all,0
d,kk,ux,0
*get,RigElem,elem,,num,max
RigElem=RigElem-1
RigNode=kk-1
ddel,fricnode,all

LUMPM,1

fini

!!!!!!!!!!!!!!!!!!!!!!!!!!!!!!
!!!                          !!!
!!! Solve The Model           !!!
!!!                          !!!
!!!!!!!!!!!!!!!!!!!!!!!!!!!!!!

*if,gosolve,eq,1,then

/solu

! Setup Solution controls
ANTYPE,4
TRNOPT,FULL

outres,all,1
kbc,1
autots,on
lnsrch,off
```

```
! Apply Friction and Add Pull Force to Drill String
timint,off
time,.0002
nsub,10
f,FricNode,fx,FForce
f,kk,fy,PullLoad
solv

timint,on
ekill,Linkelem
DELTIM,.0002
time,.14
f,FricNode,fx,FForce
f,kk,fy,PullLoad
solv                    ! Solve this thing...

fini

*if,gopost,eq,1,then

/post26
zP                      ! Post macro

*endif !End if statement for post processing

*endif !End if statement to solve model
```

Appendix H – ANSYS Post-procession Code

ANSYS post processing code for Kalsi model.

```
/post26
NUMVAR,200,
FILE,file,rst,
pltime,0,.5                                    ! Time Frame

rforce,2,1000,f,y,fric_fy
nsol,3,FricNode,u,y,u_stuck
rforce,4,FricNode,f,y,Stuck_fy
esol,5,Jarelem,JarNodej,smisc,1,Jar_fy
RFORCE,6,1,F,Y,supp_fy
nsol,7,2,u,y,u_Tie
nsol,8,Jarnodei,u,y,ui
nsol,9,Jarnodej,u,y,uj
esol,10,Jarelem,Jarnodej,nmisc,3,gap_stat

ADD,11,9,8, ,Stroke, , ,1,-1,1,
DERIV,12,9,1, ,v_Hammer, , ,1,
DERIV,13,12,1, ,a_Hammer, , ,1,
PROD,14,13, , ,a_H_g, , ,1/9.807,1,1,

esol,15,RigElem,RigNode,f,y,Rig_fy

esol,32,RigElem-1,RigNode-1,f,y,Rig_1_fy

nsol,16,RigNode,u,y,u_Rig

ESOL,23,2,3,F,Y,onedown
ESOL,24,1,2,F,Y,tie
NSOL,25,2,U,Y,u_Tie
esol,26,160,158,f,y,DC-HW
esol,27,FricElem,FricNode,smisc,1,Normal
esol,28,FricElem,FricNode,smisc,2,Tangential

DERIV,30,8,1, ,v_Anvil, , ,1,
DERIV,31,30,1, ,a_Anvil, , ,1,
DERIV,32,16,1, ,v_Rig, , ,1,
DERIV,33,32,1, ,a_Rig, , ,1,

PLVAR,15
```

References

Aadnoy, B. S., Stavanger, U., & Anderson, K. (1998). Friction analysis for long-reach wells. *IADC/SPE*(39391).

Aarrestad, T. V., & Kyllingstad, A. (1994). Loads on drillpipe during jarring operations. *IADC/SPE*(24970).

Ansys theory manual. (Vol. Release 8.0)(2003). Vol. Release 8.0): Ansys Inc.

Askew, W. E. (1986). Computerized drilling jar placement. *IADC/SPE*(14746).

Badoni, D., & Makris, N. (1997). Pile-to-pile interaction in the time domain nonlinear axial group response under harmonic loading. *Geotechnique, 47*(2), 299-317.

Basic jar placement. (1995). National Oilwell Griffith.

Bathe, K.-J. (1967). The use of the electronic computer in structural analysis. *Impact, Journal of the University of Cape Town Engineering Society*, 57-61.

Bathe, K.-J. (1996). *Finite element procedures* (1st ed.). Upper Saddle River, New Jersy: Prentice-Hall Inc.

Broussard, A. N., Dacanay, J. U., Pewitt, G. A., & Walters, J. (2004). A case history: The effective use of jarring accelerators in stuck pipe situations. *IADC/SPE*(87983).

Chapra, S. C., & Canale, R. P. (1988). *Numerical methods for engineers* (2nd ed.). U.S.: McGraw-Hill Inc.

Clough, R. W., & Penzien, H. (1993). *Dynamics of structures* (2nd ed.). U.S.: McGraw-Hill Inc.

Dawson, R., & Paslay, P. R. (1984). Drillpipe buckling in inclined holes. *JPT*, 1734-1738.

Drilling jars. (1994). National Oilwell - Griffith.

Elnaggar, M. H., & Novak, M. (1994). Nonlinear model for dynamic axial pile response. *Journal of Geotechnical Engineering, 120*(2), 308-329.

Eustes, A. W. (1996). *A frequency domain approach to drillstring jarring analysis.* Colorado School of Miines, Colorado.

Fernandez, M. A., Inciarte, G., Ramones, R., Romero, J. L., & Bello, A. (2003). Dynamic analysis of stabilized drilling strings performance in low-dip wells. *IADC/SPE*(81148).

Field, D. J., Swarbrick, A. J., & Haduch, G. A. (1993). Techniques for successful application of dynamic analysis i nthe prevention of field-induced vibration damage in mwd tools. *IADC/SPE*(25773).

Gibson, M. T., Tayler, P. J., & Fuh, G.-F. (1992). Optimal applications engineering and borehole stability analysis avoids differential sticking and leads to successful openhole completion of north sea horizontal well. *IADC/SPE*(24615).

JarPRO™. (1990). Kalsi Engineering.

Jianhong, F., & Taihe, S. (1996). Dynamic analysis of bha with bent housing. *IADC/SPE*(37046).

Kalsi, M. S., Wang, J. K., & Chandra, U. (1985). Transient dynamic analysis of the drillstring under jarring operation using finite element method. *IADC/SPE*(13446).

Lerma, M. K. (1985). A study of how heavy-weight drillpipe affects jarring operations. *IADC/SPE*(14326).

Li, Z., & Li, J. (2002). Fundamental equations for dynamic analysis of rod and pipe string in oil-gas wells and application in static buckling analysis. *Journal of Canadian Petroleum Technology*, 44-53.

Logan, D. L. (1992). *A first course in the finite element method* (2nd ed.). Boston, MA: PWS-Kent Publishing Company.

Lubinski, A. (1986). Dynamic loading of drillpipe during tripping. *IADC/SPE*(17211).

Mabsout, M. E., & Tassoulas, J. L. (1994). A finite-element model for the simulation of pile driving. *International Journal for Numerical Methods in Engineering, 37*, 257-278.

McDaniel, G. L. (1982). A theoretical and experimental study of jarring. *IADC/SPE*(10549).

Nagem, R. J., & Williams, J. H. (1994). Scattering of nondispersive waves at nonlinear joints in one-dimensional structures. *Mechanics of Structures and Machines, 22*(3), 305-326.

Skeem, M. R., Friedman, M. B., & Walker, B. H. (1979). Drillstring dynamics during jar operation. *IADC/SPE*(7521).

Steidel, R. F. (1989). *An introduction to mechanical vibrations* (3rd ed.). U.S. and Canada: John Wiley & Sons Inc.

Stockard, D. M. (1980). Case histories of pile driving in the gulf of mexico. *IADC/SPE*(8554).

Tedesco, J. W., McDougal, W. G., & Ross, C. A. (1999). *Structural dynamics: Theory and applications* (1st ed.). Menlo Park, California: Addison Wesley Longman Inc.

Thorp, O., Ruzzene, M., & Baz, A. (2001). Attenuation and localization of wave propagation in rods with periodic shunted piezoelectric patches. *Smart Materials & Structures, 10*(5), 979-989.

Wang, J. K., Kalsi, M. S., Chapelle, R. A., & Beasley, T. R. (1990). A practical approach to jarring analysis. *IADC/SPE*(16155).

Bibliography

Allaire, Paul E., *Basics of the Finite Element Method*, 1st ed. Reading, Dubuque, Iowa: Wm. C. Brown Publishers, 1985.

Ansys Inc., *Ansys Theory Manual*, Release 8, 2003

Bathe, Klaus-Jürgen, *Finite Element Procedures*, 1st ed. Reading, Upper Saddle River, New Jersy: Prentice-Hall Inc., 1996.

Borseli, Arthur P., Omar P. Sidebottom, *Advanced Mechanics of Materials*, 4th ed. Reading, U.S. and Canada: John Wiley & Sons Inc., 1985.

Chapra, Steven C., Canale, Raymond P., *Numerical Methods for Engineers*, 2nd ed. Reading, U.S.: McGraw-Hill Inc., 1988.

Logan, Daryl L., *A First Course in the Finite Element Method*, 2nd ed. Reading, Boston, MA: PWS-Kent Publishing Company, 1992.

Steidel, Robert F. Jr., *An Introduction to Mechanical Vibrations*, 3rd ed. Reading, U.S. and Canada: John Wiley & Sons, Inc., 1989.

Tedesco, Joseph W., McDougal, William G., Ross, C. Allen, *Structural Dynamics: theory and applications*, 1st ed. Reading, Menlo Park, California: Addison Wesley Longman Inc., 1999.